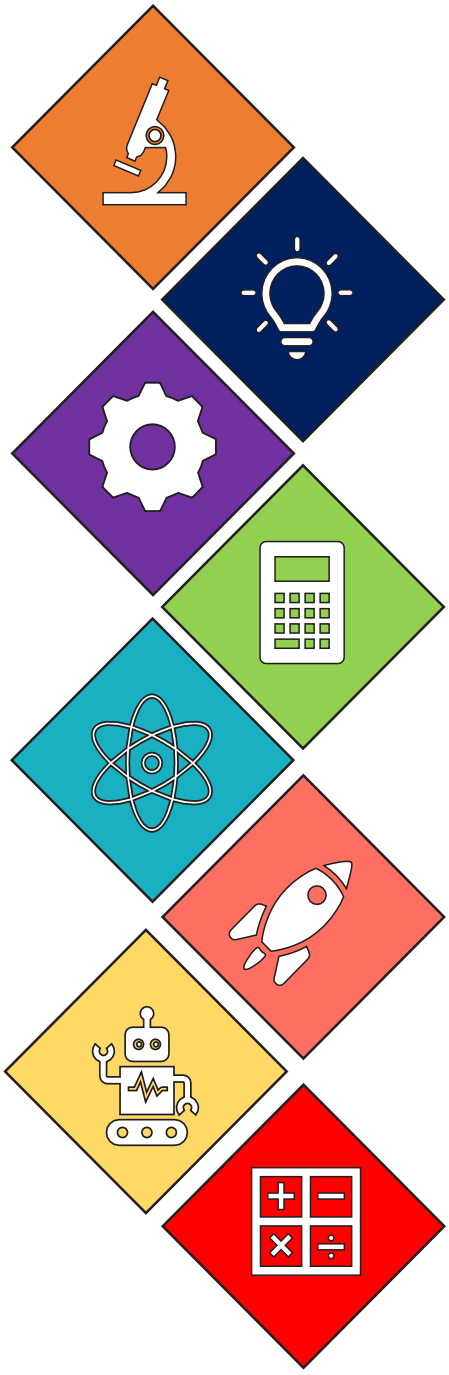

OFFICE OF UNDERGRADUATE RESEARCH
LAMAR UNIVERSITY

WELCOMES YOU

to the Ninth Annual

Texas STEM Conference

Science
Technology
Engineering
Mathematics
Medical

Archer Building

October 30th, 2021

LAMAR UNIVERSITY

Message from Lamar University's Provost and VPAA Dr. Brenda Nichols

Welcome Lamar STEM Community to the Ninth Annual Texas STEM Conference. The event brings 39 talks and posters, with 18 undergraduate presentations, 10 master level and 11 doctoral/postdoctoral level contributions. The student presenters are from Rice University, UT Austin, Auburn University, UTMB-Galveston, The University of Texas Southwestern Medical School, and the Colorado School of Mines. I congratulate all student presenters for their effort to generate quality research and for offering interesting presentations, today. We are proud of your accomplishments. We are happy to see that some presenters are Lamar's alumni. We warmly welcome you back home! I also welcome our guest speaker, Dr. Nicholas Lanning, one of the most successful undergraduate students in the STEM field that Lamar has ever had- with several awards received during his four years of academic training in our school Congratulations, Nick, for becoming an accomplished research scientist at the Air Force Research Laboratory in New Mexico. We are very proud of you and welcome to your alma mater!

Message from Lamar University's Dean of Arts and Sciences

Dr. Lynn M. Maurer

I'd like to welcome all students and faculty to the NINTH TEXAS STEM Conference. For me, as Dean of the College of Arts and Sciences, it is a pleasure to recognize this group of Biology and Computer Science students and faculty engaged in the 2021 Summer Undergraduate Research Fellowship (SURF) who will give their presentations this morning. I also congratulate the many students from our college and outside Lamar who choose the spend their Halloween weekend with us by presenting their research findings and results. We are very proud of all of you. I am thoroughly impressed by the growth of this Texas STEM conference, year after year. For this conference, dedicated researchers from prestigious schools will present at Lamar and join our cohort of students in which a significant portion of this year's attendance is from the graduate level. Our College is particularly proud to welcome Dr. Joe Watso, from the University of Texas Southwestern Medical Center and his talk on Applied Physiology research. With Dr. Watso's presence, a breakout session on Exercise Medicine and Science has been offered this year. Kudos to our student Zaid Mohammed who had a great research experience as Summer Intern of the IEEM Summer Internship Program, working closely with Dr. Joe Watso in the lab of Professor Craig Crandall.

Welcome to the Ninth Annual Texas STEM Conference at Lamar University

Acting O.U.R Director
Dr. Cristian Bahrim

Every fall season we offer two theme conferences at Lamar. Texas STEM conference celebrates its ninth edition, growing every year in significance and number of participants. This year we have a record number of graduate students presentations: 19 out of a total of 39 presentations.

Again Lamar welcomes student presenters from other schools. This year we have participants from Auburn University, UT Austin, Rice U, and Colorado School of Mines. Two of Lamar's undergraduates, Vishal Mundodi and Zaid Mohammed report results and findings from their summer research experiences at medical institutions from the University of Texas Medical School at Houston and the University of Texas Southwestern Medical Center in Dallas, respectively.

We are very proud of our eleven SURF STEM winners who got a rich research experience over summer, here, at Lamar. Their commitment to generate quality research is to be commended. Congratulations SURF winners!

This year, we have the privilege to welcome as guest speaker Dr. Nick Lanning, now an accomplished research scientist at the Air Force Research Laboratory in New Mexico. While at Lamar, as undergraduate, Nick was a student of great talent in performing research, hardworking, and committed to succeed. And indeed, he did it! We are all very proud of Nick!

Dear students, today we celebrate your dedication to achieve scholarly success. The chance to work on a research project sponsored by Lamar is due to the continuous support from Provost Nichols and President Taylor, from all academic Deans and Chairs, to whom we want to thank heartly.

Advisory Board of O.U.R. 2021-2022

Dr. Robert Kelley Bradley
College of Engineering

Dr. Bianca Easterly
College of Arts & Sciences

Dr. Gina Hale
College of Arts & Sciences

Dr. Matthew Hoch
College of Arts & Sciences

Dr. Alyse Jordan
Mary and John Gray Library

Dr. Xiangyang (Sunny) Lei
College of Arts & Sciences

Dr. Lekeitha Morris
College of Fine Arts & Communication

Dr. Nicki Michalski
College of Fine Arts & Communication

Dr. Gevorg Sargsyan
College of Business

Dr. Thinesh Selvaratnam
College of Engineering

Dr. Mamta Singh
College of Education & Human Development

Dr. Dorothy Sisk
College of Education & Human Development

Dr. Robert Worley
College of Arts & Sciences

Mr. Juan Zabala
University Advancement

Office Information:

Chemistry Suite 115
Dr. Cristian Bahrim – Chem 115B / Ms. Jenna Erwin – Chem 115A
cbahrim@lamar.edu - ext. 8290 / jerwin6@lamar.edu - ext. 8430

PLENARY GUEST SPEAK

Dr. Nicholas Lanning

Research Physicist
Air Force Research Laboratory,
Directed Energy Directorate,
Space Electro-Optics Division,
Kirtland AFB, New Mexico

R. Nicholas Lanning received a BS degree in physics and another BS in mathematics from Lamar University in 2012. He received his PhD in physics from Louisiana State University in 2018, under the guidance of the late Jonathan P. Dowling. Dr. Lanning is a theorist specializing in the spectral and transvers-spatial mode structure of photons created in nonlinear-optical interactions, the design of entangled-photon sources, and quantum communication over free-space channels. He is the PI of the quantum communication group at the Air Force Research Lab – Directed Energy Directorate – Space Electro-Optics Division (AFRL/RDS) at Kirtland AFB, NM.

Daytime Space-Earth Quantum Networking

Progress toward daytime space-Earth quantum networking includes many seminal demonstrations conducted over terrestrial free-space quantum channels. However, these experiments were all conducted under ambiguous atmospheric and channel radiance conditions, leaving their relevance to actual space-Earth links unsubstantiated. I will discuss our field experiment which validated our method for solving the daytime space-to-Earth quantum-networking problem, our optimal quantum-channel wavelength analysis, and methods for generating photon pairs optimal for daytime space-Earth channels.

References:

https://arxiv.org/abs/2107.08070, https://arxiv.org/abs/2104.10276, https://arxiv.org/abs/2006.07745

OFFICE OF UNDERGRADUATE RESEARCH
LAMAR UNIVERSITY

All events will take place on Zoom platform with **ID: 879-918-4160** *and* **password 88888**

WELCOME TO THE 9th ANNUAL TEXAS STEM CONFERENCE

8:30 AM	Conference Overview – Dr. Cristian Bahrim, Acting Director of O.U.R. Welcoming Remarks – Dr. Lynn Maurer, Dean of College of Arts and Sciences
8:45 AM	Introduction of our guest speaker, Dr. Robert Nicholas Lanning Research Physicist at the Air Force Research Laboratory, Directed Energy Directorate, Space Electro-Optics Division, Kirtland AFB, New Mexico
9:35 AM	Recognition of Dr. Robert Nicholas Lanning
9:40 AM	Recognition of Dr. Peggy Doerschuk, Distinguished University Professor Emerita of Computer Science

O.U.R. Sponsored Research
2021 Summer Undergraduate Research Fellowship (SURF)
Chair: Dr. Cristian Bahrim

COLLEGE OF ARTS AND SCIENCES — Dean Lynn Maurer

9:45 AM	**Oluwatomisin Egbewale** – Major in Computer Sciences Mentors: **Dr. Xingya Liu** and **Dr. Sujing Wang** Research in Computer Science "*Security evaluation of a cloud-based biometric authentication system.*"
10:00 AM	**Callan Noak** – Major in Computer Scienc cellses Mentor: **Dr. Sujing Wang** Research in Computer Science "*Designing Regression Models for Covid-19 Risk Prevention.*"
10:15 AM	**Nyah Sciarrilla** – Major in Biology Mentor: **Dr. Matt Hoch** Research in Biology "*The Effect of Starch Copper Oxide Nanoparticles on Differential Growth of Microbial Populations in Aquatic Environments.*"

10:30 AM **Carissa Slaughter** – Major in Biology
Mentor: **Dr. Ashwini Kucknoor**
Research in Microbiology and Parasite Immunology
"*Trichomonas vaginalis induced Toll-like Receptor Gene Expression in Cervical Epithelial Cells.*"

10:45 AM **Danielle Soileau** – Major in Biology
Mentor: **Dr. Ashwini Kucknoor**
Research in Microbiology and Molecular Biology
"*Characterization of a Novel Cell Surface Protein Coding Gene, TfAD1 in Tritrichomonas Foetus, a Cattle Pathogen.*"

11:00 AM **Coffee Break**

COLLEGE OF ENGINEERING — Dean Brian Craig

11:15 AM **Kalen Baker** – Major in Mechanical Engineering and Mathematics
Mentor: **Dr. Ping He**
Research in Mechanics and Physics
"*Theoretical Research on Sintering of Metals based on Results of Molecular Simulations.*"

11:30 AM **Alexander Bahrim** – Major in Electrical Engineering
Mentors: **Dr. Gleb Tscheslavski** and **Dr. Cristian Bahrim**
Research in Electrical Engineering and Physics
"*Development and Assessment of Hardware Model for Studying the Mechanism of Regenerative Braking System (RBS).*"

11:45 AM **Cymone Houston** – Major in Civil Engineering
Mentor: **Dr. Thinesh Selvaratnam**
Research in Environmental Engineering
"*Biological Treatment of Produced Water.*"

12:00 PM **Melissa Tan** – Major in Civil Engineering
Mentor: **Dr. Thinesh Selvaratnam**
Research in Environmental Engineering
"*Studying the Extracellular Polymeric Substances of Galdieria sulphuraria As Flocculation Aid for Improving Algal Harvesting Efficiency.*"

12:15 PM **Gabriel West** – Major in Mechanical Engineering
Mentors: **Dr. Sushil Doranga** and **Dr. Jenny Zhou**
Research in Mechanical Engineering
"*Vibration Response Prediction of Printed Circuit Boards used in the Transportation Industry.*"

12:30 AM **Lunch Break**

12:55 PM **Group Photo (in the Quad by the Setzer Center)**

Poster Session I 1:00 – 1:30pm

Chair: Dr. Gina Hale

Plenary Session – Exercise Medicine and Science

Chair: Dr. Cristian Bahrim

COLLEGE OF EDUCATION AND HUMAN DEVELOPMENT
Dean Robert Spina

1:30 PM

Damaris Thrash – Major in Exercise Science
Mentor: **Dr. Shannon Jordan**
"*Effects of Motivational Music on Post-Exercise Recovery.*"

1:45 PM

Poorna Menon[1], Lauren Richardson[2,3], Ramkumar Menon[4]
Mentor: Dr. Lauren Richardson
[1]University of Texas at Austin
[2]Department of Obstetrics & Gynecology, Division of Maternal-Fetal Medicine & Perinatal Research, The University of Texas Medical Branch at Galveston
[3]Department of Neuroscience, Cell Biology & Anatomy, The University of Texas Medical Branch at Galveston, Galveston, TX 77555 USA
[4]Department of Obstetrics & Gynecology, Division of Maternal-Fetal Medicine & Perinatal Research, The University of Texas Medical Branch at Galveston
"*The Effects of Extra Cellular Matrix Collagen Rigidity on 3-Dimensional Cultures of Fetal Membrane Cells*"

2:00 PM

Summer Intern of the IEEM Summer Internship Program
Zaid Mohammed
Institute of Exercise and Environmental Medicine,
7232 Greenville Ave, Dallas, TX 75231
Supervisor: Dr. Craig Crandall, Director of the Thermal and Vascular Physiology Laboratory and Professor of Internal Medicine at UT Southwestern Medical Ctr.
Collaborators: Dr. Joseph Watso, Dr. Luke Belval, and Dr. Josh Foster.

2:15 PM

Dr. Joseph C. Watso
University of Texas Southwestern Medical Center
7232 Greenville Ave, Room 330, Dallas, TX 75231
Mentor: Dr. Craig Crandall
"Adults with well-healed burn injuries have reduced pulmonary function decades after injury."

Afternoon Breakout Sessions

Breakout Session A1 2:30 – 3:30pm

Chair: Dr. Ian Lian – Archer 107

2:30 PM

Doctoral Research - Advanced
Manthan Shah – Doctoral candidate at Lamar University, Philip M. Drayer Department of Electrical Engineering
Mentor: Dr. Cagatay M. Tokgoz and Dr. Jing Zhang
"Efficient Radar Signature Prediction for Electrically Large Conducting Platforms Using Parallelization on the RED HPC Cluster at Lamar University."

2:45 PM

Doctoral Research - Advanced
Nader Madkour – Doctoral candidate at Lamar University, Department of Industrial Engineering
Mentor: Dr. Berna Eren-Tokgoz
"Drone and Artificial Intelligence-based evaluation of Debris for Waterways and Ports."

3:00 PM

Doctoral Research - Advanced
Premkumar Ravishankar – Doctoral candidate at Lamar University, Department of Industrial Engineering
Mentor: Dr. Berna Eren-Tokgoz
"Resilience framework of Pipeline Infrastructure Utilizing Drones and Image Processing Algorithm."

3:15 PM

Doctoral Research - Advanced
Yi Liu / Ruobing Zhao (presenter) – Doctoral candidates at Lamar University, the Department of Industrial and System Engineering
Mentors: Dr. Yueqing Li
"Effects of Directional Road Signs Combinations and Language Unfamiliarity on Driving Behavior."

3:30 – 3:45 PM **Coffee Break**

Breakout Session B1 2:30 – 3:30pm

Chair: Dr. Mamta Singh – Archer 108

2:30 PM

Graduate Research
Saumi Patel – Master candidate at Lamar University, the Department of Industrial and System Engineering
Mentors: Dr. Yueqing Li, Dr. Xinyu Liu
"Human Factor and Ergonomics evaluation of In-Vehicle Touchscreen Infotainment display."

2:45 PM

Graduate Research
Tyler Nelson – PhD program in the Applied Physics at Rice University, the Gustavsson Laboratory
Mentor: Dr. Anna-Karin Gustavsson
"Live-cell 3D Super-resolution Imaging."

3:00 PM

Graduate Research
Roberto Obregon – Master candidate at Lamar University, Department of Chemistry and Biochemistry
Mentor: Dr. Paul Bernazzani
"Analysis of Oxidized Low-Density Polyethylene to Determine the Possibility of a Recycle Stream."

3:15 PM

Graduate Research
Dylan Palmer – Master candidate at the Colorado School of Mines, Mechanical Engineering
Mentor: Dr. Brian G. Thomas
"Finite Element Analysis of Defects in Continuously Cast Steel Slabs."

3:30 – 3:45 PM **Coffee Break**

Breakout Session A2 3:45 – 4:30pm

Chair: Dr. Thinesh Selvaratnam – Archer 107

3:45 PM

Ruobing Zhao – Doctoral candidate at Lamar University, the Department of Industrial and System Engineering
Mentors: Dr. Yueqing Li
"A Preliminary Assessment of Driver's Workload in Partially Automated Vehicles and Conventional Vehicles."

4:00 PM

Prasad Pawar – Doctoral candidate at Lamar University, Nanobiomaterials and Bioprocessing Laboratory (NABLAB), Research in Chemical Engineering, Department of Chemical Engineering
Mentor: Dr. Clayton S. Jeffryes
"Microwave-assisted demulsification of tight crude oil-water emulsions."

4:15 PM

Rishi Bharadwaj – Doctoral candidate at Lamar University, Philip M. Drayer Department of Electrical Engineering
Mentor: Dr. Cristian Bahrim
"Energy suppression of a laser beam on a glass surface assisted by a stronger coupling laser."

Breakout Session B2 3:45 – 4:30pm

Chair: Dr. Matt Hoch – Archer 108

3:45 PM

Undergraduate Research
Vishal Mundodi
Department Microbiology and Molecular Genetics, University of Texas Medical School at Houston, 6431 Fannin St. Houston, TX 77030
Mentor: Dr. Peter J. Christie
"Targeted Plasmid Delivery Using Surface Displayed Adhesions."

4:00 PM

Doctoral Research - Advanced
Nurul Azam – PhD candidate at the Auburn University, Department of Electrical and Computer Engineering
Mentor: Dr. Masoud Mahjouri-Samani
"Laser Based Synthesis of Two-Dimensional (2D) Quantum Materials."

4:15 PM

Graduate Research
Tyler Martin – PhD candidate at Rice University, Department of Mechanical Engineering
Mentor: Dr. Daniel Preston
"Powering Soft Wearable Devices Using Body Heat."

Poster Session II 4:30 – 5:30pm

Chair: Dr. Clayton Jeffryes

Special Session 5:30 – 5:45pm

Presenter: Dr. Keivan Davami

Research in the Department of Mechanical Engineering at the University of Alabama - Tuscaloosa

Keivan Davami

Assistant Professor, University of Alabama

PhD, Nanotechnology, Postech University
MS, Mechanical Engineering, University of Tehran
BS, Mechanical Engineering, University of Najad Abad

Dr. Davami joined the department of mechanical engineering at the University of Alabama as an Assistant Professor in summer 2019 after serving as an assistant professor in the department of mechanical engineering at Lamar University. Prior to joining Lamar, he was a research fellow at the U.S. Naval Research Laboratory and a postdoctoral research scholar at the University of Pennsylvania. Dr. Davami's research interests are focused on advanced manufacturing and surface modification techniques, in particular, additive manufacturing and laser shock peening, as well as metamaterials and micro- and nano-fabrication. His research on plate metamaterials and self-healing additively manufactured materials received national and international media attention. Dr. Davami's research has been supported by federal agencies such as the National Science Foundation, the Department of Defense, the Department of Energy, as well as state funding organizations. He has been a PI and Co-PI in over $11M funded projects. He won an NRC Research Associateship award from the National Academies of Sciences for a proposal related to the phase transformations of materials.

Recognition of our guest speaker Dr. Robert Nicholas Lanning

OFFICE OF UNDERGRADUATE RESEARCH
LAMAR UNIVERSITY

Certificate of Appreciation

Dr. Robert Nicholas Lanning

Research Physicist, Air Force Research Laboratory
Directed Energy Directorate - Space Electro-Optics Division

In recognition for his outstanding talk at the
9th Annual Texas STEM Conference

Cristian Bahrim, Ph.D.
Acting Director of O.U.R.

October 30th, 2021

Brenda Nichols, Ph.D.
Provost and VPAA

Recognition of Dr. Peggy Doerschuck, Distinguished University Professor Emerita of Computer Science

OFFICE OF UNDERGRADUATE RESEARCH
LAMAR UNIVERSITY

Recognition of Service

To Professor Peggy Doerschuk, Ph.D.

Distinguished Professor Emerita and University Professor

for mentoring and inspiring generations of STEM students and
for leading The Award-winning STARSTEP program at Lamar University

Cristian Bahrim, Ph.D.
Acting Director of O.U.R.

Brenda Nichols, Ph.D.
Provost and VPAA

Certificate offered on Thirtieth of October 2021 at the Nineth Texas STEM Conference

Award Winners

Best SURF Presentations

First place

Alexander Bahrim
Research in Electrical Engineering and Physics
"*Development and Assessment of Hardware Model for Studying the Mechanism of Regenerative Braking System (RBS).*"

Second place

Carissa Slaughter
Research in Microbiology and Parasite Immunology
"*Trichomonas vaginalis induced Toll-like Receptor Gene Expression in Cervical Epithelial Cells.*"

Third place

Gabriel West
Research in Mechanical Engineering
"*Vibration Response Prediction of Printed Circuit Boards used in the Transportation Industry.*"

Best Undergraduate Presentation in non-OUR Sponsored Research

First place

Poorna Menon
Research in Cell Biology
"*The Effects of Extra Cellular Matrix Collagen Rigidity on 3-Dimensional Cultures of Fetal Membrane Cells.*"

Second place

Vishal Mundodi
Research in Microbiology
"Targeted Plasmid Delivery Using Surface Displayed Adhesions."

Third place

Talon Weaver
Research in Space Science
"Toroidal magnetic clouds in solar wind."

Best Master Level Oral Presentation

Tyler Martin
Research in Material Science
"Powering Soft Wearable Devices Using Body Heat."

Award Winners

Best Master Level Poster Presentation

First place: **Caitlyn Clark**
Research in Chemistry
"Physical Tuning of Photo-Chemical Response in Biverdazyl Biradicals."

Runner-up: **Anthony Osu**
Research in Microbiology and Parasite Immunology
"Trichomonas vaginalis induced Toll-like Receptor Gene Expression in Cervical Epithelial Cells."

Runner-up: **Fatih Omeroglu**
Research in Industrial and System Engineering
"Effect of Background Music on Task Performance."

Best Doctoral Presentation of Advanced Research

First place: **Ruobing Zhao**
Research in Industrial and System Engineering
"Effects of Directional Road Signs Combinations and Language Unfamiliarity on Driving Behavior."

Runner-up: **Nader Madkour**
Research in Industrial and System Engineering
"*Drone and Artificial Intelligence-based Evaluation of Debris for Waterways and Ports."*

Best Doctoral Presentation of In-Progress Research

Prasad Pawar
Research in Nanobiomaterials and Bioprocessing
"Microwave-assisted demulsification of tight crude oil-water emulsions."

Congratulations!

A big "Thank You!" to all judges for their time in assessing student presentations at the 9th Texas STEM Conference

Advisory Board members:

Dr. Robert Kelley Bradley

Dr. Bianca Easterly

Dr. Gina Hale

Dr. Matt Hoch

Dr. Alyse Jordan

Dr. Xiangyan Sunny Lei

Dr. Nicki Michalski

Dr. Lekeitha Morris

Dr. Gevorg Sargsyan

Dr. Thinesh Selvaratnam

Dr. Dorothy Sisk

Dr. Mamta Singh

Dr. Robert Worley

Colleagues Faculty:

Dr. Paul Bernazzani

Dr. Berna Eren-Tokgoz

Dr. Sushil Doranga

Dr. Ping He

Dr. Xingyu Liu

Dr. Cagatay Tokgoz

OUR liaisons:

Dr. Ian Lian

Dr. Clayton Jeffryes

Dr. Sujing Wang

Dr. Chun-Wei Yao

OFFICE OF UNDERGRADUATE RESEARCH
LAMAR UNIVERSITY

Posters

Posters to be set up after 12:00 p.m. Friday 10/29
or 8:00 a.m. Saturday 10/30

Poster session I : 1:00 – 1:30 PM
Poster session II : 4:30 – 5:15 PM

Chairs: Dr. Gina Hale and Dr. Clayton Jeffryes

Poster 1

Graduate Research

Presenter: Claire Elizabeth Alexander

Mentor: Dr. Maryam Vasefi
Department of Biology, Lamar University
Research in Biology

Cannabidiol (CBD) Signaling through Serotonin Receptor Subtype 1 (5-HT1AR)

Poster 2

Graduate Research

Presenter: Maryam Bahrami

Co-author: Lac Nguyen
Mentor: Dr. Robert Bradley
Department of Industrial and Systems Engineering, Lamar University
Research in Nanotechnology

Progress in Carding Single Wall Carbon Nanotubes

Poster 3

Graduate Research

Presenter: Caitlyn Clark[1]

Co-author: Emily Ingram[1]
Mentors: Ozge Gunaydin-Sen[1], David Brook[2]
[1]Department of Chemistry and Biochemistry, Lamar University
[2]Department of Chemistry, San Jose State University, San Jose, CA 95192
Research in Chemistry

Physical Tuning of Photo-Chemical Response in Biverdazyl Biradicals

Poster 4

Undergraduate Research

Presenter: Jesus Esquivel[1]
Co-authors: T. Thuy Minh Nguyen[1], Mien Jao[2], and Paul Bernazzani[1]
[1]Department of Chemistry and Biochemistry, Lamar University
[2]Department of Industrial and Environmental Engineering

Research in Forensic Chemistry

Remediation of Contaminants in Dredged Soil: A Gas Chromatography Analysis

Poster 5

Graduate Research

Presenter: Md Abrar Jamil[1]
Co-authors: Gregory D. Twing [1,2]
Mentors: Suying Wei[1], and Sylvestre Twagirayezu[1]
[1]Department of Chemistry & Biochemistry
[2]Department of Chemical Engineering, Lamar University

Research in Chemistry

Evaluation of Molecular Rotational Resonance Technique for Fast Monitoring Sulfur Dioxide in Ambient Air

Poster 6

Undergraduate Research

Presenter: Mariela Marquez
Mentors: Dr. Paul Bernazzani and Dr. T. Thuy Minh Nguyen
Department of Chemistry and Biochemistry, Lamar University

Research in Forensic Chemistry

Gas Chromatographic Analysis of the Effect of Aniline on Plant Cell Lipids

Poster 7

Undergraduate Research

Presenter: Poorna Menon[1]
Co-authors: Lauren Richardson[2,3], Ramkumar Menon[4]
[1]University of Texas at Austin
[2]Department of Obstetrics & Gynecology, Division of Maternal-Fetal Medicine & Perinatal Research, The University of Texas Medical Branch at Galveston
[3]Department of Neuroscience, Cell Biology & Anatomy, The University of Texas Medical Branch at Galveston,
[4]Department of Obstetrics & Gynecology, Division of Maternal-Fetal Medicine & Perinatal Research, The University of Texas Medical Branch at Galveston

Research in Cell Biology

The Effects of Extra Cellular Matrix Collagen Rigidity on 3-Dimensional Cultures of Fetal Membrane Cells

Poster 8

Graduate Research

Presenter: Fatih Omeroglu

Mentor: Dr. Yueqing Li

Department of Industrial and Systems Engr, Lamar University

Research in Industrial Engineering

Effect of Background Music on Task Performance

Poster 9

Graduate Research

Presenter: Anthony Osu

Mentor: Maryam Vasefi

Department of Biology, Lamar University

Research in Biology

Glutamate Receptor Interactions in Alzheimer's Disease

Poster 10

Undergraduate Research

Presenter: Joshua Smith[1]

Mentor: Sylvestre Twagirayezu[1]

Co-authors: Zhao Jianbao[2] and Brant Billinghurst[2]

Department of Chemistry and Biochemistry, Lamar University

[2]Canadian Light Source Inc, Saskatoon, SK S7N 2V3

Research in Biochemistry

Synchrotron-based Attenuated Total Reflection (ATR) Infrared Spectroscopy of Artificial Gasoline Blend

Poster 11

Undergraduate Research

Presenter: Talon Weaver[1]

Mentors: Dr. Evgeny Romashets[2] and Dr. Cristian Bahrim[2]

[1]Department of Civil and Environmental Engineering, Lamar University

[1]Department of Physics, Lamar University

Research in Space Science

Toroidal magnetic clouds in solar wind

Oluwatomisin Egbewale

Major in Computer Science

Mentor: Dr. Xingya Liu and Dr. Sujing Wang

Research in Computer Science

Department of Computer Science

Security Evaluation of a Biometric Authentication System

During the Spring semester of my freshman year in college, I submitted a research proposal to Lamar University's Office of Undergraduate Research. The proposal was accepted. Within a few months, I was set to carry out a major academic project in the summer of 2021. Prior to the time, I had no experience in elaborate research, so I approached the summer with a mixture of excitement, worry, and hope.

From the onset, I knew the major challenge I had was an insufficiency in knowledge. Related academic projects I had previously carried out revolved around collecting data from a population and then deducing facts from the statistics. This rarely ever tasked my knowledge; the information needed was usually a 'given'. But my summer 2021 research was established in an unfamiliar direction. I put forward a proposal to explore the vulnerabilities of a biometric authentication system. More so, my aim was to have results that would be contributory to the cybersecurity and Computer Science field at large. Similar projects had been carried out by individuals and organizations in the past, but the approach was usually based on exploitation methods from outside the biometric-enabled device. This approach almost always involved cloning/retrieving the actual fingerprint or other biometric of an authorized user. But my intention was to exploit a biometric authentication system from within. I knew this would involve writing and understanding lines of code that were beyond my level of knowledge at the time, but for some good reason, most likely my passion, the challenge appealed to me.

Of course, the most visible asset I gained in the research period was knowledge. I ended the summer with more confidence in my knowledge than at the start of the summer. Also, given the task and the apparent *novelty* of the idea, I needed creativity to achieve the aim of the proposal. I had a clear idea of what I wanted to accomplish, but in addition to knowledge, there was need for a level of inventiveness on how to route the journey. This is certainly a skill I acquired as the summer unfolded: imagination. I am confident that I spent more time thinking about a way forward than I did working in the Computer Science laboratory – way more time. Most of the additional skills I gained are abstract but essential; two of them were patience and endurance. I specifically

mention these two skills because we (I and my mentors) did not start making any real progress until mid- July. This was late for a project which had a runtime from June 2 – August 10.

Prior to the project, my career goal was well defined along the lines of cybersecurity, so I chose a research path that would complement this ambition. The research opened me up to the dynamics and intelligence involved in the field: hackers constantly find new methods of breaching system software; security experts continuously do the same but for the purpose of patching up perceived vulnerabilities in the software. The cycle is unending. This area of Computer Science demands a need to always learn and relearn; that was my experience in the summer. So overall, my undergraduate research reinforced my interest in cybersecurity.

Our research was not without results. Perhaps the most important result was that we were able to intercept the communication channel within a biometric authentication system and capture any information that would be transmitted at the instance of a user's authentication on a biometric-enabled device. This was essentially the breakthrough moment in our research. We strongly believe our finding can potentially unlock *any* biometrically locked device. After this finding, we encountered obstacles that prevented us from making a full discovery and proving our belief. We would have set out to confront them, but time constrained us. We needed to:

- develop a filter to 'sieve' out irrelevant information that may have been captured, as not all the transmitted information would be related to the user's biometrics.
- develop a program to automatically store the captured information in a local file so that the information can be sent out anytime to unlock the same device.
- develop a program to send out the captured information in the same sequence it came in so that the information can be accepted by the device.

Several dynamics to the above have been omitted, as they are not explainable within two pages.

Summarily, the research was an enriching experience, academically and career-wise. As has been indicated already, a continuation of the project is possible, hopefully at a much higher level of my academic journey. I also plan to present the results of the research at the Texas STEM (Science, Technology, Engineering and Mathematics) conference coming up in Fall 2021 and at the Annual Undergraduate Research Expo at Lamar University in Spring 2022. My gratitude goes to my two mentors, Dr. Sujing Wang and Dr. Xingya Liu, as well as the Office of Undergraduate Research.

Callan Noak

Major in Computer Science

Mentor: Dr. Sujing Wang

Research in Computer Science

Department of Computer Science

Designing Regression Models for Covid-19 Risk Prevention

Abstract

The purpose of this project is to create regression models for the number of new daily cases and new daily deaths due to Covid-19 in each state in the US. These models can then be used to analyze the current pandemic as well as provide valuable information for future pandemics. The information provided by our models can allow people to make more informed decisions that has the potential to save more lives in the future. The models for this project were created and selected using a combination of statistical analysis and data science.

The data for this project was downloaded from John Hopkins University public dataset. The timeframe for the data is between Jan 23rd, 2020 and July 28th, 2021. We used different Python data modeling packages to model and analyze our data. The two major packages used for this project was Pandas and Sklearn. The main challenge of this project was designing a regression model that best fits the data. There are many regression models in literature. We chose linear, polynomial, decision tree, and support vector regression. We measured the efficiency of each model using the Mean Squared Error (MSE) and the Coefficient of Determination (R2). Both the MSE and R2 are a measurement of how close the model fits the data. The MSE is an absolute measurement and R2 is a relative measurement. For MSE, the smallest value indicates the best fit. For R2, the value closest to 1 indicates the best fit.

Results

The first model we developed is the linear regression model. A linear regression model is best used when the data seems to follow a straight line. Unfortunately, the COVID-19 data had many curves, therefore the linear model did not fit the data well. The linear model for the new daily cases for the state of Texas is shown in Figure 1.

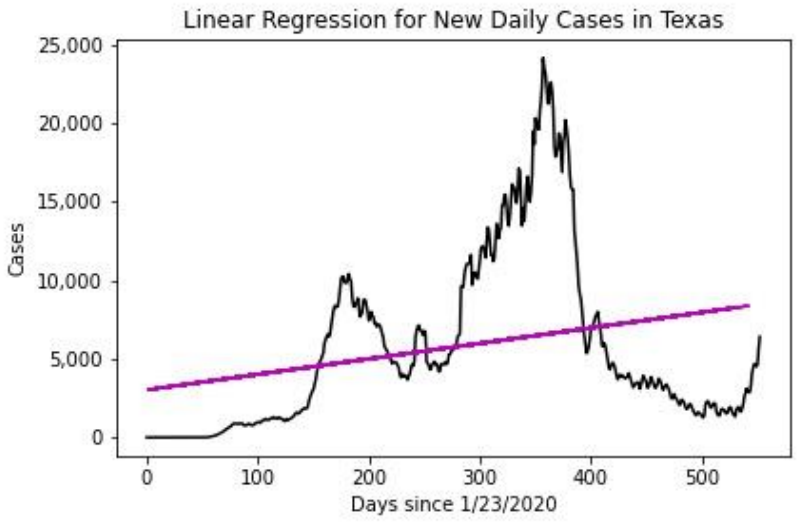

***Figure 1**: Linear Regression for Daily Cases in Texas*

The second model developed is the polynomial regression model. We also introduced a rolling average to reduce the noise of our data. We took a rolling average of 14-days to create all subsequent models. The polynomial regression model was better than the linear model but still did not fit the data very well. The polynomial model for the new daily cases for the state of Texas is shown in Figure 2.

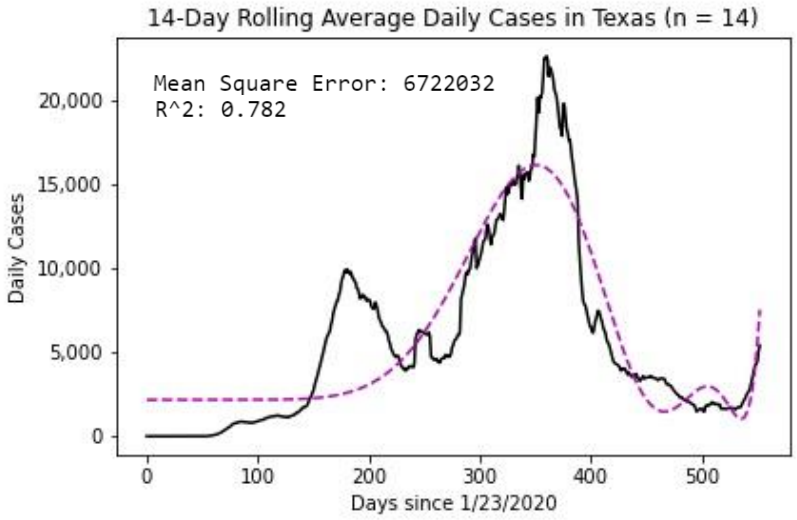

***Figure 2**: Polynomial Regression for Daily Cases in Texas*

The next model was the decision tree regression model. This model turns the data into a tree with many different nodes. All nodes are broken down into two categories, decision nodes and leaf nodes. This model fitted our data better than linear regression and polynomial regression models, The decision tree model for the new

daily cases for the state of Texas is shown in Figure 3. However, decision tree regression model might overfitting the data. One of the requirements for a good model is that it can predict other data sets in addition to the one that was used to create it. If a model is too reliant on one dataset it will not be useful for other datasets.

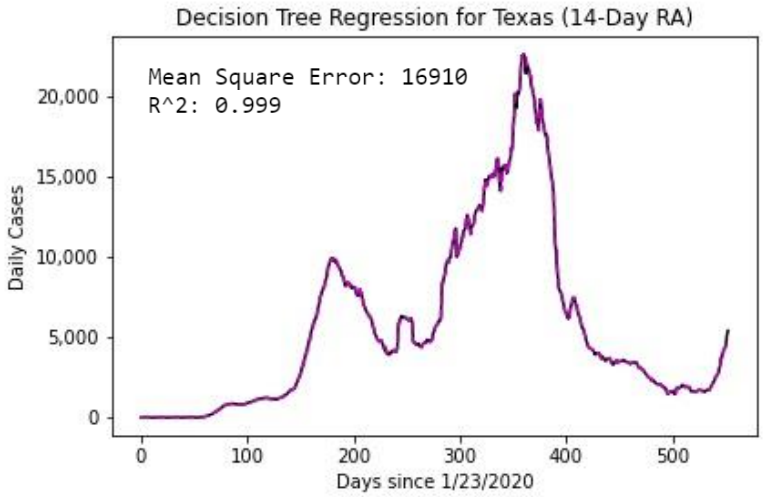

***Figure 3**: Decision Tree Regression for Daily Cases in Texas*

The final model we developed was a support vector regression model. This model allows to ignore error within a certain threshold when creating a model. The points closest to the model are the support vectors and dictate what shape the model makes. The model tries to get as many data points as possible within that error threshold. This model was the best at predicting our data with the smallest MSE and R2 closest to 1 compared with the other three models. The support vector models for the new daily cases and new daily deaths for the state of Texas are shown in Figures 4 and 5 respectively.

Conclusion

We were able to successfully develop four regression models for each chosen state in U.S.A. This research can be extended to include more countries besides the United States. It is also possible that there are even better regression models that fit the data better than the models used in this project. It would also be interesting to see if a different model would be better for the data as the pandemic progresses. We plan to continue this project and present at the STEM and other academic conferences.

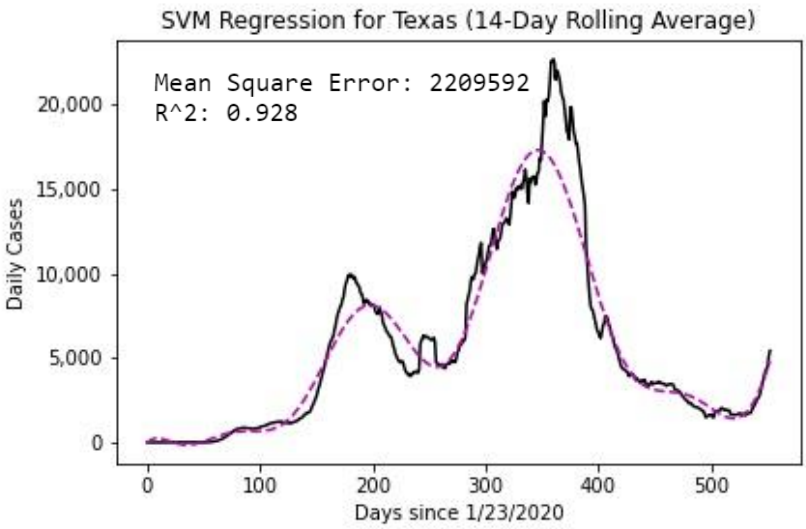

***Figure 4**: Support Vector Regression for Daily Cases in Texas*

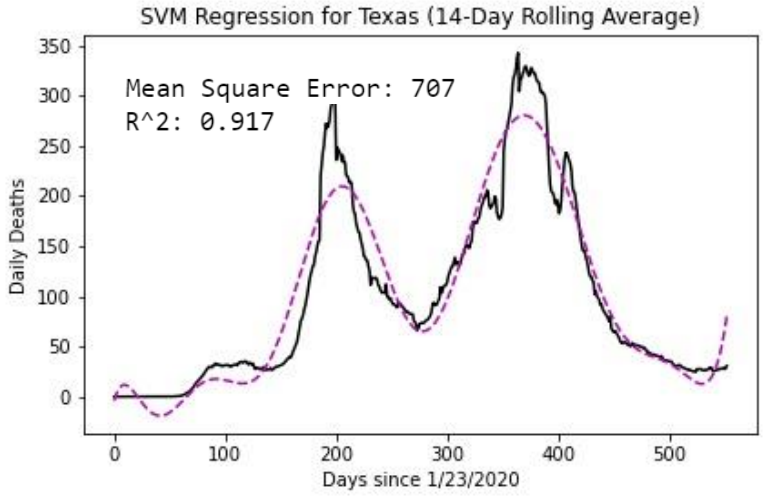

***Figure 5**: Support Vector Regression for Daily Deaths in Texas*

Nyah Sciarrilla

Major in Biology

Mentor: Dr. Matt Hoch

Research in Biology

Department of Biology

The Effect of Starch Copper Oxide Nanoparticles on Differential Growth of Microbial Populations in Aquatic Environments

Throughout my Summer Undergraduate Research Fellowship (SURF) program, I got to perform my own research project with my mentor, Dr. Matt Hoch, and in doing so I developed into a stronger researcher. My research involves the effects of starch copper oxide nanoparticles (SCuONPs) on the composition and function of microbial communities in rice crop water. This is important because mineral copper oxide nanoparticles (CuONPs) are currently used as herbicides and fungicides in agriculture, but they can be harmful to the environment. SCuONPs are potentially a cleaner, more effective alternative, but their effects on microbial communities are not known. I hypothesized that bacterial taxa in the rice crop water will respond differently to SCuONPs, with some stimulated by organic components and others inhibited by CuO.

To test this hypothesis, rice crop water was collected, distributed into four replicates for each treatment, then incubated under ambient condition for a total of seven days. The treatments used were a control (unamended), low concentration of mineral-only CuONPs (30 µM Cu), low concentration SCuONPs (30 µM Cu), and high concentration SCuONPs (300 µM Cu). Every day, bacterial count samples were preserved in 2% formaldehyde and α-glucosidase activity was measured by fluorometry to assess starch degradation. On day one, day four, and day seven, samples were assayed for bioorthagonal noncanonical amino acid tagging (BONCAT) to assess levels of protein synthesis and filtered for subsequent metagenomic DNA extraction and 16SrDNA sequencing to determine bacterial taxa. The density of SYBR Green stained bacteria and BONCAT fluorescence intensity were determined flow cytometry (FCM). High and low BONCAT intensity populations were then collected by fluorescence activated cell sorting (FACS), filtered, and DNA extracted. All DNA extracts were sent for metagenomic 16Sr DNA sequencing. Sequence analysis will use QIIME2 workflows to assess the relative population composition of the total microbial communities, as well as populations with lower and higher growth, based on BONCAT-FACS.

Prior to performing the main experiment to test my hypothesis, I had to develop and test all my methods using pure cultures of bacteria and aquatic bacterial communities in John Gray Pond water. Most challenging was the BONCAT procedure, whose application to natural bacterial communities is still fairly new. The BONCAT procedure was first tested on Staphylococcus epidermidis cultures, using stationary phase cells as a control and cells stimulated in growth by amending to 10 mM glucose for 4 hours. The BONCAT procedure did indeed work, as the population amended with glucose showed increased activity compared to the control as determined by epifluorescence microscopy and FCM cell-specific fluorescence (Fig. 1).

For the main experiment, both the bacterial density (Fig. 2) and DNA extract concentrations (not shown) followed similar trends among treatments over time. The high concentration of SCuONP treatment showed significant cell death and growth inhibition, and the mineral CuONP treatment did not reach the maximum bacterial density in the control and low SCuONP treatments by Day 4 (Fig. 2). There was a decrease in cell density after four days in the control and lower CuONP treatments, which is consistent mortality due to viral lysis or heterotrophic protists feeding on the bacteria rather than Cu toxicity alone. (Fig. 2). The flow cytometer plots of forward scatter versus SYBR Green used for counting cells (Fig. 3) were generally similar in the Control and low mineral CuONP treatments, but there was some selection of higher DNA content cells in the low SCuONP treatment, possibly in response to the added organic content. However, a toxic response was evident in the high SCuONP treatment, consistent with CuO production of reactive oxygen species damaging DNA.

The α-glucosidase activity was measured each day to observe any starch degradation (Fig. 4). The low SCuONP treatment had significantly greater enzyme activity at Day 2 through Day 7 than any other treatment. The initial lag in activity for this treatment may be explained by catabolic repression due to the presence of glucose in the SCuONP preparation. The lowest enzyme activity was in the high SCuONP treatment and is consistent with both prolonged catabolic repression due to 10-fold greater glucose than in the low SCuONP treatment and CuO toxicity driven cell loss.

BONCAT analysis by FCM was performed on Days 0, 4, and 7. The Day 0 BONCAT assays and negative controls (Fig. 5) demonstrate the efficacy of the assay for protein synthesis and minimal non-specific staining. All of Day 4 and 7 BONCAT samples were analyzed, and two to three levels of cells-specific protein synthesis (growth rate proxy) were cell sorted by FCM-FACS (Fig. 6). Both treatments with the organic SCuONP had a population of fast-growing populations (P3 gate) whose appearance was consistent with the 10-fold difference in concentrations. Specifically, this population appeared first in the low organic SCuONP treatment at Day 4 then disappeared by Day 7. Whereas in the high organic SCuONP treatment it sustained

itself through Day 7, when there was also a loss of all low activity (P1 gate cells). All cell sorts were filtered, DNA extracted, and are at this time in the process having the 16SrDNA of the metagenomes sequenced for bacterial taxa analysis.

When I took a microbiology course required for my biology major my freshman year of college, I developed an interest in microbiology. Through this research fellowship, I was able to delve into that interest in a way that I would not have gotten to do otherwise. I also came into college with my mindset that research was not an option for me, as I did not see myself enjoying it. After finishing my SURF project, my perspective has changed on research, and I now see that I could potentially enjoy doing more research in the future. I also learned many new techniques and skills during my research fellowship. Through this opportunity, I learned how to operate multiple instruments that I had not used before, including a flow cytometer, epifluorescence microscope, and spectrophotometer. I also got very adept at using pipets, and I got to use a repeat pipet, which I had not gotten to use before my SURF project. Lastly, through this project, I was given the opportunity to perform a fairly new technique, BONCAT, and I had to get in contact with one of the authors of the paper to do so.

Although the SURF program finished in August, I was not completely done with analysis all BONCAT results, cell sorting and DNA extractions for sequencing and bacterial community analysis. In early fall I began collaborating with Michael Shannon (BS Biology Major) for FCM-FACS of BONCAT samples. All cell sorts were then filtered, DNA extracted, and are at this time in the process having the 16SrDNA of the metagenomes sequenced for bacterial taxa analysis. We will specifically know which bacterial taxa were inhibited by CuO versus benefited from the organic constituents of SCuONPs.

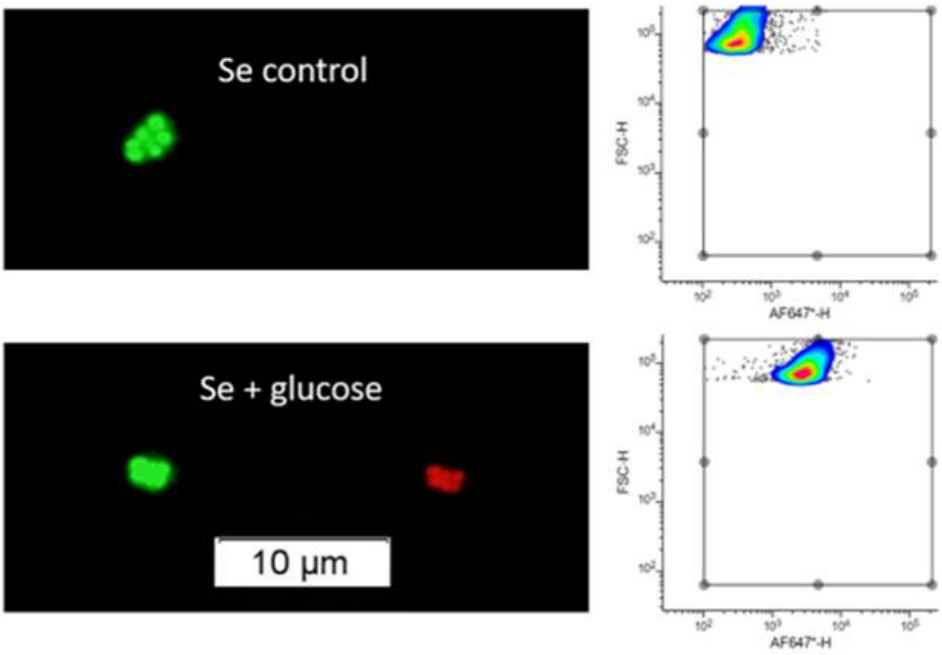

Figure 1. *Epifluorescence microscopy of SYBR Green stained and BONCAT active (red) S. epidermidis stationary phase control (top left) versus culture amended with glucose (bottom left); Flow cytometry results of forward-scatter (relative cell size) versus BONCAT AlexaFluor 647 fluorescence for control (top right) and glucose amended (bottom right) the S. epidermidis cultures.*

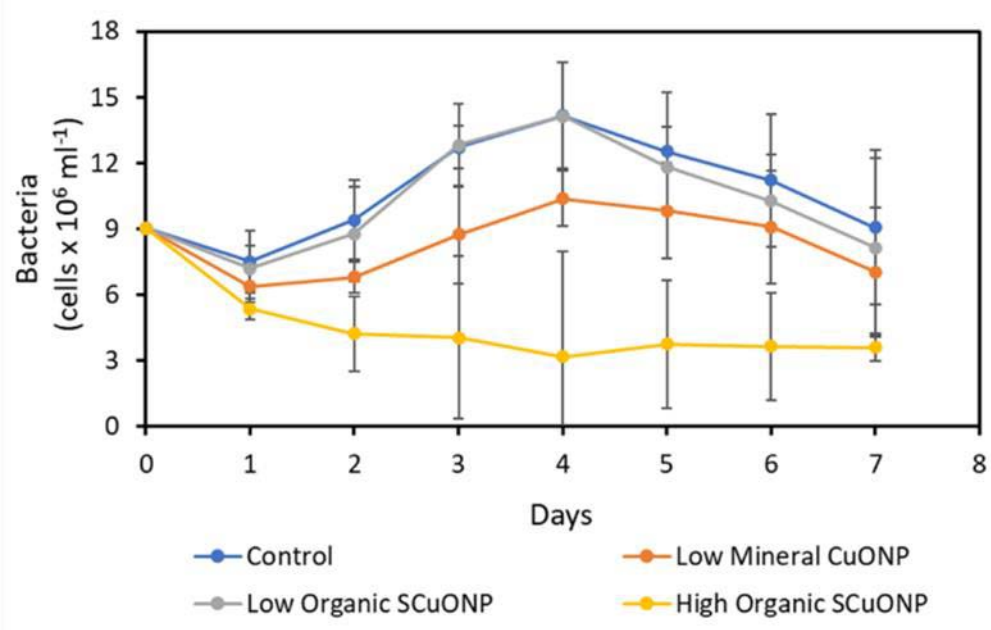

Figure 2. *Mean (± SD) daily bacterial density of each treatment determined by SYBR Green staining and FCM.*

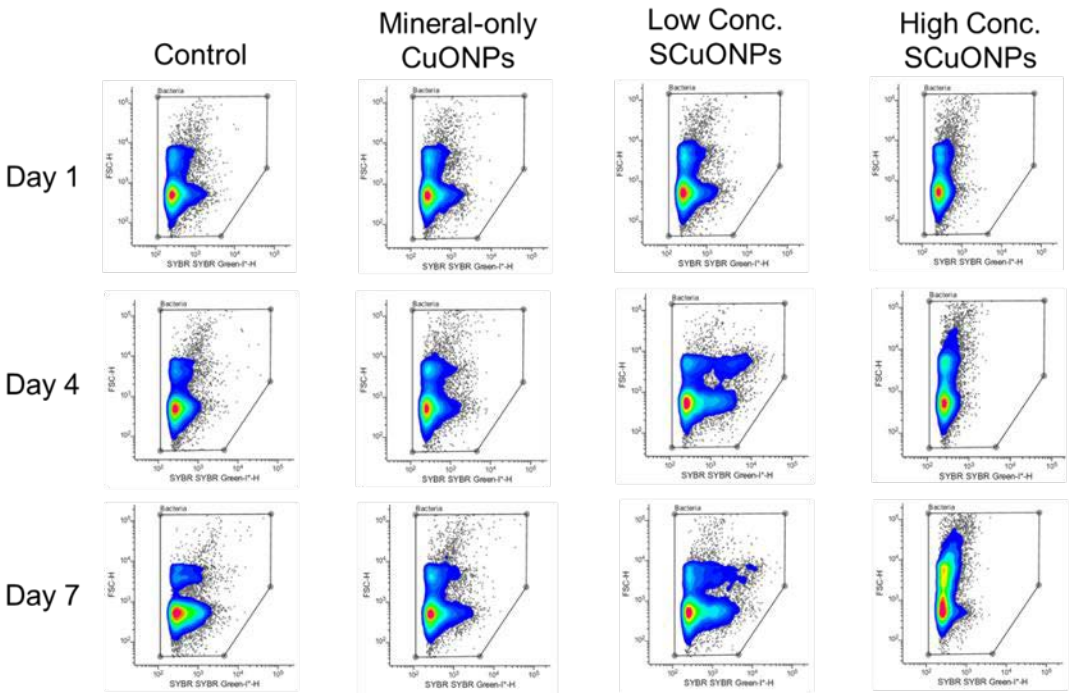

Figure 3. *Bacterial count flow cytometry plots of forward-scatter versus SYBR Green cell-specific fluorescence of DNA for replicate #4 of each treatment on days 1, 4, and 7.*

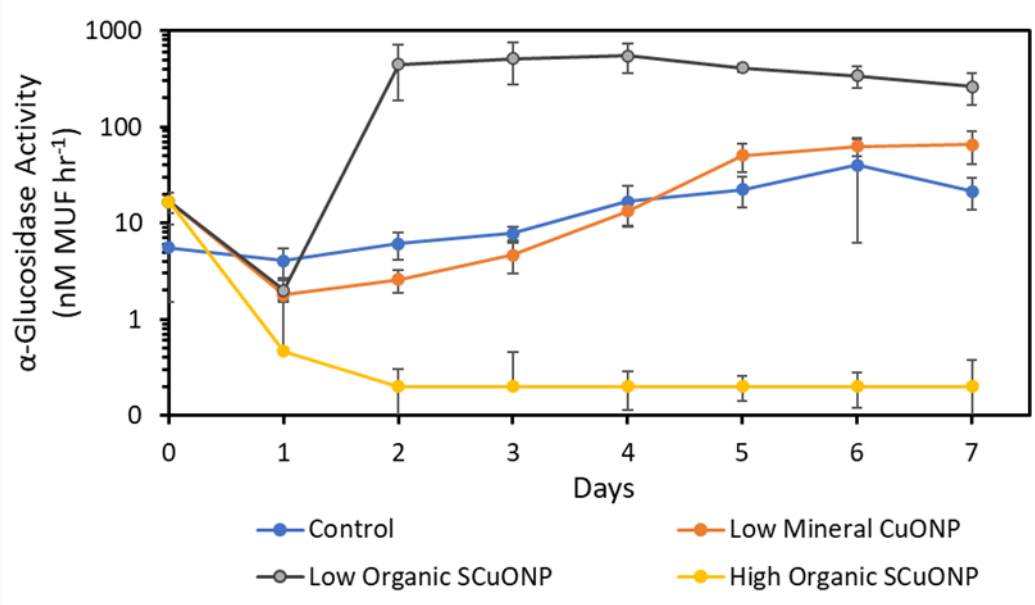

Figure 4. *Mean (± SD) daily α-glucosidase activity of each treatment.*

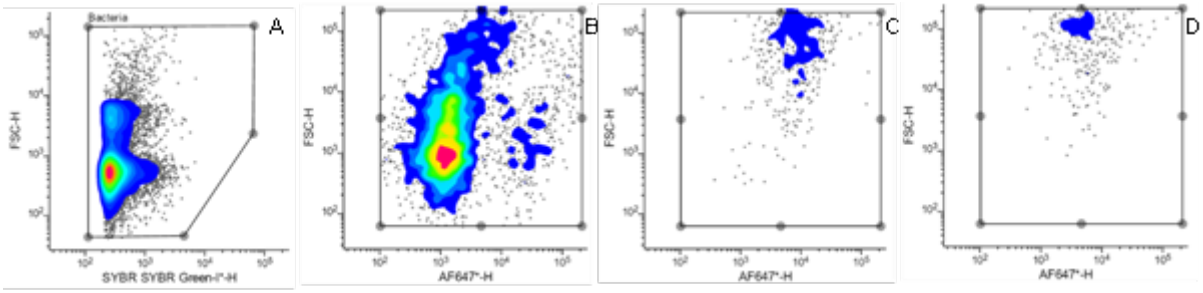

Figure 5. *Flow cytometry plots of the Day-0 rice crop water control for SYBR Green bacteria count (A) and AlexaFluor 647 dye fluorescence of the normal BONCAT assay involving incubation with the methionine analog, L-homopropargylglycine (+HPG; B), incubation with both +HPG and chloramphenicol, a prokaryotic-only protein synthesis inhibitor (C), and incubation without HPG to assess non-specific binding of AlexaFluor 647 dye (D). The PMT setting differed for FCM between SYBR and AF647 plots.*

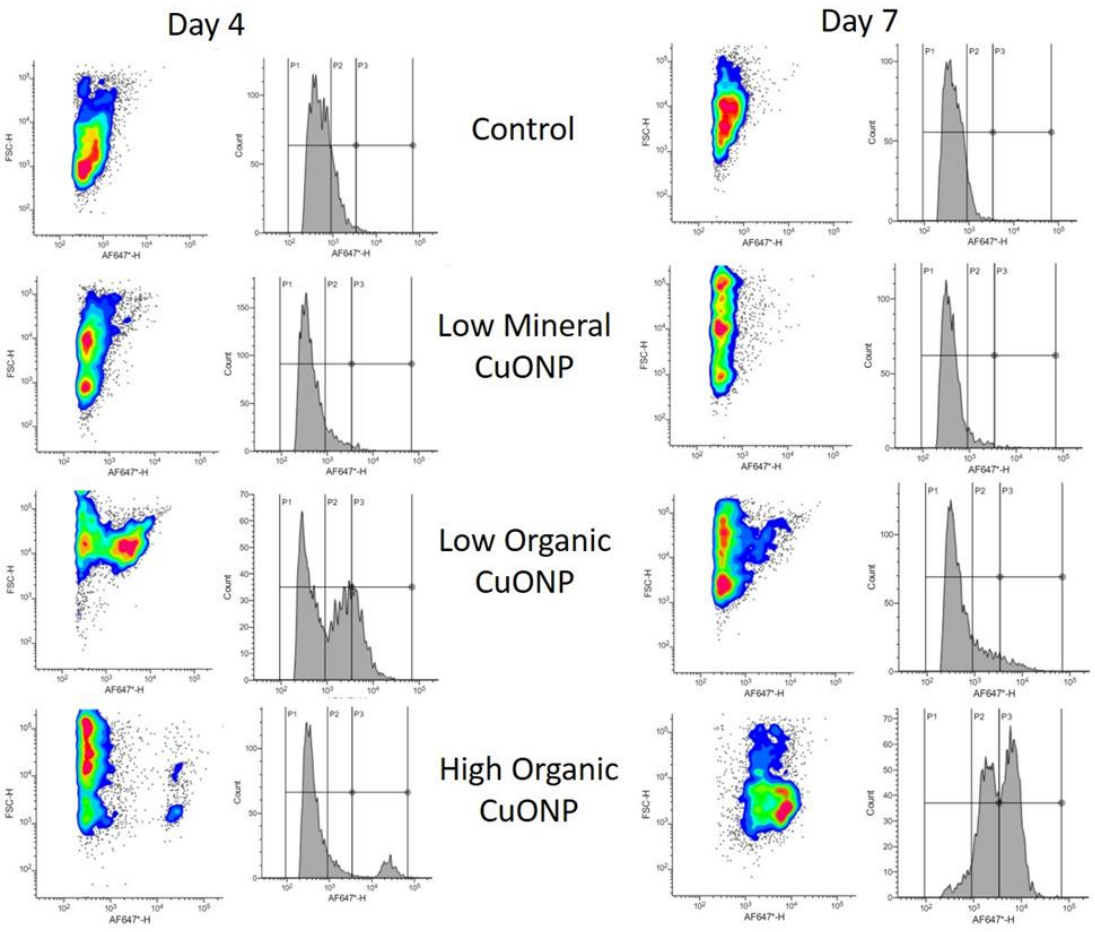

Figure 6. *Flow cytometry plots of FCM versus BONCAT-AF647 fluorescence and the histogram of the latter with three sorting gates, P1, P2, P3, of increasing cell-specific protein synthesis of control and three treatments for Day 4 and Day 7 samples.*

Carissa Slaughter

Major in Biology

Mentor: Dr. Ashwini Kucknoor

Research in Microbiology and Parasite Immunology

Department of Biology

Trichomonas vaginalis Induced Toll-like Receptor Gene Expression in Cervical Epithelial Cells

Research Hypothesis

During the 2021 Lamar University Summer Undergraduate Research program we were able to determine gene expression of Toll-Like receptors in cervical epithelial cells, understand cytokine expression, compare differences in cytokine responses, analyze TLR activation, study innate immune responses induced by *Trichomonas vaginalis*, and understand the pathways that could provide potential targets against *Trichomonas* infections for chemotherapy.

Data Analysis - Development of the Project

Parasites

Trichomonas vaginalis is a pear or circular shaped unicellular protozoan contracted through venereal transmission during sexual contact in intercourse and causes the Trichomoniasis infection in their definitive host – humans (Schumann and Plasner, 2020; Shiadeh, *et al*., 2016). Extracellular trichomonas adheres to the vaginal epithelium which disintegrates the tissue creating an immune response while also exponentially reproducing by longitudinal binary fission, affecting both the vaginal microbiota and immunity of the host (CDC, 2017; Mercer and Johnson, 2018). The nutrients *Trichomonas vaginalis* needs for survival, vaginal glycogen, are taken by feeding on the epithelial tissue by the trogocytosis mechanism where the protozoan nibbles or will completely phagocytosize the lymphoid cells (Coleman, *et al*., 2013; Mercer and Johnson, 2018). These pathogens are categorized by four flagella which appear to be amphitrichous, however are lophotrichously flagellated with an axostyle, ranging in size of 5 micrometers to 32 micrometers. Unlike organisms with mitochondria, trichomonas has hydrogenosomes creating their ATP and hydrogen, and *Trichomonas vaginalis* is unable to survive outside

of a human host as there are no existing intermediate host (Shiadeh, *et al*., 2016). In the United States trichomonas is the highest transmitted sexually transmitted parasite that is not a virus (Tsevat, *et al*., 2017). 7.4 million cases are diagnosed every single year and given its' name, *Trichomonas vaginalis*, infects mostly women, but also infects men, and in both cases most times, one in every two women, the host is asymptomatic (Coleman, *et al*., 2013; Gunn and Pitt, 2012; Mercer and Johnson, 2018). As a self-diagnosis, change in discharge color as in green or unusual textures may indicate the need for further inspection by a gynecologist or urologist to diagnose the infection. For clinical diagnostic testing there are three main tests: one – during a pelvic exam, a swab will collect specimen culture from the infected person to be viewed on a wet-mount with light microscopy, 2 - rapid antigen testing, and 3 – nucleic acid molecular tests (Coleman, *et al*., 2013). Unfortunately, because the host does not know they are infected the parasite infection becomes chronic, which leads to further long-term issues. *Trichomonas vaginalis* has a relation with other sexually transmitted diseases such as a proneness to Human Immunodeficiency Virus and other additional risks include having other sexually transmitted diseases, multiple sex partners, or misusing intravenous drugs (Shiadeh, *et al*., 2016). In the genital tract trichomonas can cause deformities, cervical neoplasia which are new masses on the cervix, and inflammation of the uterus and vagina in women causing pelvic inflammatory disease (Coleman, *et al*., 2013). The protozoan can also infect the upper genital tract leading with 30% giving salpingitis, or inflammation in the fallopian tubes, in women (Tsevat, *et al*., 2017). During pregnancy, the trichomonas parasite can cause low birth weight as well as rupture of the membranes resulting in premature delivery (Shiadeh, *et al*., 2016). Infertility in women with a history of *Trichomonas vaginalis* increase the likelihood of infertility twice as much (Gunn and Pitt, 2012) and treatment to manage the protozoan is with either of the oral metronidazole, which cures nine of ten patients, or tinidazole curing closer to ten of ten patients. Prevention includes protected sex and monogamous sexual relations (Shiadeh, *et al*., 2016). During pregnancy metronidazole medicated treatment is given, and the prescription is not found to correlate with congenital deformities yet is more closely monitored (Coleman, *et al*., 2013). *Trichomonas vaginalis* elicits host inflammatory responses that promotes cell proliferation and dysregulation of cell cycle.

Figure 1. *Trichomonas vaginalis* captured from Britannica (Leu, A. L., n.d.).

Toll-like Receptors

Toll-like receptors or Innate Immune System receptors identify pathogens, to determine the molecular mechanism for host defense. There are intracellular and extracellular, which are located on the plasma membrane, receptors to focus on a response and defend the host. TLR 1, 2, 4, 5, 6 and 10 are within the cell, while TLR's 3, 7, 8, and 9 are located externally. Because Trichomonas vaginalis is located outside the vaginal epithelium and most pathogenic protozoans correlate with TLR 4, we chose to focus on Toll-like receptor 4.

Experiment

Several cell cultures, molecular and immunological techniques such as establishing parasite and HeLa cell cultures, co-culturing Parasites and Human Cell Lines (Interaction), Polymerase Chain Reactions, Reverse Transcription-Polymerase Chain Reaction, gel electrophoresis, proinflammatory cytokine response, measurement of adherence, immunohistochemistry staining, TUNEL staining, and Enzyme Linked Immunosorbent Assay were performed. Initially, the culturing of both *Trichomonas vaginalis* and the epithelial gastrointestinal and cervical cells were established. For the parasites, Tryptose-Yeast Extract Medium 1,000mL Diamond's Medium is composed of 500mL dH20, 20 grams of Tryptose, 10 grams of yeast extract, 5 grams of maltose, 1 gram of cysteine, 0.2 grams of ascorbic acid, 0.8 gm kh2po4, 0.8 grams of k2h2po4. For the complete media when growing the Trichomonas protozoan, per 50 milliliter flask, 36 mL of the Tryptose-Yeast Extract Medium, 4 mL of Horse Donor Serum, 40 microliters of Penicillin-Streptomycin or Antimycotic-Antifungal Antibiotic (and 20 microliters of additional Gentamicin are needed if the cells are contaminated with bacteria), and 500 microliters of *Trichomonas* cells are required. The Cells are then incubated in human-like conditions at 37 Celsius and 95% CO2. The epithelial cells are cultured using a different media, known as DMEM. The complete media for both HeLa and CaCo2 cells both require 5 milliliters of Fetal Bovine Serum, 45 milliliters of plain media, and 0.5 milliliters of AA-Antibiotic. For each 50mL flask, 9 milliliters of complete media, 100 microliters of AA-Antibiotic, and 500 microliters of epithelial cells were used. The epithelial cells were also cultured in the incubation system mimicking a human's carbon dioxide level and temperature. To begin the interaction of Trichomonas and the epithelial cells, counting each portion was done with a light microscope on a 5 by 5 glass slide to measure the exact number of cells. The number of cells were then calculated, with scientific notation, with a 1:3 ratio – *Trichomonas* to epithelial respectively, into microliters. The different variants of Trichomonas were then manually pipetted into the single epithelial tissue layer for the interaction. 2 mL of the Tryptose-Yeast extract, 4 mL of DMEM media along with the epithelial cells and injected Trichomonas vaginalis cells were co-cultured for either 30 minutes or two hours. Next, the flask would be trypsinized with trypsin, which is an enzyme

which removes the epithelial cells from the treated side of the flask, enabling the process of centrifugation. After the centrifugation, the remaining cells began the ribonucleic acid isolation process with Trizol, in preparation for both the polymerase chain reaction and reverse transcription polymerase chain reaction. After the amplification process was finalized, the samples sat in 4 degrees Celsius to later be analyzed with gel electrophoresis.

Results

Experiment 1 - Polymerase Chain Reaction to determine the primer annealing temperatures and TLR gene amplification. Genomic DNA from Hela Cells were isolated and verified on the gel to determine the integrity of the DNA. Next, primers corresponding to TLR genes and an internal control GAPDH genes were used to amplify the respective genes. PCR samples were verified on the agarose gel to determine the expected amplicon sizes. All primers successfully amplified the expected amplicons.

Experiment 2 – Reverse Transcription – Polymerase Chain Reaction- Total RNA was isolated from Hela cells alone and Hela cells interacted with Trichomonas cells. Total RNA was separated on gel to determine the quality. 1ug of total RNA was used in reverse transcription PCR to determine the expression of TLRs in response to Hela activation with Trichomonas cells. Results showed that TLR 4 was increased in expression when HeLa cells encountered Trichomonas, TV-123 isolate when compared to HeLa cells alone or HeLa interacted with another TV isolate TV-6.

Experiment 3 – Enzyme Linked Immunosorbent Assay- ELISA assay was performed using the supernatant collected from cell culture flasks after the interaction with Trichomonas cells. The supernatant was diluted in various ratios and used in the ELISA assay to determine the cytokine gene expression using the Iinterleukin-6, antibody. As shown in the graph below, there was an induction of IL-6 over the basal levels (~200 pg/ml) in presence of Trichomonas cells. TV123 isolate showed enhanced induction of IL-6 when compared to TV6, indicating that different strains of Trichomonas will have different degree of host immune response. This result is consistent with the previous experiment results, in that TV123 interaction resulted in induction of TLR-6 as well as the pro-inflammatory cytokine IL-6.

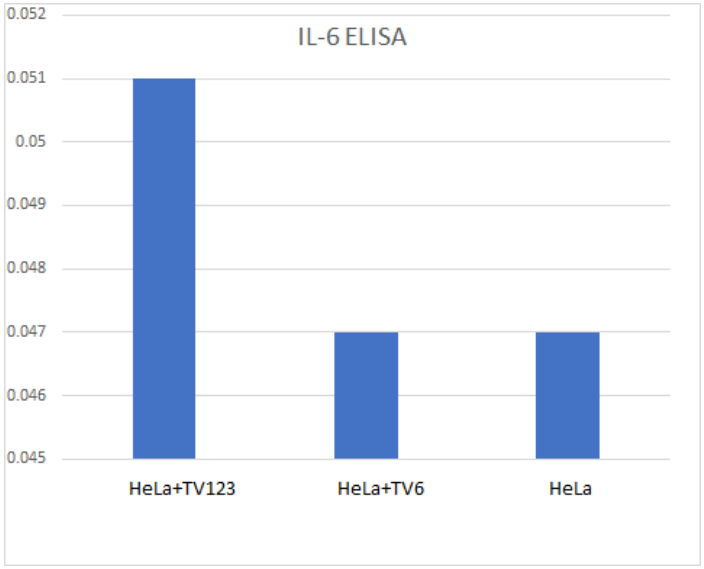

Experiment 4 – Measurement of Adherence Assay, TUNEL Staining, Immunohistochemistry staining – To correlate the TLR and cytokine gene expression with Trichomonas binding an adherence assay using fluorescent dyes is underway.

Conclusion and future directions:

TLR gene expression analysis showed that TLR-4 was induced in Epithelial cells that came in contact with *Trichomonas vaginalis*. We also verified the cytokine gene expression (IL-6) using ELISA, and the cytokine gene expression correlated with that of the TLR-4 gene expression, as expected.

References:

CDC. 2017. *CDC - DPDx - Trichomoniasis*. Centers for Disease Control and Prevention. doi: cdc.gov/dpdx/trichomoniasis/index.html.

Coleman, J. S., *et al*. 2013. *Trichomonas vaginalis* Vaginitis in Obstetrics and Gynecology Practice: New Concepts and Controversies. Obstetrical and Gynecological Survey 68: 43-50. doi: 10.1097/OGX.0b013e31827fb7d.

Gunn, A., and S. J. Pitt. 2012. Parasitology: An Integrated Approach. Wiley-Blackwell, Hoboken, New Jersey, p. 7-8, 37-38, 43-45, 54-57, 70-74, 114-126.

Leu, A. L. (n.d.). Encyclopedia Britannica. doi: britannica.com/science/Trichomonas-vaginalis.

Mercer, F., and P.J. Johnson. 2018. *Trichomonas vaginalis*: Pathogenesis, Symbiont Interactions, and Host Cell Immune Response. Trends in Parasitology 34: 8. doi: 10.1016/j.pt.2018.05.006.

Schumann, J. A., and S. Plasner. 2020. Trichomoniasis. StatPearls Pubblishing, National Library of Medicine. doi: ncbi.nlm.gov/books/NBK534826/.

Shiadeh, M. N., *et al*. 2016. Human parasitic protozoan infection to infertility: a systematic review. Parasitology Research 115: 469-477. doi: 10.1007/s00436-015-4827-y.

Danielle Soileau

Major in Biology

Mentor: Dr. Ashwini Kucknoor

Research in Microbiology/Molecular Biology

Department of Biology

Characterization of a novel cell surface protein coding gene, TfAD1 in *Tritrichomonas* foetus, a cattle pathogen.

My name is Danielle Soileau, and I worked with Dr. Ashwini Kucknoor this summer to characterize a novel cell surface protein coding gene, TfAD1 in Tritrichomonas fetus, a cattle pathogen. Bovine trichomoniasis is caused by the protozoan *T. foetus* and is a common disease in the beef industry, costing US cattle ranchers an estimated $650 million annually. Adherence to host epithelial cells is the primary step in the pathogenesis of *T. foetus,* mediated by cell surface proteins. If this initial attachment is destroyed, then the parasite cannot cause infection in the host. My proposal was aimed at characterizing a novel cell surface protein in *T. foetus,* using homolog of TvAD1 gene from related human trichomonad. This novel gene will be disrupted using siRNA gene disruption technique to study the function of this gene. The long-term goal is to understand the importance of similar cell surface proteins in *T. foetus* pathogenesis, by using reporter genes to verify the cellular localization and gene silencing to understand the functions of TvAD1 homologs in *T. foetus*. My specific research hypothesis for the summer project was that A TV homolog TVAD1 is present in *T. foetus*, and it will play a role in promoting adherence to bovine epithelial cells.

This summer, I have followed a tight schedule with various processes including establishing parasite and bovine epithelial cells through PCR application and gene sequencing, work on RNA expression via SiRNA knockdown experiments, and measured the adherence of TVAD1 to bovine epithelial cells. The project was started by familiarizing myself with the basic cell culture technique. *T . foetus* was grown using diamond media, supplemented with donor horse serum and antibacterial and antifungal antibiotic at 37 degrees Celsius in an incubator. For gene characterization, DNA primers were designed based on the TvAD1 gene sequence from TrichDB- T. vaginalis gene sequences and a PCR was performed on T. vaginalis and *T. foetus* genomic DNA. We first analyzed the TVAD1 gene sequence from Trich Database, and designed primer sets to be used in our study. The primers were ordered from Invitrogen. We then grew *T. foetus* cultures (three isolates, TF31, TfK and TFF6).

Genomic DNA was isolated and verified on the gel to determine the quality and quantity. Genomic DNA was then used to amplify TfAD1 gene using TVAD1 primers. After standardizing the annealing temperature, we were able to amplify the gene from *T. foetus*. The amplicon size and gene sequence matched that of TVAD1. We then determined the expression of TfAD1 in the three *T. foetus* isolates, both in *T. foetus* cells that were grown in the flasks, and the *T. foetus* cells that were grown in presence of host epithelial cells. Results showed that TfAD1 expression increased in *T. foetus* cells that encountered the cells, further confirming that TfAD1, like TVAD1 is an adherence related gene, whose expression is increased during the process of adherence.

The amplified fragment was sequenced, and TVAD1 gene sequences were compared to *T. foetus* genomic DNA sequences. The amplified gene and its sequences were confirmed to be matching the expected size based on TV genome database. Next, RNA isolation was carried out from two isolates of *T. foetus*, Tf31 and Tff6. Total RNA was used for gene expression analysis using RT_PCR method. *T. foetus* cells were grown axenically at 37 degrees Celsius and were co-incubated with host epithelial cells, to mimic the infection status. When RNA was compared for gene expression between Tf and TF that encountered epithelial cells, an increase in gene expression was observed in those cells that were c- incubated with epithelial cells, suggesting that TfAD1 gene plays a role in helping parasites bind or stick well to host cells.

Next, we wanted to determine if we can knock-down the TfAD1 gene expression and determine its effect on *T. foetus* adherence to host cells. We employed the relatively new technique called antisense oligo knockdown experiment. We designed two antisense oligos to TfAD1 gene sequence using Antisense oligo generating software. We got two antisense oligos (A and B) synthesized by Sigma Aldrich. 100 uM of the antisense oligos were introduced into the cells by electroporating the cells using 320V current. Following transfection, cells were allowed to recover on ice for 10 min and then allowed to grow under normal conditions. RNA was isolated from the transfected cells at 24 and 48 hrs, and RT-PCR was carried out to determine if the gene expression was affected. Antisense oligo A showed decreased expression of TfAD1 compared to antisense oligo B in Tf31 isolate. This result suggests that the antisense oligo A was able to interfere with the mRNA of TFAD1 And aided in the decreased gene expression. Currently, the transfected cells are being tested for the adherence capacity to host cells. When it came to challenges, the most difficult adversities that we faced were getting cells to grow and dealing with contamination issues. It took a lot of patience and sometimes a little bit of luck for cells to grow properly. Often the safest approach was to ensure our workspaces were cleaned with seventy percent of ethanol. Overall, I learned more than I ever imagined before starting this project. Not only did I learn new lab processes, I learned how to organize a professional project, and how to speak more confidently in front of my peers.

During my first presentation, I was exceedingly nervous. SURF gave me otherwise not feasible scenarios where I got to listen to and discuss with older students on how to present a project in a professional setting. Surf gave me a better appreciation for research, and I would like to continue being involved in research as a doctor in the future. In the future, I plan to attend medical school and eventually become a doctor. Working with Dr. Kucknoor during this research project opened a new molecular world to me. Not only did it foster new interests and help me understand topics I had learned in class before, but it has also pushed me to want to continue being involved in and supporting research projects in the future.

In a world where it feels like we are currently under attack by an invisible enemy, COVID-19, it is crucial to keep exploring across the terrain not seen by the naked eye. Many of the processes I learned such as the PCR process is technology that was used to help fight against the spread of COVID-19. The skills I learned this summer are priceless and will hopefully be able to help me understand more diseases in the future. In the future, we plan to present at the Texas STEM conference, and at the Annual Undergraduate Research Expo at Lamar in 2022. With the combined efforts of the entire student lab of Dr. Kucknoor, we plan to publish a scholarly article based off years of cumulative research that has been put into the study of Trichomonas. Like any path found in science or medicine, students have passed the baton of knowledge under the guidance of Dr. Kucknoor to harvest a wealth of knowledge worthy of publishing.

Since there is little to no knowledge is known about *T. foetus*, continuation of the project is the wish of this lab. The significance of this research, if successful, will provide the functional role of adhesion proteins in host parasite interaction. The results will potentially identify novel therapeutic targets for bovine trichomoniasis, which is otherwise a neglected parasitic disease in the cattle industry. Knockdown of genes by degrading mRNA will result in the cells not having the TVAD1 protein. As a result, we can investigate the function of this gene towards parasite adherence to host cell. If indeed the knockdown of TfAD1 results in poor adherence, then TfAD1 protein can be further studied to determine potential target strategies to inactivate this protein.

Kalen Baker

Major in Mechanical Engineering

Mentor: Ping He

Research in Mechanics and Physics

Department of Mechanical Engineering

Theoretical Research on Sintering of Metals based on the Results of Molecular Simulations

Introduction

Sintering is the process able to fuse a fine powdered material into a single object, which is of significance because it forms a near net set object reducing wasted material and processing time. Another benefit is that this process occurs below the melting point of the same bulk material, which can save a significant amount of energy needed to manufacture a final product. Here in Houston and Beaumont area, a common use of sintering is laser cladding Stellite™ to valve seats and disks to improve wear resistance. Other uses include the nuclear fuel pellets, crystal lenses, and flexible electronics. While this sintering is of commercial interest, modeling of it is quite complex because of the many contributing factors such as powder size, contamination, molding process and heating method. Efforts have been made modeling different aspects such as density, grain growth, pore distribution and shape. Of interest here, this study uses two models, i.e., the Master Sintering Curve (MSC) and Molecular Dynamics (MD).

The goal is to use data gathered from the MD system as the input information to the MSC model to predict of the bulk material properties primarily grain size, grain growth, elastic strength, and diffusion mechanism:

$$-\frac{dL}{Ldt} = \frac{\gamma\Omega}{kT}\left(\frac{\Gamma_v D_v}{G^3} + \frac{\Gamma_b \delta D_b}{G^4}\right)$$

where γ is surface energy, Ω is atomic volume, k is Boltzmann's constant, T is temperature, Γ is group of condensed geometric constants, D is diffusion coefficient δ grain boundary thickness, and G is mean grain diameter. The subscripts v and d delineate whether it is diffusion through the volume or grain boundary, respectively. This equation of the MSC model uses the shrinkage measurements ($-\frac{dL}{Ldt}$) and the thermal history during processing from multiple samples to generate a curve that can be used to predict the behavior of any other

samples of the same material (1). For a developed process, the MSC model poses no challenge because the material selection and initially processing is set. However, if a new supplier for raw material must be found or the firing schedule of the component being produced is changed, then developing new materials is particularly expensive in time and resources, especially for the pre-processed or exotic alloy (2,3).

An MD model, however, can perform simulations of most materials under varied conditions, if a suitable molecular potential set exists for the system to be modelled. The primary limitation of a MD simulation is the size because the potential calculates between an atom and each of its neighbors so that the computational load increases dramatically with the simulation size that limits most simulations to the nanometer size of material.

Experiment

The purpose was to combine the best of both models to allow the input information gained from MD simulations of a material to formulate a Master Sintering Curve so that material properties could be predicted in advance of actual processing of samples to save the expense of material at the cost of computer processing time but also allowing the simulation results to be scaled up to bulk material. Material selection started with the ability to find a completed potential system that could be provided to our MD software, LAMMPS (4). Based on our previous work, the potential system has been narrowed to a particular type known as the Embedded Atom Method (EAM) (5) because of its ability to accurately assess the long-range characteristics at the conditions required for sintering. Then, reference data was needed to compare the results to (6). Titanium was chosen due to the large amount of data available as well as its commercial importance. From the reference data, the temperature range was from 800K to 1600K (7), and a set of 10 simulations has been run at 100K intervals in our computational facility.

Results

Initially qualitative analysis showed complete fusion of the material and an expected rearrangement and final geometry of the material. With all simulations an MSD calculation was made, and a curve generated and shown in Figure 2. On comparison however, this proved to be a problem that the generated MSD is much higher than the reference values the suspected cause of this is the potential or the MSD calculation and because of the crystal transition very little data exists for the hcp structure of Titanium.

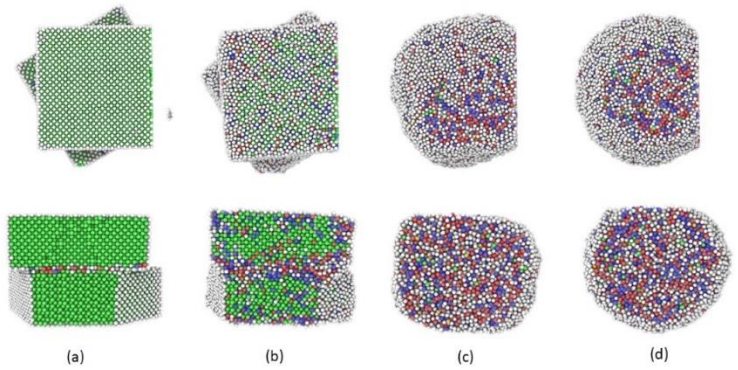

Fig 1: Evolution of material at timesteps: a) 5, b) 100, c)155, d) 235. Given as a top and cut away to see interior colors represent crystal structure: green is fcc, red is hcp, blue is bcp, and white is non-specified

The previously stated potential problems can be seen in Figure 1, where the structure rapidly shifts from fcc to both hcp and bcc, and in Figure 3, where the high temperature deviation is obvious as the number of timesteps to complete a begins to rise rapidly. The MSD calculation deviations could be of three possible types: 1) the original bound for the calculation now contains a surface due sphericalization of the grain, which would have an artificially high diffusion due to surface motion, 2) the transition of the crystal structure is being seen as diffusion because the MSD is calculating displacement, and 3) the MSD was made wrong. Because of the EAM and MSD error, the diffusion was never found to be accurate enough to commence MSC curve generation. Due the intense nature of generating an EAM potential, efforts are now underway to validate the MSD made by LAMMPS. LAMMPS makes periodic dump files that contain position and velocity data that will allow for a manual formulation of the MSD and to ensure that a surface wasn't inadvertently captured a new simulation is being developed that only contains bulk material. Later, a new EAM will still need to be reformulated using the right structure and allowance for excited states.

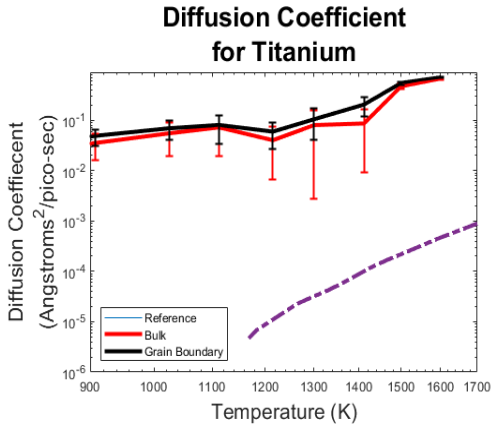

Fig 2: Calculated diffusion Coefficient.

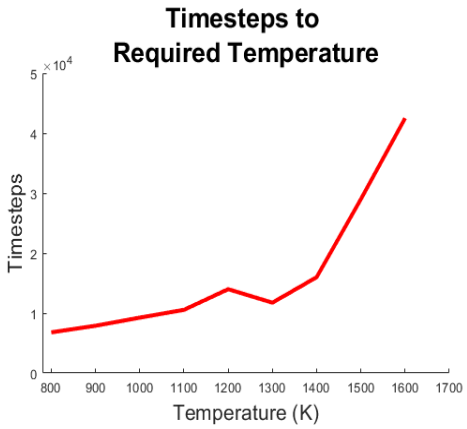

Fig 3: Total timesteps in a simulation.

References

1) H. Su and D. Johnson, "*Master Sintering Curve: A Practical Approach to Sintering*", *J Am Ceram Soc*, 79, 3211-17 (1996).

2) Chuvil'deev, V.N., et al. "*Ultrastrong Nanodispersed Tungsten Pseudoalloys Produced by High-Energy Milling and Spark Plasma Sintering*." *Doklady Physics,* 56, 109 (2011)

3) Mingjun Shi, et al. "*Preparation and Properties of Titanium Obtained by Spark Plasma Sintering of a Ti Powder-Fiber Mixtures*." *Materials*, 12, 2510 (2018).

4) S. Plimpton, *"Fast Parallel Algorithms for Short-Range Molecular Dynamics*", *J Comp Phys*, 117, 1-19 (1995).

5) Daw, M.S. and Baskes, M.I. *"Embedded-atom method: Derivation and application to impurities, surfaces, and other defects in metals."* Phys. Rev. B., 29, 6443 (1984).

6) Kadkhodaei, Sara, and Davariashtiyani, Ali. "*Phonon-assisted Diffusion in Bcc Phase of Titanium and Zirconium from First-Principles."* Phys. Rev. Materials, 4, 043802-1 (2020).

7) Robertson, I., and Schaffer, G. *"Some Effects of Particle Size on the Sintering ofTitanium and a Master Sintering Curve Model."* Metall. Mater. Trans. A, 40, 1968 (2009).

8) A. Stukowski, "*Visualization and analysis of atomistic simulation data with OVITO – the Open Visualization Tool*." *Modelling Simul. Mater. Sci. Eng*. 18 (2010).
9) R. M. German, Sintering Theory and Practice., Wiley-VCH (1996).

Alexander Bahrim

Major in Electrical Engineering and Minor in Mathematics

Mentors: Dr. Gleb Tcheslavski and Dr. Cristian Bahrim

Research in Electrical Engineering and Physics

Department of Physics and Department Electrical Engineering

Opto-Electronic Laboratory

Development and Assessment of Hardware Model for Studying the Mechanism of Regenerative Braking System (RBS)

Abstract

As an increasing number of electric motor vehicles (EV) are reaching consumers, increasing the charge stored by an electric battery and its efficiency has become a priority of the EV industry to compete with combustion (gas) vehicles. The solution car manufacturers are turning to is termed as regenerative braking system (RBS). In this project, we build an RBS model to study its efficacy in various conditions, we estimate the mechanical energy generated by the system and its portion that was transformed into electrical energy and stored, and finally estimate real world efficiency. The purpose of this research is (1) learning about how RBS works and is built, (2) designing and building a charging circuit for storage of energy on a capacitor, and (3) analyzing the efficiency of our RBS for various RPMs. Trials of different combinations of capacitors and resistors led us to successfully build and test an efficient experimental configuration with 30% efficiency at 1,000 RMP. Our results predict a possible efficiency of 51% for 2,000 RPM, which corresponds to real-world applications.

Keywords

regenerative braking system (RBS); electric vehicles (EV); permanent magnet synchronous motor (PMSM); revolutions per minute (RPM); “motor-flywheel-generator” system (MFG)

1. Literature Overview

An RBS most commonly involves a brushless motor called Permanent Magnet Synchronous Motors (PMSM) due to its efficient design (described later, in the section: *Theory Behind RBS*) and is used in conjunction with a capacitor to recharge the battery. The system is used to recapture the kinetic energy lost in vehicle braking, thus significantly reducing a vehicle’s overall energy consumption, and at the same time increasing battery

longevity. The regenerative braking system (or RBS) is an *energy recovery mechanism* associated to slowing down a moving vehicle or object by converting its kinetic energy into electric that can be either used immediately or stored until needed. In our research, an RBS was built by using a motor-flywheel-generator (MFG) system to study the rotational energy of the flywheel, and its conversion into electrical energy. The efficiency of such energy conversion is carefully studied.

2. Preliminary Research

An electric motor in electric vehicles (EV) offers an environmentally friendly solution to the widely common combustion (gas) motor. According to CAR Magazine [1], the longest-range for EV on the market is 379 miles for the Tesla Model S. Compared to a study done in 2016 by the US Dept. of Energy [2], gas vehicles have an average-range of 412 miles with the longest-range vehicle at a staggering 700 miles. The EV industry is behind; however, the solution may not only be found in the battery's storage capacity, but also in the efficiency of energy conversion inside electric motors today. We started by building a model RBS system using a motor, a generator, a cylinder of steel to connect the two pieces, and an RC circuit to test the efficiency of our hybrid RBS system, with the purpose of suggesting an improvement in the EVs' battery-operating electric motors.

3. Materials

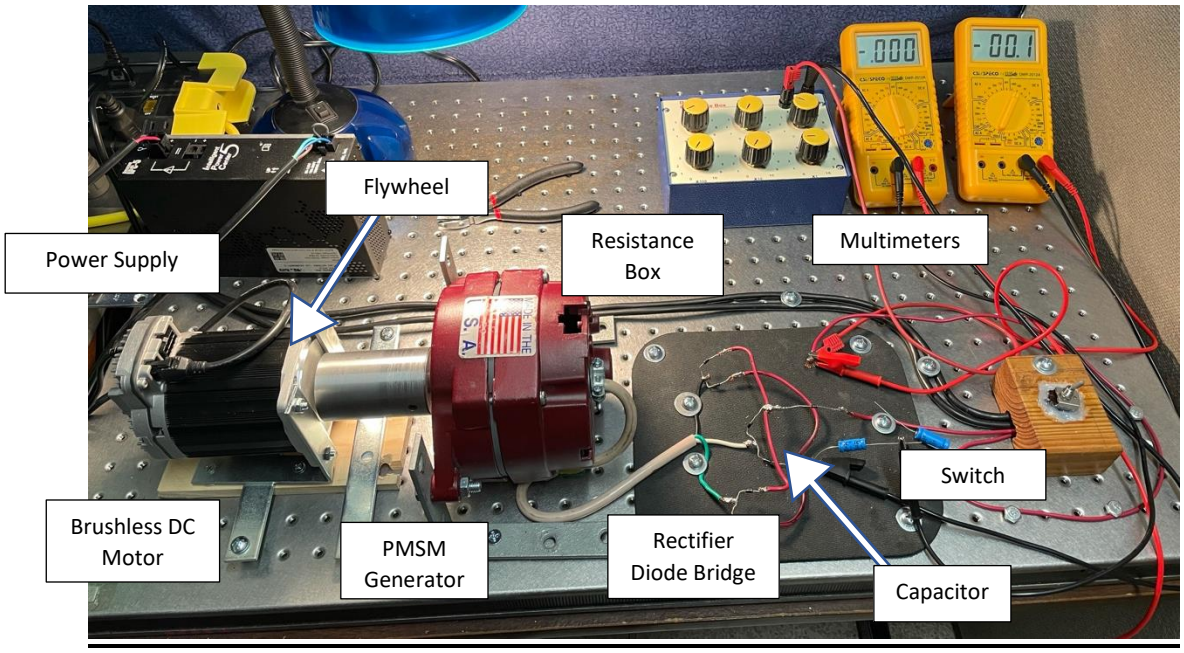

Figure 1 *Overview of our RBS model constructed in the laboratory*

The first item acquired for the setup was a robust Newport-like breadboard table. Finding an original and functional PMSM motor for the research was not possible. Building a proper PMSM was a difficult task due to the complexity of the motor and needing a very large power supply to power. Our option was to a *create hybrid RBS system:* First, we purchased a brushless DC motor (BLDC) from ClearPath Integrated Servo Motors (Figure 1, bottom left) powered by an IPC-5 DC power supply (Figure 1, top left). The ClearPath Software gave us full control of RPM of the desired RPM while using a computer. The second item acquired was a spare wind turbine PMSM (Figure 1, bottom centered) found in our EE department's storage room. The PMSM served the purpose of acting as a generator for our RBS system, thus demonstrating a complete RBS found in EV.

To build the flywheel (Figure 1, top centered), a steel cylinder was purchased, drilled, and polished to conjoin the shafts of the motor shaft with the generator shaft. In the case of my research, we decided to use only a capacitor to capture the voltage delivered by the generator system. A battery has the capacity to produce electric power through various reactions (i.e. chemical), while a capacitor stores charge for delivering electric power. This option was adopted due to cost, and because for our study, we need to measure the energy produced by the PSMS system and stored for further usage (i.e. for powering a car tractional system). Therefore using a capacitor (Figure 1, bottom right), I was able to store this energy and accurately test the efficacy of the RBS without further loss in energy transfer to car battery. Besides several capacitors (of 100, 500 and 6,300 μF) and wires, we used a 2-phase switch (Figure 1, bottom right) connected the circuits of the motor and of the generator, 4 separate multimeters (Figure 1, top right [two displayed]), 7 diodes to direct and convert AC to DC voltage also called a rectifier diode bridge (Figure 1, bottom centered), rheostat/resistance box (Figure 1, top centered [resistance box displayed]), and finally the "Analog Discovery Kit", allowing us to use an oscilloscope function to display the signal produced by the AC generator as well as rectified in a DC signal by the diode bridge.

4. Process and Experimental Model

4.1 Theory Behind RBS – In real-world applications, RBS works by using a motor-generator system to successfully convert kinetic energy from the rotation of the flywheel (which is a motor's shaft – cylinder coating – generator's shaft) system to recharge the capacitor when it is not being used. The electromotive force (EMF) of an electric motor provides a much greater supply of voltage to a capacitor than a normal car battery recaptures as voltage from a classical alternator. In RBS, the voltage is supplied from the kinetic energy of the wheels which is otherwise lost to thermal energy in physical braking pads. Figure 1 shows the principle of energy conversion from kinetic into electric in RBS. While braking, the EV will naturally slow down due to friction, but the decelerating

traction is used toward recharging the capacitor**.** To understand how an RBS works, one must first investigate its components.

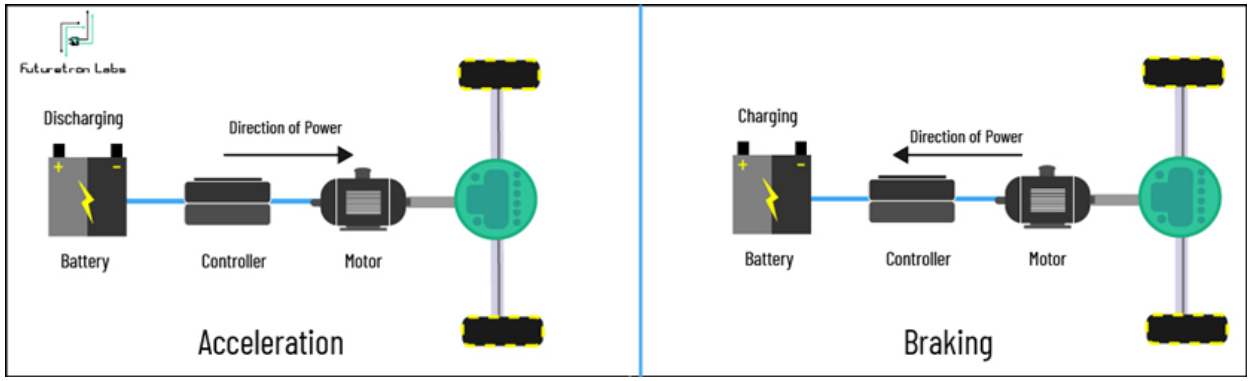

Figure 2 *Principle of RBS Diagram (accessed from Futuretronlabs Inc.). The image is from* [*https://futuretronlabs.in/blog/index.php/2019/09/12/regenerative-braking-system/*](https://futuretronlabs.in/blog/index.php/2019/09/12/regenerative-braking-system/)

EV can use either AC or DC motors. A motor is an electrical device that converts electrical energy into mechanical energy. [4] Although there are several types of electric motors, according to *Embitel* [3], the most widely used motors are a brushless DC motor (BLDC) and a AC permanent magnetic synchronous motor (PMSM). Both serve as a better alternative to the standard AC induction motor and have higher power density and efficiency. "BLDCs have high starting torque, high efficiency and low maintenance" according to Ritvik Gupta [5]. There are no differences between BLDC and PMSM besides the driving current and detection of rotor position. Most automotive manufactures use PMSM motors due to their high performance and sinusoidal EMF signal, whereas BLDC generates a trapezoidal signal. "[A] system consisted by PMSMs processes excellent dynamic performance, high precision, and wide speed range."[6] For companies such as Ford and Toyota, they both use PMSM motors in their electric vehicle variations. Tesla Model X also uses PMSM, while their Model S uses the AC induction. Both AC and DC motors can work for an RBS.

A PMSM (shown in Figure 3) is a brushless motor, as opposed to brushing motors found in farm machinery, stair lifts, and chemical injection pumps. For PMSM, the magnetic rotor uses solid magnets. The continuous rotation of the magnets caused by the polarity of the stators and coils allow the motor to smoothly rotate the axle and convert the electromagnetic energy into mechanical energy for generating the rotation of the car wheels.

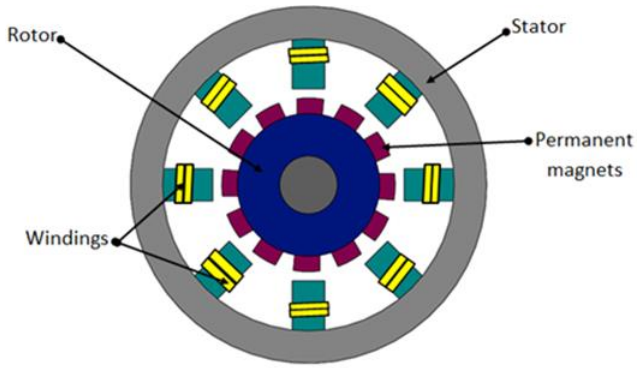

Figure 3 *Schematic design of a PMSM (accessed from Embitel [3]). The permanent magnets rotate on the rotor caused by the polarity of the stators allowing the system to generate power. The image is from* https://www.embitel.com/blog/embedded-blog/brushless-dc-motor-vs-pmsm-how-these-motors-and-motor-control-solutions-work

4.2 Designing a Circuit for RBS and Understanding its Mechanism- we designed and built the circuit in 2 phases:

Phase 1 *- The power supply is powering the motor and accelerates the flywheel. Figure 4 shows a power supply controlling the RPM of the motor-generator shaft and flywheel. A voltmeter is used to measure the voltage distributed in the circuit.*

Phase 2 *– When the voltage from the power supply is cut off from the motor the kinetic energy (KE) from the wheels is directed into electric energy and stored on the capacitor as voltage, V_C (see Figure 4). The generator (PMSM) converts KE into AC which is then converted by a lab made diode rectifier bridge (built with 7 diodes) of with negligible resistance. This newly converted AC to DC voltage is next captured by the capacitor as V_C. The rheostat serves to protecting the capacitor from voltage overload.*

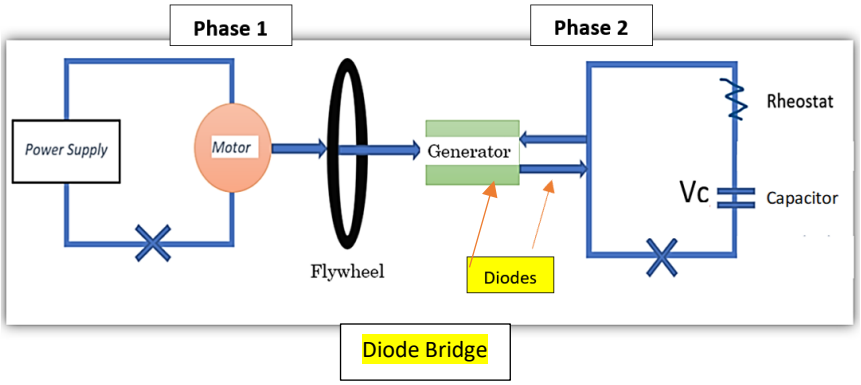

Figure 4 *Schematic of the RBS system. Phase 1 consists of the powering of the flywheel system and Phase 2 contains the charging of the capacitor.*

5. Methodology and Calculating relevant quantities for our study

5.1 Calculating Moment of Inertia- The energy of rotation (E_r) is given in the equation below

$$E_r = 2I \times (\pi f)^2 \qquad [1]$$

where *f* is the RPM in Hertz, and *I* is the moment of inertia for the flywheel with the two shafts on the motor side and the generator side. From the general formula of moment of inertia for a solid cylinder,

$$\mathrm{I} = \frac{1}{2}\,\mathrm{mr}^2 \qquad [2]$$

we calculate the moment of inertia of the flywheel, which has two chambers (see figure 2) of radii $R - r_1$ and $R - r_2$,

$$\mathrm{I} = \frac{1}{2}\sum_{i=1}^{2} \mathrm{m_i}(\mathrm{r_1^2} + \mathrm{r_2^2}) \qquad [3]$$

and where R is the radius of the initial steel solid cylinder.

Figure 5 shows the chambers of the flywheel. For our flywheel *I is 0.003555 kg* m^2. Hereafter, the system built will be called the "motor-flywheel-generator" (MFG) system. Finally, we need to calculate the energy of rotation as:

$$E_r = \frac{1}{2}\,I\omega^2 \qquad [4]$$

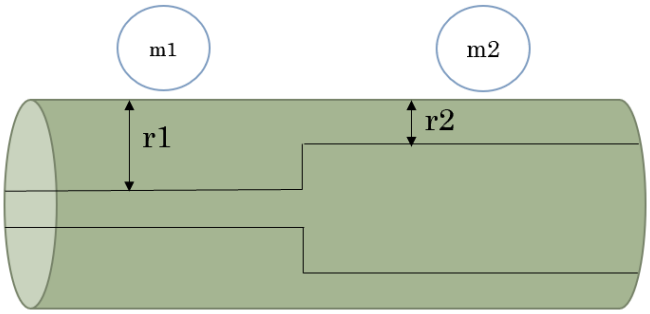

Figure 5 *Flywheel Diagram – We have drilled two chambers to fit in the shafts of the motor (left) and generator (right)*

5.2 Oscilloscope v. Multimeter Measurements –First tests used an oscilloscope to (1) precisely measure the voltage output from the AC generator, (2) study the sinusoidal AC signal and its root-mean-square (rms) voltage value (labelled V - rms in Table 1), as well as (3) the time of extinction from voltage peak to zero. But the response of the oscilloscope to voltages (lower than 24V) became quickly an issue. Therefore, we had to use multimeters, instead of oscilloscopes for larger voltages. Table 1 shows our comparison study: Using 4 different

lower RPMs, the multimeter was found to give a reading comparable to the oscilloscope reading, thus allowing us to read larger voltages and move forward with higher RPM trials toward the real-world RPM values for EV.

5.3 Extinction Time Using the Oscilloscope- Extinction time is the time it takes for the highest peak of the AC sinusoidal signal to reach zero after voltage is cut off (called phase 2 in Figure 4).

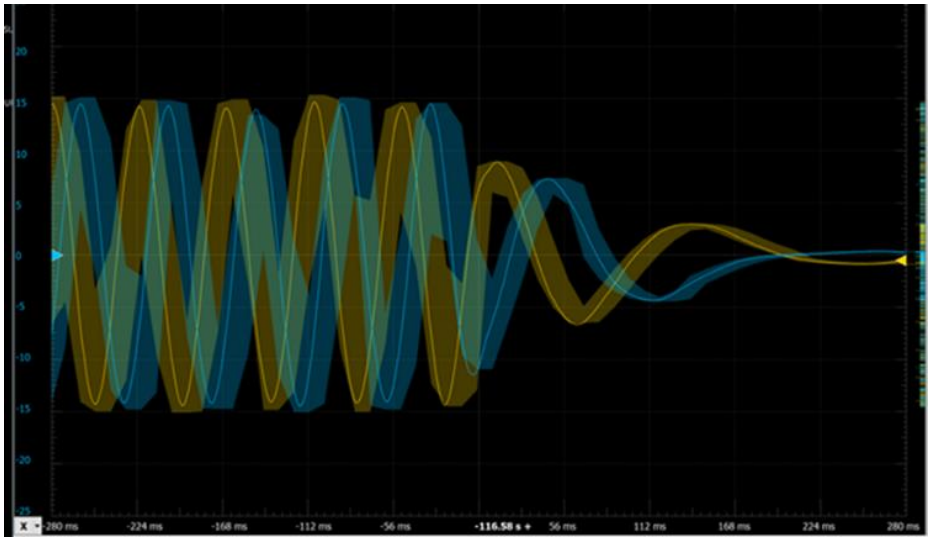

Figure 6 *Example of extinction time shown graphically by the oscilloscope*

Figure 6 is a signal from the AC PMSM generator before the rectifier diode-bridge, for a random study case at 150 RPM. The two curves corresponded to the two pair channels of the 3-phase AC generator output signal. They were in sync, as they should be. This analysis was also a diagnostic test that the AC generator is functioning normally. We compare the extinction time with the characteristic time (CT) of the RC charging circuit after the rectifier diode bridge.

$$CT = R\ (Ohms)\ x\ C\ (Farad) = t_{1/2} / ln\ (2), \qquad [5]$$

where $t_{1/2}$ is the time for charging half the voltage on the capacitor. *R* is the Ohmic resistance of the circuit and *C* is the capacitance of the capacitor which receives the mechanical energy of MFG system, as V_C voltage. Reason for this is because as the current flows, the capacitor charges until the voltage reaches *V-rms*. In a typical RC circuit, the complete charging of the capacitor is reached after a time which is about 5 times the $t_{1/2}$ value.

The duration of the voltage peak (DVP) ~~duration~~ is another important time, which is typically very short, of about 0.0001 seconds. In our case, CT needs to be short enough to avoid loss of voltage after the peak voltage has passed. If the CT is too short, then the capacitor cannot capture much voltage from the AC generator. If the

CT is too long as compared to DVP, then the voltage from AC generator rectified by the diode bridge is lost in discharging the capacitor mostly through heat dissipation.

Table 1 Study on four lower RPM values for comparing the V - rms reading from the oscilospcope with the voltmeter reading. The extinction time of the AC voltage signal before the diode bridge (from Figure 6) is also reported for each RPM.

RPM	V-rms (volts)	V-meter (volts)	Extinction time (sec)
50	3.308	3.28	0.45
100	6.63	6.61	0.43
150	10.014	10.05	0.4
200	13.36	13.46	0.42

Table 1 indicates that at low RPMs, the extinction time of the rectified voltage signal is 0.42 ± 0.02 seconds. This meant that the characteristic time for the charging RC circuit (that acts as battery in many real-world applications) should be much less than 0.4 seconds. According to equation [5], we can decrease CT, using low R and C, but to store large charge on the capacitor, its capacitance C should be large. Therefore, for practical purposes the only way to decrease CT is by lowering the resistance R of the RC circuit. The final trails of testing different combinations of resistance and capacitance will lead us to optimum results.

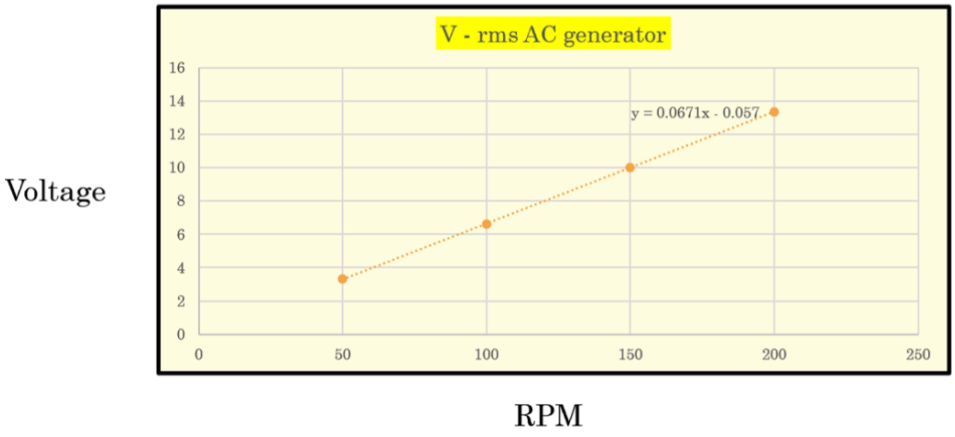

Figure 7 *V – rms at low RPMs. The best fitting linear function is reported.*

From Figure 7, we observe that V – rms follows a linear trend for these low RPMs. Adopting the linear regression formula V – rms = 0.0671 x rpm – 0.057, generated by the best linear fit, we predicted V – rms values past 200 RPM, where the oscilloscope was not operational. This linear regression allowed us to predict the range of voltages expected at larger RPMs.

5.4 Finding the optimum values for R and C for charging efficiently the capacitor - First, we worked with typical commercial capacitors used in circuitry today (of 100, 500 μF) and larger resistances to protect the RC system. The results of our study is shown in Table 2.

Table 2 Trials for finding optimal R and C for better efficiency

Trial 1 1650 Ohm V - cap (volts)	One capacitor 100 μF Charging time (seconds)	Capacitor's Energy (Joule)	RPM	Efficiency
2.19	0.174	0.000240	100	0.12%
3.206	0.194	0.000514	150	0.12%
5.81	0.214	0.001688	200	0.22%
8.07	0.253	0.003256	250	0.27%

Trial 2 1650 Ohm V - cap (volts)	Two capacitors in series 50 μF Charging time (seconds)	Capacitor's Energy (Joule)	RPM	Efficiency
3.173	0.136	0.000252	100	0.13%
4.98	0.16	0.000620	150	0.14%
7.489	0.172	0.001402	200	0.18%
9.7278	0.204	0.002366	250	0.19%

Trial 3 100 Ohm V - cap (volts)	Two Capacitors in Series 50 μF Charging time (seconds)	Capacitor's Energy (Joule)	E rotational (Joule)	RPM	Efficiency
7.438	0.098	0.001383	0.1949	100	0.71%
9.957	0.096	0.002479	0.4386	150	0.57%
15.099	0.093	0.005699	0.7797	200	0.73%
18.7	0.089	0.008742	1.2183	250	0.72%

Our initial studies used load resistances of hundreds or thousands of Ohms. We choose resistor boxes for having easy to manipulate adjustable resistances. We looked for settings where the CT was at most a quarter of the average extinction time value (of 0.42 ± 0.02 seconds) from Table 1. From the study of efficiency reported in Table 2, we observe that in order to have a better efficiency, and at same time, for lowering the characteristic time we must lower the load resistance.

5.5 Finding the Best Characteristic Time - By lowering the load resistance, we greatly reduce the energy dissipated in the RC circuit. This attempt opened the door for a larger voltage which would go from the AC generator and rectifier (the diode bridge) to the capacitor. But at large voltages, 100 μF or 500 μF capacitors would most likely break down. Thus, we have acquired a large capacitor of 6,300 μF. This choice of large C requires to reduce greatly the load resistance for retaining the peak voltage (see the discussion before). For dropping CT in these circumstances, we moved to using a rheostat (instead of resistor box) which can have a very small resistance.

6. Results and Discussion

6.1 Studies when resistances of 1Ω and 5 Ω are separately used with a 6,300 µF capacitance - First, we chose to study the charging of the capacitor using a rheostat of R = 5 Ω and 1 Ω.

Table 3 Comparing the efficiency in energy transfer between the MFG system and capacitor, for two separate resistances of 1Ω and 5Ω, and a 6,300 µF large capacitor.

RPM	V - rms	V - cap	E - cap	V - cap	E - cap	V - Cap / V - rms	V - Cap / V - rms	Efficiency	Efficiency
	(Joule)	R = 5 Ω	R = 5 Ω	R = 1 Ω	R = 1 Ω	R = 5 Ω	R = 1 Ω	R = 5 Ω	R = 1 Ω
50	2.93	0.82	0.0021	0.71	0.0012	27.99%	24.23%	4.28%	2.51%
100	6.52	1.64	0.0085	1.73	0.0094	25.19%	26.52%	4.36%	4.84%
150	9.80	2.51	0.0198	2.69	0.0228	25.62%	27.46%	4.52%	5.20%
200	13.29	3.50	0.0374	3.67	0.0467	26.30%	27.58%	4.80%	5.99%
300	19.50	5.78	0.1052	6.23	0.1221	29.64%	31.93%	6.00%	6.96%
400	26.13	8.12	0.2079	8.36	0.2200	31.08%	31.98%	6.66%	7.05%
500	32.93	10.40	0.3409	11.32	0.4034	31.59%	34.36%	7.00%	8.28%
600	39.97	12.97	0.5302	13.75	0.5955	32.46%	34.40%	7.56%	8.49%
700	46.73	15.68	0.7741	16.84	0.8933	33.54%	36.03%	8.11%	9.35%
800	53.67	19.41	1.1868	20.45	1.3173	36.17%	38.11%	9.51%	10.56%
900	60.27	23.10	1.6809	23.63	1.7594	38.33%	39.21%	10.65%	11.14%
1000	66.87	26.50	2.2121	27.70	2.4170	39.63%	41.43%	11.35%	12.40%

The AC generated voltage rectified by the diode-bridge, provides V – rms. We have calculated the percentile ratio between the capacitor voltage and the V-rms from the AC generator rectified by the diode bridge, for assessing the voltage transfer from MFG to the capacitor, and reported the results in Table 3, together with the efficiency in energy transfer from the rotational energy of the MFG system into the electrical potential captured by the capacitor for the available RPMs generated by our ClearPath motor. From Table 3, one can see that the efficiency of our system increases with RPM, which is essential for transferring this study to a real-world application in EV industry. The top value is about 12% for the largest RMP we can reach. This value is close to our 16% target value, but at much lower RMP than in real-world cars.

6.2 Comparing results with Two Resistances of 0.02Ω and 1 Ω and the same capacitance of 6,300 µF – As compared to Table 2, in the case of very low resistance used in Table 3 the efficiency is greatly improved to values desired in real-world applications. However, these values are not yet satisfactory.

Therefore, we choose to drop the resistance to a minuscule 0.02 Ω value. With R = 0.02 Ω and C = 6,300 µF, the CT became 0.00012 seconds, and it was comparable with the duration of the peak voltage of the AC

generator. From Figure 6, the DVP is about 0.0001 seconds. However, the results reported in Table 4 for R = 0.02 Ω, do not show an improvement as compared to the two cases reported in Table 3. Still a 12% efficiency can be reach at the largest RPM value of 1,000, which in itself is a good result for the efficiency our RBS system.

RPM	V - rms (Joule)	V - cap R = 0.02 Ω	E - cap R = 0.02 Ω	V - cap R = 1 Ω	E - cap R = 1 Ω	V - Cap / V - rms R = 0.02 Ω	V - Cap / V - rms R = 1 Ω	Efficiency R = 0.02 Ω	Efficiency R = 1 Ω
50	2.93	0.72	0.0021	0.71	0.0012	22.16%	24.23%	3.32%	2.51%
100	6.52	1.55	0.0085	1.73	0.0094	22.97%	26.52%	3.88%	4.84%
150	9.80	2.75	0.0198	2.69	0.0228	26.96%	27.46%	4.67%	5.20%
200	13.29	3.33	0.0374	3.67	0.0467	24.72%	27.58%	5.50%	5.99%
300	19.50	5.83	0.1052	6.23	0.1221	29.08%	31.93%	6.10%	6.96%
400	26.13	8.68	0.2079	8.36	0.2200	32.34%	31.98%	7.28%	7.05%
500	32.93	10.93	0.3409	11.32	0.4034	32.58%	34.36%	7.72%	8.28%
600	39.97	13.01	0.5302	13.75	0.5955	32.29%	34.40%	7.60%	8.49%
700	46.73	14.80	0.7741	16.84	0.8933	31.39%	36.03%	7.22%	9.35%
800	53.67	19.90	1.1868	20.45	1.3173	37.05%	38.11%	9.99%	10.56%
900	60.27	24.27	1.6809	23.63	1.7594	40.33%	39.21%	11.75%	11.14%
1000	66.87	27.60	2.2121	27.70	2.4170	41.44%	41.43%	12.31%	12.40%

Table 4 Same structure as Table 3, but for 0.02 Ω and 2 Ω resistance and 6,300 μF capacitance

6.3 Comparing All Three Resistances with Capacitance at 6,300 μF - When we looked to the experimental peak voltage absorbed by the capacitor (shown in Figure 8) as a function of the RPM range from Table 1, we observe for all three cases defined by the three resistances of 0.02 Ω, 1 Ω, and 5 Ω a perfect parabolic variation (a polynomial of order 2) for larger RPMs than 300, as opposed to the simpler linear variation from Figure 7. In Figure 8, we give an example for R = 5 Ω and take 3 trials for checking the consistency of our results. As one can see in Figure 9, the best fitting with a polynomial of order 2 has a high R^2 precision.

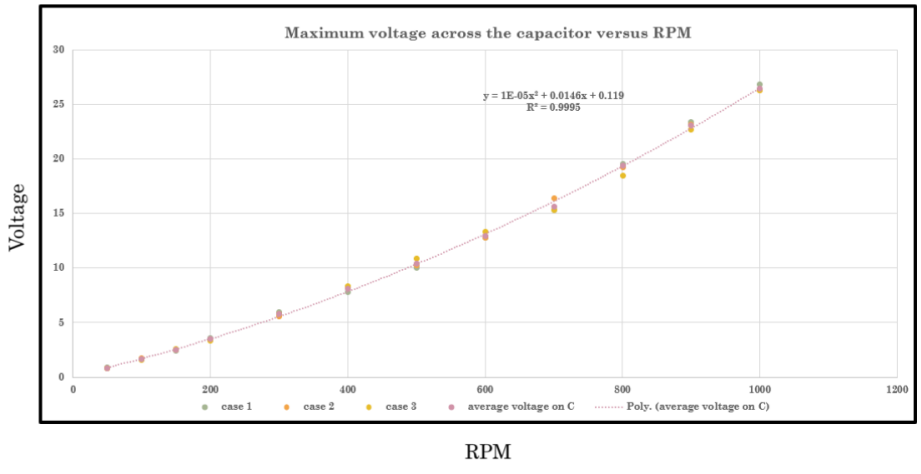

Figure 8 *Parabolic trend-line for voltage capacitance (V-cap) versus RPM for a wide range of RPMs allowed by our ClearPath motor.*

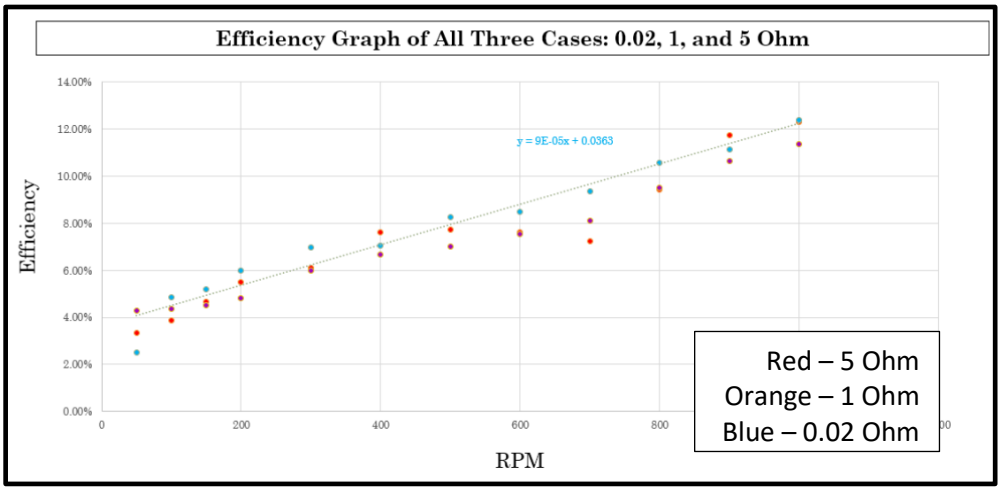

Figure 9 *The efficiency for the three resistances included in Tables 4 and 5, and using the same 6,300 μF capacitance. The best fitting function is shown for the case at 1 Ω, as an example.*

6.4 Comparing Three Capacitances with the Lowest Load Resistance of 0.02Ω - The impact of using a combination of capacitors on the efficiency of charging a large capacitor.

We took the analysis route with two case studies in mind. If two capacitors are wired in parallel, the equivalent capacitance increases. If they are wired in series, the equivalent capacitance decreases. In the former wiring case, we offered more room for energy to be transferred from the AC generator to the capacitors, but we lose the critical parameter, CT, which naturally increases for two identical capacitors wired in parallel. Thus, CT doubles, according to equation [5]). For a series combination, we decrease the equivalent capacitance, and with the two identical capacitors, we half the CT value.

Using the lowest load resistance available, of 0.02Ω, we minimize the energy lost through dissipated heat (i.e., due to collisions in the load resistance). The results are shown in Table 5 for efficiency. Here, the parallel and series combination of two capacitors of 6,300 μF are compared with measurements using one similar capacitor. All the measurements are done with R = 0.02 Ω.

Table 5 Comparing the efficiency for three Capacitances at same load resistance 0.02 Ω

RPM	Efficiency % for R = 0.02Ω in All Three Cases		
	12,600 µF	3,250 µF	6,300 µF
50	1.45%	6.81%	3.32%
100	1.83%	14.22%	3.88%
150	2.20%	15.89%	4.67%
200	2.33%	17.10%	5.50%
300	2.65%	17.73%	6.10%
400	2.84%	18.30%	7.60%
500	2.98%	19.98%	7.72%
600	3.38%	22.12%	7.60%
700	3.49%	22.29%	7.22%
800	3.76%	23.80%	9.44%
900	4.03%	28.66%	11.75%
1000	4.68%	**29.97%**	12.31%

One can see that a series combination can significantly increase the efficiency as revealed in the previous study reported in Tables 3 and 4. With a resistance of R = 0.02 Ω and two 6,300 µF capacitors in series (equivalent to 3,150 µF), we reached a maximum of **29.97% efficiency at 1000 RPM for the system**, which surpasses greatly the goal of 16% energy regain in an efficient RBS as discussed in [6].

6.5 Expanding from Our Results to Real-World Situations – "Automobile engines that can have rotational speeds of 500–7000 RPM" [7]. Domestic cars run typically at 2,000 RPM moving forward, and idle at 1000 RPM. From the best polynomial fitting function for a series combination of capacitors, we found that at 2,000 RPM: (1) from Figure 10, the maximum voltage delivered can be 133 volts (an increase by 7.7 times from 17 volts at 1000 RPM), and (2) from Figure 11, the efficiency can reach an astonishing 51% (from about 30% at 1,000 RPM)! These numbers encourage further exploration on the implementation of these ideas in car industry and successfully demonstrate the effectiveness of RBS in real-world applications.

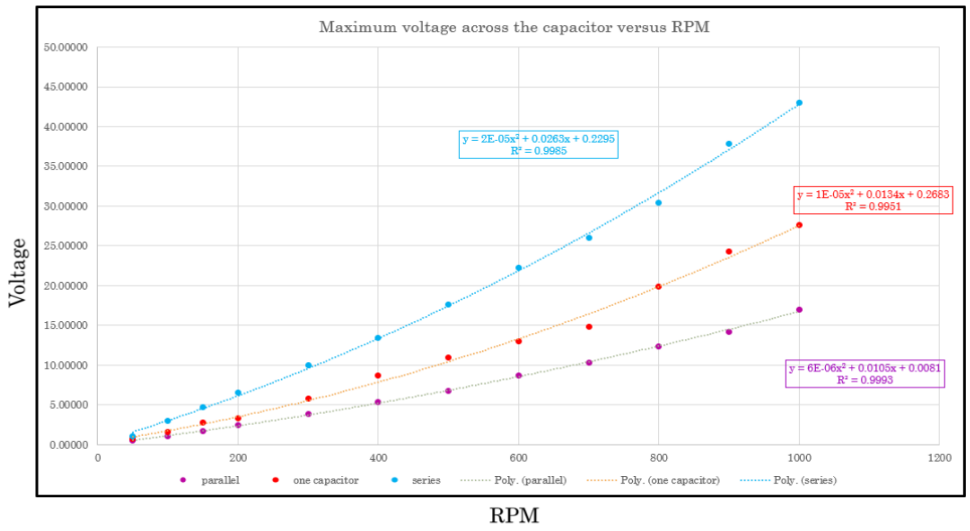

Figure 10 *The maximum capacitor voltage extracted from the rectifier diode bridge at the peak voltage from the AC generator for R = 0.02 Ω and C = 6,300 µF (from Table 5). A similar parabolic-trend-line of different curvatures can be observed, which increases in slope as the capacitance decreases (the lowest curve is for the highest C value of 12,600 µF).*

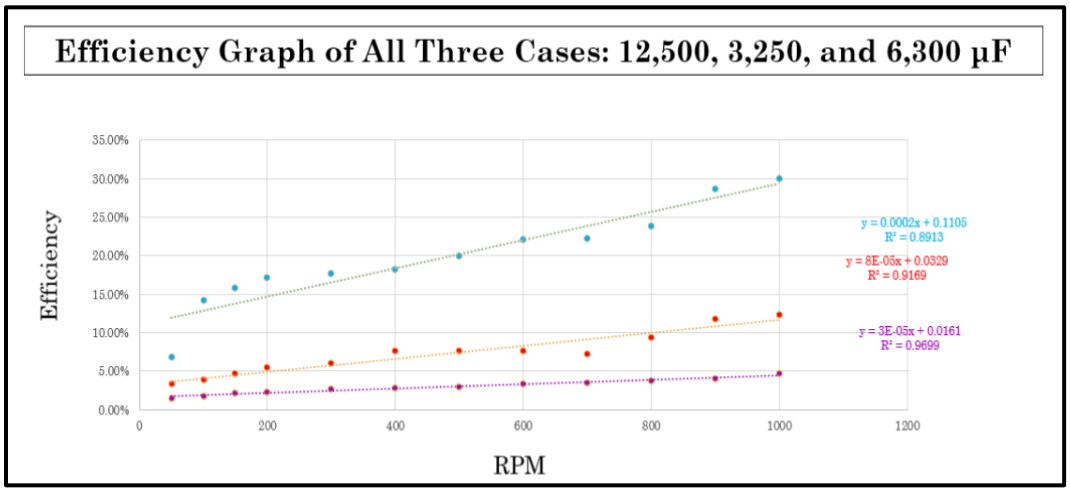

Figure 11 *Plot of the efficiency in charging the three capacitors from Table 5 using the same 0.02 Ω resistance. In each case, the best polynomial fitting function is reported.*

Conclusion:

According to Doyle "Regenerative braking allows the range of the EV to be extended; however, the efficiency of capturing this energy is reported to vary from 16% to 70% [8]". Our hypothesis that we can build an RBS system with efficiency greater than 16% has been proved to be accurate. When using our RBS to real-world RPM, we find nearly 30% efficiency at 1,000 RPM. When extrapolating our data beyond 1,000 RPM, we find 51% efficiency at 2,000 RPM. This research suggests that an RBS can increase the overall single charging of a battery to meet and surpass the average gas-mileage consumption for combustion vehicles. Thus, EVs with RBS are presumably more efficient than combustion vehicles, on top of being more environmentally friendly, and can extend the lifespan of a physical braking system. EV manufacturers and any industry that uses electric motors can take advantage of our findings and inspire others to utilize RBS in their applications. This research helped demonstrate that the EV industry can meet range demands, benefit all forms of electric motors, and further help the environment by making EVs the transportation standard of the future.

References

[1] Alistair Charlton (2019). The longest-range electric cars of 2019: new EVs with the most charge. [online] CAR Magazine. Available at: https://www.carmagazine.co.uk/electric/ longest-range-electric-cars-ev/. [Accessed 17 Feb. 2021].

[2] Energy.gov. (2019). Alternative Fuels Data Center: How Do All-Electric Cars Work? [online] Available at: https://afdc.energy.gov/vehicles/how-do-all-electric-cars-work. [Accessed 17 Feb. 2021].

[3] Sasmita (2019). Motor Control Solutions: Brushless DC vs PMSM Motor Controller. [online] Embitel. Available at: https://www.embitel.com/blog/embedded-blog/brushless-dc-motor-vs-pmsm-how-these-motors-and-motor-control-solutions-work [Accessed 20 Feb. 2021].

[4] Kim, Sang-Hoon. "Chapter 10 - Brushless Direct Current Motor." *Electric Motor Control: DC, AC, and BLDC Motors*, 2017, pp. Page 389–416.

[5] Gupta, R. (2020). Electric Vehicles and Its Different Types | Explained. [online] The GoMechanic Blog. Available at: https://gomechanic.in/blog/electric-vehicles-types-explained/. [Accessed 20 Feb. 2021].

[6] Huazhong, Xu, and Ma Sha. "Research and Simulation of Pmsm Based on Coordination Control Technology." *Procedia Engineering*, vol. 16, 2011, pp. 157–162., doi:10.1016/j.proeng.2011.08.1066.

[7] Kosky, P. G., et al. *Exploring Engineering: An Introduction to Engineering and Design*. Academic Press, 2021.

[8] Doyle, Aisling. "2 - Traction Energy and Battery Performance Modelling." *Electric Vehicles: Prospects and Challenges*, edited by Tariq Muneer, Elsevier, 2017, pp. 93–124.

Cymone Houston

Major: Civil and Environmental Engineering

Mentor: Dr. Thinesh Selvaratnam

Research in Environmental Engineering

Department of Civil and Environmental Engineering

Biological Treatment of Produced Water

Introduction:

Produced water (PW) is a byproduct that comes out of the ground with oil and gas during oil and gas exploration and production. PW's chemical and physical characteristics vary based on the reservoir characteristics and on the extraction process. PW is one of the largest waste streams generated in the Oil and Gas industry and is estimated to be around more than 110 billion barrels per annum in the world in 2019, out of which, 21 billion barrels is produced by North America alone [1]. PW contains various aromatic and aliphatic hydrocarbons, phenols, polycyclic aromatic hydrocarbons, heavy metals (e.g., Cu, Pb, Zn, Ni, Cd, Cr), and additives (e.g., antifoam, biocides, scale, and corrosion inhibitors) which are added to the extraction process to increase efficiency and prevent operational issues [2]. Given the complex chemical and physical nature of the PW, it is paramount to treat and dispose of the PW safely, otherwise, the PW contaminants can severely impact the receiving water bodies, soils and air [3].

Over the years, multiple chemical and biological treatment techniques have been developed for PW treatment, including coagulation-flocculation, electrocoagulation, hydrocyclone, membrane filtration, gas flotation, etc [4]. However, reinjection to the disposal wells been the mostly preferred method for PW treatment in the oil and gas industry. The cost of treating one barrel of PW is $0.775, whereas the reinjection cost is 0.75-8 $/barrel [5]. Currently, most of the generated PW is reinjected into the disposal wells, and it is more expensive to reinject than to treat the PW. The cost of treating one barrel of PW is $0.775, whereas the reinjection cost is 0.75-8 $/barrel [5]. In addition to the high cost of these treatment techniques, significant input of chemicals and incomplete removal of metals are still the main limiting factors with the existing treatment processes [6]. This leads to the need for a more sustainable pathway to treat the PW.

The traditional removal of containments happens to be costly, labor intensive and environmentally unsustainable. In contrast, algal bioremediation of produced water has benefits of being environmentally cautious and reliable to treat produced water. Thus, the pollutants in PW serve as nutrients for the algae and other microorganisms inhabiting the produced water. However, significant dilution of produced water is often required in algal-based systems due to complex chemical contaminants present in PW.

Materials and Methods:

As a product of my previous research, *Galdieria sulphuraria* showed the best performance. Additionally, this algal strain can sustain high temperatures. It has a low pH, tolerates high salt and metal concentrations. *Galdieria sulphuraria* can outcompete wastewater pathogens and can handle a variety of chemicals. Therefore, in the current research it was used to treat the produced water as such. The strain of algae grown on-site and was grown under 24 hrs of continuous illumination inside the incubator at 42°C. A 16/8 hour- light and dark cycle with a temperature of 28°C. The carbon dioxide levels inside the incubator were kept around 3% and were measured every morning. Hence, giving the microorganisms an environment to increase in biomass for experimentation.

Cyanidium media (CM) was used as the standard growth media for *Galdieria sulphuraria*. In the early stages of the research, the development of large-scale culture was needed. The incubator's CO_2 levels were kept at a constant rate between 2-3% (vol/vol). All flaks used were autoclave prior to usage. To start the small-scale reactors to grow the bulk number of algae needed, CM was added to the bottom of the flasks. The algae was then added, and the flasks was placed into the incubator. Thus, the algae being in the incubator optimal density (OD) of the algal growth was then measured every morning with the spectrophotometer. The biomass density was analyzed within the confides of 'ash dry weight'. All OD value of *G. sulphuraria* were taken from 750 nm. As a result of the algae was tested for ammonia nitrogen and phosphate-phosphorus The HACH DR 3900 (HACH, Colorado, USA) with the HACH vials and powders gave different measurement ranges for each sample. The tasks of ammonia and phosphate measurement was preformed every other week. Once the algae needed a larger space to grow, they were transferred to larger Erlenmeyer flasks. Once a bulk amount of media was created the algae was then transferred into 10 mL reactors inside the incubator. Therefore, the continuation of the growth would create enough culture to be moved to 10 L large scale reactors. The 10 L large scale reactors were kept in lab temperature control room at 40°C. The OD of these 10 L reactors were taken every day to ensure the biomass growth.

Discussion:

The 1 L reactors were tubular bubbling bioreactors in an in-lab temperature control room at 40°C. The light cycle conditions were 12/12 while the CO_2 levels were kept at 2-3% (vol/vol). The two conditions in the 1 L reactors consisted of 5 tubes with control media and 5 tubes containing 20% PW. This experimental setup lasted for 7 days in the 1 L reactors. As a result, the reactors containing 20% PW showed the best results. The final biomass with the control media was 5.38 ± 0.680 g L^{-1} while the 20% PW had a biomass of 3.20 ± 0.396 g L^{-1} (Figure 1). The nutrient removal in the 1 L reactor showed significant results (Figure 2). The ammoniacal removal was greater in the 20% PW with a 97% outcome. In contrast to the control media only removing 41% of all ammoniacal nitrogen removal. The 20% PW in the case of ammoniacal nitrogen removed almost all the chemical completely. The phosphate removal of with 20% PW removed 33%.

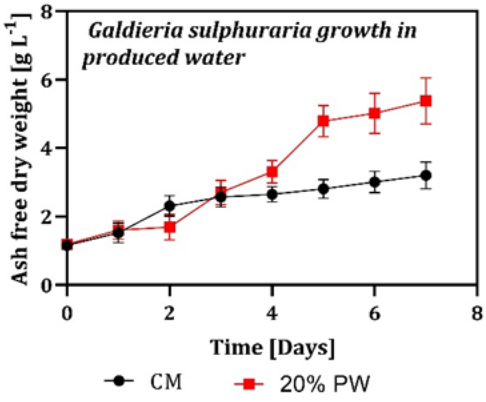

Figure 1: *G. Sulphuraria* growth 20% PW

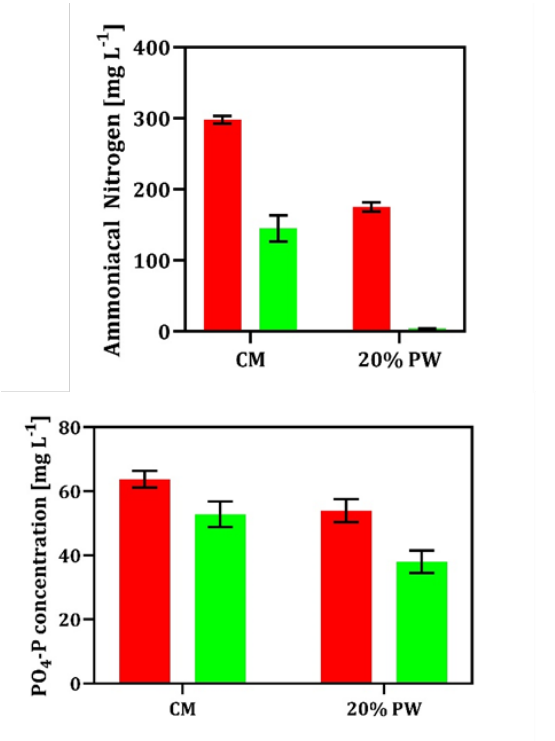

Figure 2: Ammoniacal and Phosphate Removal

Conclusion:

G. Sulphuraria for bioremediation is sufficient for removing Ammoniacal nitrogen and PO_4-P in PW. Additionally, the collective biomass and substantial nutrient removal indicates the benefits of agal based systems. Therefore, further experiments in 10 L reactors are needed to evaluate the nutrient removal and biomass growth in pilot-scale reactors. Thus, leveraging the data obtained from these pilot scale reactors to optimize the systems' performance in real life applications.

References:

[1] Global produced water volumes, produced Water Society, Webpage accessed on 02/20/2021. (https://www.producedwatersociety.com/resources/chart-data/global-produced-water-volumes)

[2] A. Fakhru'l-Razi, A. Pendashteh, L.C. Abdullah, D.R.A. Biak, S.S. Madaeni, Z.Z. Abidin, Review of technologies for oil and gas produced water treatment, Journal of Hazardous Materials, 170 (2009) 530-551.

[3] T. Bakke, J. Klungsøyr, S. Sanni, Environmental impacts of produced water and drilling waste discharges from the Norwegian offshore petroleum industry, Marine Environmental Research, 92 (2013) 154-169.

[4] P. Das, M. AbdulQuadir, M. Thaher, S. Khan, A.K. Chaudhary, G. Alghasal, H.M.S.J. Al-Jabri, Microalgal bioremediation of petroleum-derived low salinity and low pH produced water, Journal of Applied Phycology, 31 (2019) 435-444.

[5] A. Szép, R. Kohlheb, Water treatment technology for produced water, Water science and technology : a journal of the International Association on Water Pollution Research, 62 (2010) 2372-2380.

[6] A.F. Talebi, S.M.M. Dastgheib, H. Tirandaz, A. Ghafari, E. Alaie, M. Tabatabaei, Enhanced algal-based treatment of petroleum produced water and biodiesel production, RSC Advances, 6 (2016) 47001-47009.

Melissa Tan

Major in Civil and Environmental Engineering

Mentor: Dr. Thinesh Selvaratnam

Research in Environmental Engineering

Department of Civil and Environmental Engineering

Studying the Extracellular Polymeric Substances of *Galdieria sulphuraria* as Flocculation Aid for Improving Algal Harvesting Efficiency

Introduction

Some of the most promising sources of biodiesel come from microalgae. Unfortunately, because of their small sizes and low biomass densities, harvesting microalgal biomass in an economical way has proven to be a significant challenge. Filtration and centrifugation consume a considerable amount of energy and can be costly, whereas flocculation uses less energy and is a low-cost process. While this is true, it is also known that alum- and ferric-based inorganic flocculants and synthetic organic flocculants can be toxic to aquatic organisms [1]. However, naturally occurring or microorganism-derived flocculants seem to be a sustainable alternative [1] as they are non-toxic and offer high flocculation efficiency [2]. Extracellular polymeric substances (EPS) is a biopolymer secreted by algae. EPS contains many biomolecules with a wide range of potential applications. One specific application lies in the flocculation process for algal biomass harvesting. In this study, EPS was extracted from the microalga *Galdieria sulphuraria* and used to conduct flocculation experiments to assess the feasibility of using EPS to improve algal harvesting efficiency.

The strain of the microalga *G. sulphuraria* was cultivated in an environmentally controlled incubator. The strain was grown under 24 hours of continuous illumination inside of incubators at 42ºC. The carbon levels inside of the incubators were maintained at around 3%. The cultures that were obtained were streaked onto agar plates. The plates then formed single colonies, which were used to create axenic cultures. The cultures were streaked under the Labconco purifier to avoid any contamination. After media preparation, the media was sterilized through an autoclave at 121ºC. All of these conditions were met in order to grow *G. sulphuraria* without any contamination.

The EPS of *G. sulphuraria* was extracted through centrifugation. After the EPS was centrifuged at 4000 rpm for 40 minutes, the supernatant was kept and stored inside a fridge for 90 days. Before conducting any flocculation experiments, the EPS was taken out of the fridge to get to room temperature. It is important to note that each flocculation experiment requires a large amount of culture, which can take over a month to grow for one experiment. In this case, nearly two months were spent growing and maintaining the cultures. Because of the limited amount of large-scale reactors in the lab, only three flocculation experiments were conducted.

Methods

The optical density (OD) value was taken at 750 nm from each sample after a tenfold dilution for every experiment. The OD values were used to calculate the biomass density. Each sample was taken from the center of each reactor as not to disturb the algae that had settled at the bottom. The OD values would decrease as time passed as there would be fewer algae present in the center than in the bottom of the reactor. A lower OD value would indicate that more algae have settled to the bottom of the reactor.

Experiments

For the first flocculation experiment, 50-mL reactors were used, and three different conditions were tested using five replicates for each condition. For Test A, 1 mL/L of EPS was added. For Test B, 2 mL/L of EPS was added. The control samples had no EPS added. The initial OD value of the culture was measured to be 2.25 OD, which roughly translates to 1.125 g/L of algal biomass. After adding the respective amounts of EPS to the reactors of Test A and Test B, the solutions were thoroughly mixed and set to the side. The OD values of all 15 reactors were then taken after 10 minutes, 30 minutes, 1 hour, and 2 hours. A tenfold dilution was made to each sample before measuring its OD value. An interesting observation was made shortly after mixing the EPS into the samples. Floating on the surfaces of the reactors of Tests A and B were unidentified molecules (Fig. 1). This observation was not further examined and maybe an area of interest to future study. Essentially, this experiment was conducted to determine if changing the amount of EPS would affect the harvestability. As can be seen from the results, the EPS had clearly worked best in the first 10 minutes as the OD values for Tests A and B had lowered over 70% compared to the control lowering around 30% from the initial OD value (Fig. 2). Alternatively, after 30 minutes, all 15 reactors seemed

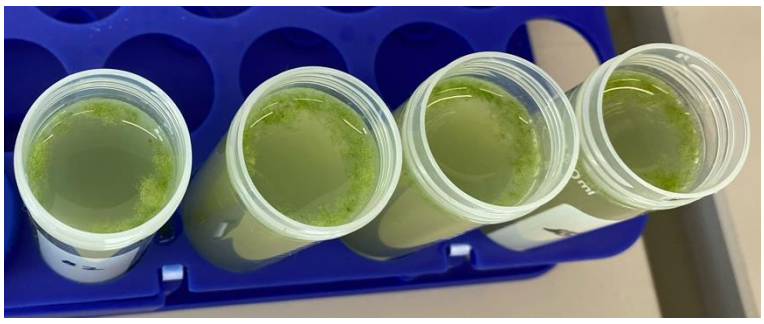

Figure 1. Molecules in Tests A and B

to have nearly the same OD values. This shows that the EPS drastically increased the harvesting efficiency for at least the first 10 minutes.

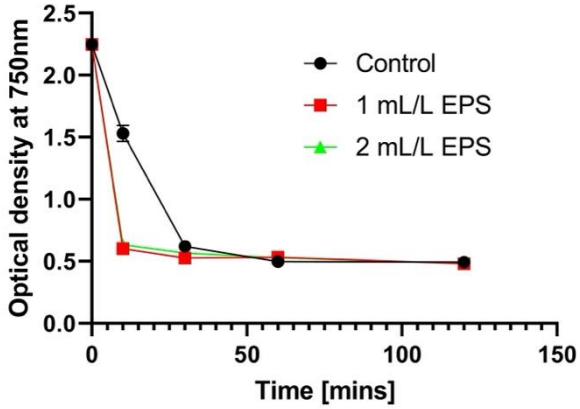

Figure 2. Experiment 1 (Optical Density)

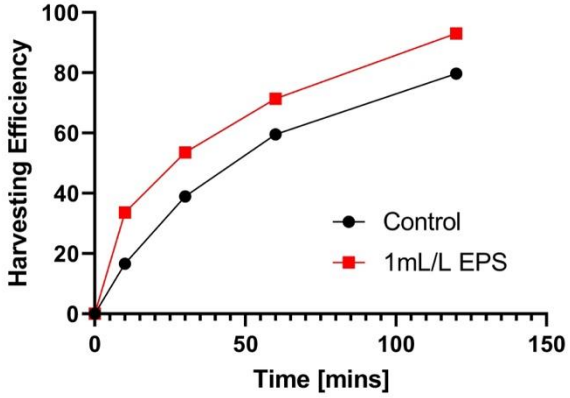

Figure 3. Experiment 2 (Harvesting Efficiency)

For the second flocculation experiment, 1-L column reactors were used, and two different conditions were tested using four replicates. For Test C, 1 mL/L of EPS was added for every 700 mL of working volume, and the control samples had no EPS added. The OD value of the initial culture was 3.30 OD, which means that there was approximately 1.65 g/L of algal biomass. The OD values of all 8 reactors were taken after 10 minutes, 30 minutes, 1 hour, and 2 hours. It was found that the reactors with the added EPS settled faster than the control samples at all times. This indicates that the reactors with EPS had a higher harvesting efficiency (Fig. 3).

For the third flocculation experiment, two conditions were set as the OD values were predetermined to be 0.6 OD (0.3 g/L of algal biomass) and 1.2 OD (0.6 g/L of algal biomass). In order to concentrate the cultures, they were centrifuged at 4000 rpm for 10 minutes. The supernatant was discarded, and the centrifuged algal biomass was kept to make two concentrated cultures. For this experiment, 50-mL reactors were used for two different conditions. Test D used the culture with the value of 0.6 OD, and Test E used the culture with the value of 1.2 OD. Each test had 4 reactors as their control and 4 reactors with 2.5 mL/L of EPS added, so there were a total of 16 reactors used in this experiment. The OD values of all 16 reactors were taken after 10 minutes, 30 minutes, and 1 hour. This experiment was conducted to see if a higher amount of EPS (compared to 1 mL/L of EPS in Experiment 1) mixed with varying concentrations of cultures would affect the harvestability. Throughout the experiment, the reactors with the EPS had a higher harvesting efficiency compared to their controls.

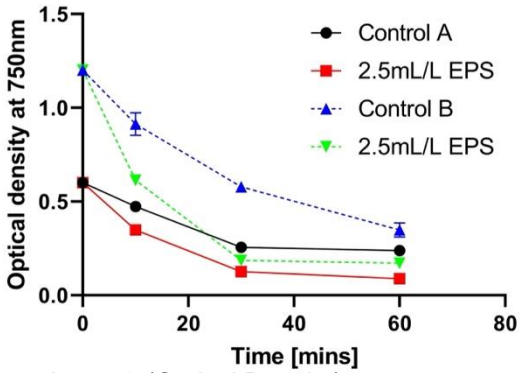

Figure 4. Experiment 3 (Optical Density)

Conclusions

Due to the limited time and unavailability of large reactors, only a limited number of experiments were able to be conducted. The addition of EPS seemed to improve short-term harvesting efficiency up to 2 hours. Moreover, the harvesting efficiency was observed to be higher within the first 30 minutes. Even so, more detailed experimentations are needed to make a conclusive argument that the addition of EPS improves algal harvesting efficiency.

References

[1] Yang, L.; Zhang, H.; Cheng, S.; Zhang, W.; Zhang, X. Enhanced microalgal harvesting using microalgae-derived extracellular polymeric substance as flocculation aid. ACS Sustainable Chem. Eng. 2020, 8, 4069−4075.

[2] Rashid, N.; Park, W.; Selvaratnam, T. Binary culture of microalgae as an integrated approach for enhanced biomass and metabolites productivity, wastewater treatment, and bioflocculation. Chemosphere 194 (2018) 67-75.

Gabriel West

Mentors: Dr. Sushil Doranga and Dr. Jenny Zhou

Research in Department of Mechanical Engineering

Department of Mechanical Engineering

Vibration Response Prediction of Printed Circuit Boards used in The Transportation Industry

The in-service vibrations that occur within a transport vehicle during operation can compromise its electronic systems, thus, decreasing the vehicle's reliability. Printed circuit boards (PCBs) and Printed Circuit Board Assemblies (PCBAs) predominantly experience failure due to such vibrations. The objective of this research was to select a best candidate material properties model for PCBs and PCBAs based on the dynamic response under various vibration excitations. The isotropic and orthotropic properties models of the PCBs available in the existing literature were numerically simulated using the finite element (FE) based tool and the obtained results were compared through direct experimentations, conducted in a bare PCB using the impulse hammer and a modal shaker. Comparisons of the responses between the theoretical and the experimental results showed that the theoretical orthotropic model of the PCB was close to the experimental model. In addition, the experimental results suggest that the modulus of elasticity of the PCBs varies across the lateral, longitudinal and vertical directions.

1. Introduction

When evaluating PCBs the observations must begin at the base level of the composition of the PCB itself. The specific composition that is evaluated in this research is a six-layer configuration with both isotropic and orthotropic mechanical properties. Testing the two different setups is crucial as the difference between isotropic and orthotropic shows the baseline behind why simulation of just an isotropic PCB (as done in most existing literature and industry) simply is not accurate enough to create a reliable baseline for later in the research due to the differences in the mechanical properties.

2. Simulation

For this project a large portion of the work to create the baseline values was done via harmonic simulation and was done through DSS Solidworks Simulations tool. The simulations specifically were linear harmonic tests. In total, eight of these tests were simulated to see the response of our 4 different models **[table 1]** of PCB which were found in existing literature in clamped-free and clamped-clamped configurations **[figures 1 & 2]**. Model 1 is the control for an isotropic PCB, this is being simulated to give a quick glimpse of how much the response of an isotropic PCB varies from multiple different orthotropic PCBs (Models 2, 3, & 4). The simulation portion of this experiment is of extreme importance as it shows how under perfect conditions the PCB should react. Models 2, 3, and 4 are used primarily to use as comparisons to relate with the experimental data to have a rough estimate of what the properties of the physical PCB are.

Material Property	Model 1 Isotropic	Model 2 Ortho 1	Model 3 Ortho 2	Model 4 Ortho 3
E_x (Pa)	1.50E+10	1.69E+10	1.90E+10	2.30E+10
E_y (Pa)	1.50E+10	1.69E+10	2.30E+10	1.90E+10
E_z (Pa)	1.50E+10	7.40E+09	4.00E+09	4.00E+09
G_{xy} (Pa)	5.30E+09	7.60E+09	1.97E+10	1.97E+10
G_{xz} (Pa)	5.30E+09	3.30E+09	1.97E+10	1.97E+10
G_{yz} (Pa)	5.30E+09	3.30E+09	1.97E+10	1.97E+10
ν_{xy}	0.39	0.11	0.1	0.1
ν_{xz}	0.39	0.39	0.4	0.4
ν_{yz}	0.39	0.39	0.38	0.38
Mass Density (kg/m^3)	1910	1910	1900	1900

Table 1: Mechanical Properties found in literature

3. Manufacturing

The manufacturing of this experiment was a huge component of the project as it had to be completely designed and built from scratch. The best option for material for the apparatus would be a solid metal like billet aluminum due to its known mechanical properties as well as it being one solid piece, but due to budget constraints it was decided to make the apparatus' components via 3D printer which used a PLA extrusion. This was convenient due to the relative ease of making changes if necessary and reprinting pieces if needed in a short time span. However, during experimentation of the physical PCB it was found that the PLA which has a Young's Modulus range of 0.05- which is low enough where the simulations and physical experimentation could be thrown off slightly. Also due to the large range the value picked for the stands in the simulation may not exactly match the material the physical apparatus is made of.

4. Experimentation

The experimentation for this project consists of two configurations one being a clamped-clamped configuration **[figure 1]**, and the second being clamped-free **[figure 2]**. The first test was used to find the natural frequencies of the physical PCB. This test used the modal hammer **[figure 3]** to test the response of the PCB through an impulse test which showed the response through a range of 0-500 Hz. The hammer tests were done for both the clamped-free and clamped-clamped configurations. For the second phase of experimentation the modal shaker was introduced to the testing apparatus **[figure 4]**. These tests were modal time history tests which were used take the natural frequencies found in the first experiments and applied a small range of frequencies around them to see the response of the PCB around the natural frequencies. This is done to have more precise dynamic responses of the PCB.

Figure 1: Clamped-Clamped Configuration

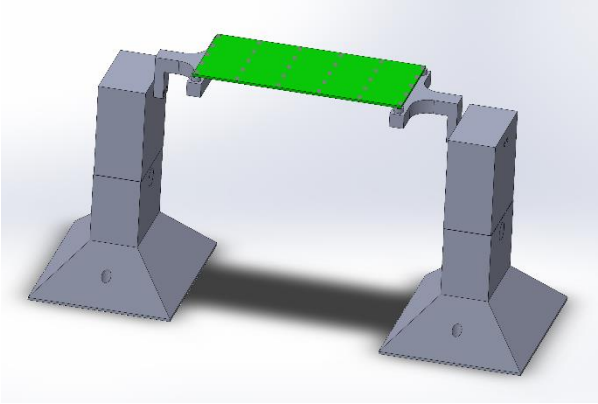

Figure 2: Clamped-Free Configuration

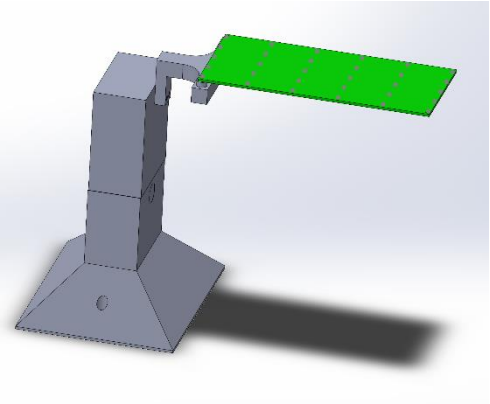

Figure 3: Impulse Hammer

Figure 4: Modal Shaker

5. Results

The first test done was the linear harmonic (hammer) tests during these tests the clamped-clamped configuration gave extremely consistent values that can be shown in Table 2. When testing the clamped-free configuration however the issues of sensitivity, and major feedback noise come into play which prevented the

ability of getting solid frequency values. Due to the inconclusive testing to make up for it the modal testing for clamped-free had to be over wider ranges and were based off the simulation of Model 3 as it is so similar.

Experimental Natural Frequencies	
Linear Harmonic Tests	Clamped-Clamped (Hz)
Test 1	58.6
	82
	127
Test 2	58.6
	82
	127
Test 3	58.6
	82
	127

Table 2: Hammer Test Results

During the simulations of the four model PCBs the responses of all four can be seen in **[figures 5 & 6]**, but as the first natural frequencies had the largest response the focus of the experimentations went to the first natural frequency of the PCB. When viewing **[figures 7 & 8]** the relationship of Model 3 and the experimental results the mechanical properties of Model 3 became the benchmark values to relate as its first natural frequency was at 56.54 Hz with a response of 55.90 G in the clamped-clamped configuration and 17.65 Hz and a response of 30.93 G in the clamped-free configuration. These values most closely relate to the experimental data collected of 17.04 Hz and 28.32 G for clamped-free and 55.13 Hz and 54.79 G in the clamped-clamped setup. These results show the necessity of properly simulating a PCB as if it is not done it will drastically change the results to the point where the simulation is useless as it won't supply realistic data.

Figure 5: Total simulation response C-F

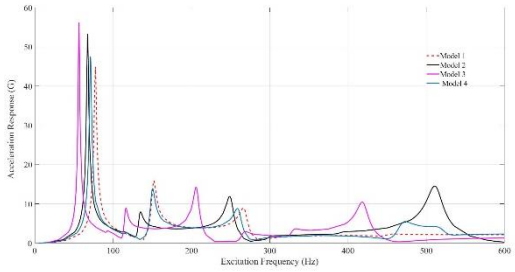

Figure 6: Total simulation response C-C

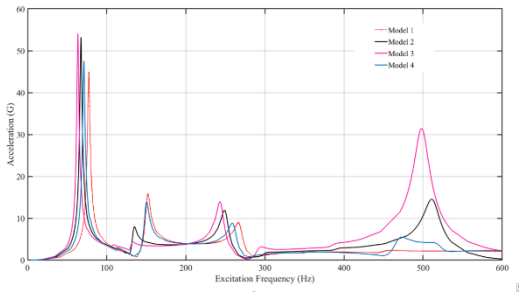

Figure 7: First Frequency Shaker Results C-F

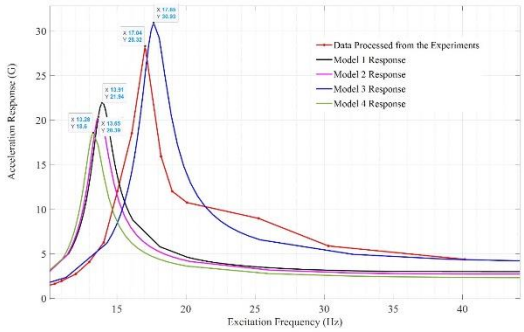

Figure 8: First Frequency Shaker Results C-C

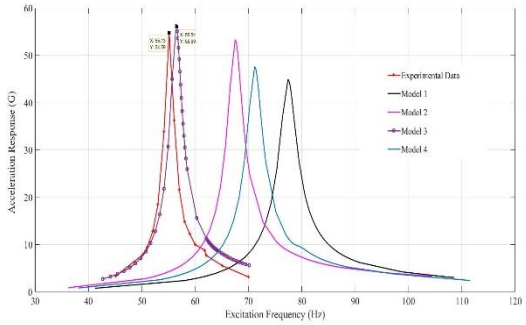

6. Conclusions

In the present work the dynamic responses of printed circuit boards have been examined with simulations and experimentation.

During the simulations and experimentations, the natural frequencies of 1 isotopic PCB and 4 orthotropic PCBs have been extracted and compared among one another to examine the relationships between each model. It has been determined that the dynamic responses and therefore the natural frequencies of an isotropic and orthotropic PCB do not match. This is due to the comparison of simulation and experiment showing a high degree of similarity between each other.

7. Future Works

The first of the future works will be compiling the responses of the physical experiments to determine the mechanical properties of the physical PCB to complete further research of the PCB. The next is to repeat this physical experimentation we did in the present works, but with a printed circuit board assembly (PCBA) to determine the differences on dynamic response due to the added mass. As the present work was done to see if simulating an isotropic PCB would be a valid option due to its simplicity; the future work would be to determine if the increase in mass of a PCBA would warrant a large enough difference in dynamic behavior to warrant its own full simulation as opposed to simulating a bare PCB with the correct mechanical properties.

References:

1. Somashekar, V. N., et al. "Vibration response prediction of the printed circuit boards using experimentally validated finite element model." *Procedia Engineering* 144 (2016): 576-583.
2. Thraza, M. Mary, and V. N. Somashekar. "Modelling and simulation of effect of component stiffness on dynamic behaviour of printed circuit board." *International Journal of Pure and Applied Mathematics* 118.17 (2018): 75-89.
3. Amy, Robin Alastair, Guglielmo S. Aglietti, and Guy Richardson. "Accuracy of simplified printed circuit board finite element models." *Microelectronics Reliability* 50.1 (2010): 86-97.
4. Kalyani, Uday H., and Mark Wylie. "Modal finite element analysis of PCBs and the role of material anisotropy." *Vibroengineering PROCEDIA* 32 (2020): 75-80.
5. F. Arabi, A Garcia, J.-Y Deletage, H. Fremont. "*Vibration Test and Simulation of Printed Circuit Board."* (2018).

Damaris Thrash

Major in Exercise Science

Mentor: Dr. Shannon Jordan

Research in Exercise Science

Department of Health and Kinesiology

Effects of Motivational Music on Post-Exercise Recovery

Previous studies have been conducted to analyze the physiological effects listening to motivational music has on exercise performance. For music to be considered "motivational", literature suggests a tempo of 120-140 bpm if it is expected to elicit a positive response during high-intensity exercises. However, there is a scarcity of research analyzing the effects of music during the post-exercise recovery period (EPOC). Due to this, my research study was meant to examine the effects of types of music on exercise recovery.

With OUR support, my mentor Dr. Shannon Jordan and I were able to carry out this project. With the funds provided, we purchased materials needed to conduct this experiment, including filters, hoses, and headgear for the Lamar University Health and Kinesiology Department's ParvoMedics Metabolic Cart (in order to measure metabolic gas exchange variables) and the book *Applying Music in Exercise and Sport* by Costas I. Karageorghis. This textbook provided the Music Brunel Rating Inventory (MBRI), a validated survey tool that was used to assess the degree to which is deemed motivational.

While working on this research project, I learned many new skills that will be beneficial to me in the future, as one of my goals is to attend graduate school. These new skills include becoming more proficient in taking exercise blood pressure, analyzing data, and using Excel. Dr. Jordan has also taught me how to calibrate and perform maintenance on the metabolic cart, as well as analyze lactate samples.

For this experiment, our goal was to recruit ten healthy, college-age (non-smokers, 18-30 years) participants. Each participant completed an initial evaluation – including providing an informed consent and a PARQ+ (an IRB approved screening tool). Participants meeting the criteria performed a treadmill exercise test to determine their aerobic fitness level (VO_{2peak}). Throughout the test heart rate (HR), blood pressure (BP), and lactate were monitored, along with metabolic gas exchange. Next, participants performed at 70% of their VO_{2peak} for three different exercise trials in which they would listen to different types of music during the recovery period of each session. Participants completed three trials in random order:

Exercise	**Recovery**
Motivational Music	No Music
Motivational Music	Motivational Music
Motivational Music	Calming Music

Exercise recovery was determined based on post-exercise gas exchange data, heart rate, blood pressure, and blood lactate. Data were organized into an excel sheet and analyzed in the statistical program SPSS. A total of ten participants have completed all exercise trials.

Our findings showed no difference in recovery when comparing the three different trials. This conflicts with our research hypothesis that calm music, or no music would allow the participants to recover more quickly during the EPOC. In the attached data table, you can see the means ± SD for heart rate, systolic and diastolic blood pressure, lactate, VO2 (absolute and relative), ventilation (VE), respiratory rate (RR), and respiratory exchange ratio (RER). When the statistical analysis was performed in SPSS, there were no significant differences between music trials for any physiological variable associated with recovery during the EPOC.

Throughout this process, there were challenges we faced and overcame, one being when a participant's braces made it difficult to fit the mouthpiece in their mouth correctly, causing it to pop out in the middle of their run. Since the trial was not completed, the participant had to reschedule while the team retrieved a mouthpiece that was shaped differently and more suitable for the participant's condition. Another problem manifested itself with scheduling and the number of participants able to complete all five visits of the experiment. Originally, we aimed to have fifteen or more participants sign up in order to have ten totals, accounting for attrition. We recruited thirteen participants. One dropped out due to being a front-line worker and not having time off work. Another took a full-time job in another city. The third person who dropped out of the study was uncomfortable walking on a treadmill and had trouble keeping their balance.

Personally, I also found monitoring blood pressure to be a little challenging; it can be difficult to detect Korotkoff sounds (the sounds emitted while recording a person's blood pressure) when the person being monitored is active; their constant movement can affect the gauge, and their footfalls can make it difficult to hear. For this experiment, motivational music was required during exercise at a certain volume, adding to the noise levels. However, as I grew more experienced, I also grew more confident in my readings.

While I have not yet had an opportunity to present my research at any conference or venue to date, I hope to do so at both the Ninth Texas STEM Conference and the 2022 Texas American College of Sports Medicine meeting. We plan to extend our recruitment efforts further into the fall in order to obtain more participants

beyond our initial goal of ten participants in order to have a larger data set to present at the ACSM conference in the spring. This will also give us a more robust data set to prepare a manuscript for a publication in a peer-reviewed scientific journal within the field of exercise science.

This experience fueled my interests for this topic and my love for the study of exercise science in general. Not only has it made me more confident in my abilities and what I want my future career to revolve around, but it has created a much more curious mind and stimulated a great and newfound appreciation for research within me as well. If I had known how much I would come to enjoy research through this experience beforehand, I would have applied for SURF and all the opportunities if offers sooner. As it is, I cannot wait for future chances to conduct more studies.

	Exercise Intensity During 20-minute Exercise Trials				
	Absolute VO2 (L/min)	Relative VO2 (ml/kg/min)	Percent VO2max	Max Heart Rate (bpm)	Percent HRmax
No music	2.1 ± 0.7	24.29 ± 6.57	70.1 ± 4.59	187 ± 7	81.4 ± 4.7
Motivational	2.1 ± 0.6	23.73 ± 6.44	72.3 ± 4.8	188 ± 7	82.8 ± 5.4
Calm	2.1 ± 0.7	23.13 ± 6.71	69.8 ± 4.7	188 ±	83.4 ± 6.7

The goal for each 20-minute exercise session was to have the participants exercise at 70% of their VO2max…or maximal aerobic capacity. In this table, you can see the percent VO2max was similar between treatment groups and we were able to hold the exercise intensity steady in order to ensure that any results were not due to different exercise intensities between trials.

		No Music	Motivational Music	Calm Music
Heart Rate (bpm)	IPE	136 ± 12	146 ± 13	135 ± 14
	7 Min Post	98 ± 9	100 ± 8	100 ± 8
	15 Min Post	92 ± 8	91 ± 8	91 ± 9
SBP (mmHg)	IPE	152 ± 18	165 ± 25	160 ± 17
	7 Min Post	131 ± 13	131 ± 18	131 ± 18
	15 Min Post	124 ± 7	124 ± 9	121 ± 8
DBP (mmHg)	IPE	75 ± 7	77 ± 8	77 ± 7
	7 Min Post	82 ± 6	82 ± 7	82 ± 4
	15 Min Post	82 ± 6	83 ± 8	81 ± 6
Blood Lactate (mmol/L)	IPE	4.2 ± 2.3	4.7 ± 2.6	4.5 ± 2.1
	7 Min Post	3.0 ± 1.6	3.1 ± 1.6	3.1 ± 2.0
	15 Min Post	2.1 ± 0.9	2.0 ± 1.1	2.1 ± 1.1
	No significant differences between treatments for any time point			
	SBP= Systolic Blood Pressure; DBP=Diastolic Blood Pressure			

Our findings showed no significant differences during the EPOC, or recovery stage between treatments, for the variables measured. Data in this table depicts the 15-minute EPOC period. IPE stands for Immediately post exercise. Participants had stopped exercising and stood still on the treadmill for the IPE measurements. Participants then sat quietly for the remainder of the 15-minute EPOC period, where measurements were taken at 7 and 15 minutes post exercise. Data represented in this table are heart rate, systolic and diastolic blood pressure, and blood lactate.

		No Music	Motivational Music	Calm Music
Absolute VO2 (L/min)	IPE	0.7 ± 0.2	0.7 ± 0.2	0.6 ± 0.2
	7 Min Post	0.4 ± 0.1	0.7 ± 1.2	0.4 ±0.1
	15 Min Post	0.3 ± 0.1	0.3 ± 0.1	0.3 ± 0.1
Relative VO2 (ml/kg/min)	IPE	8.50 ± 2.25	7.86 ± 2.32	7.15 ± 2.38
	7 Min Post	4.20 ± 1.20	3.82 ± 1.17	4.11 ± 1.46
	15 Min Post	3.69 ± 0.94	2.99 ± 1.11	3.89 ± 1.24
Ventilation (L/min)	IPE	20.18 ± 6.06	19.94 ± 3.76	19.10 ± 5.55
	7 Min Post	11.48 ± 4.03	9.61 ± 2.48	10.25 ± 2.17
	15 Min Post	9.89 ± 4.33	7.17 ± 1.82	8.63 ± 2.57
Respiratory Rate (bpm)	IPE	21.00 ± 3.61	22.40 ± 3.10	22.80 ± 2.90
	7 Min Post	18.67 ± 3.94	19.70 ± 3.56	17.90 ± 4.56
	15 Min Post	16.11 ± 4.26	15.20 ± 2.30	16.20 ± 2.30
Respratory Exchange Ratio	IPE	1.13 ± 0.11	1.13 ± 0.07	1.14 ± 0.05
	7 Min Post	0.97 ± 0.12	0.95 ± 0.06	1.02 ± 0.14
	15 Min Post	0.85 ± 0.07	0.90 ± 0.11	0.83 ± 0.05

Data represented in this table are absolute and relative VO2, ventilation, and respiratory rate during each measurement period of the EPOC. Respiratory exchange ratio, which is the ratio of expired volume of CO_2 to O_2 is also reported in this table. No significant differences were found between different treatment conditions.

POSTERS

In alphabetical order

Poster 1 / Graduate Research

Presenter: Claire Elizabeth Alexander

Mentor: Dr. Maryam Vasefi

Department of Biology, Lamar University

Research in Biology

Cannabidiol (CBD) Signaling through Serotonin Receptor Subtype 1 (5-HT1AR)

Cannabidiol (CBD) is a cannabinoid associated with anxiolytic, antidepressant, and neuroprotective effects, with the potential to treat multiple psychiatric disorders due to its variety of molecular targets including 5-HT1AR and the endocannabinoid system. A recent study revealed that chronic CBD-mediated desensitization of 5-HT1AR induced an anxiolytic effect in rodents, though this effect has not been observed in humans. Moreover, SSRIs exert antidepressant effects via desensitization of 5-HT receptors, though these drugs may have unpleasant side effects. Thus, the objective of this study is to observe a dose-dependent and time-dependent 5-HT1AR desensitization effect of CBD in human SH-SY5Y cells. The underlying signaling cascade will be elucidated via western blot, RT-PCR, and agonist-antagonist studies. CBD-mediated endocannabinoid signaling as a contributor to these effects will be investigated by confirming the utility of 5-HT1AR-ERK1/2 signaling in receptor desensitization. This study will reveal that CBD desensitizes 5-HT1AR via a similar mechanism to SSRIs, supporting the utility of CBD as a novel anxiolytic and antidepressant alternative to currently available pharmaceuticals.

Poster 2 / Graduate Research

Presenter: Maryam Bahrami

Co-author: Lac Nguyen

Mentor: Dr. Robert Bradley

Department of Industrial and Systems Engineering, Lamar University

Research in Nanotechnology

Progress in Carding Single Wall Carbon Nanotubes

Single wall carbon nanotubes (SWCNTs) have the form of graphene sheets rolled into seamless tubes. They are known for valuable features such as, possibly, the highest tensile strength, high strength/weight ratio, excellent electrical and thermal conductivity, and resistance to chemical corrosion. SWCNTs, despite their significant properties, are challenging to convert from raw as-produced form into yarn or thread, a process known as spinning. According to the literature, there are two methods for SWCNT spinning: 1) wet spinning which requires the addition of liquid or polymer that must be removed in a later step and 2) direct spinning in which the spinning process occurs simultaneously with SWCNT production. We present work that could lead to a new method for SWCNT spinning which overcomes the previous methods disadvantages. The presented work is based on carding, an initial step in production of wool yarn, to process dry as-produced SWCNT material. We tested different strategies to extract SWCNTs from carding arrays, and to study the degree of alignment we set up SEM and TEM analysis. Progress on our research will be presented.

Poster 3 / Graduate Research

Presenter: Caitlyn Clark[1]

Co-author: Emily Ingram[1]

Mentors: Dr. Ozge Gunaydin-Sen[1] and Dr. David Brook[2]

[1]Department of Chemistry and Biochemistry, Lamar University

[2]Department of Chemistry, San Jose State University, San Jose, CA 95192

Research in Chemistry

Physical Tuning of Photo-Chemical Response in Biverdazyl Biradicals

Photo-physical properties of small organic molecules are significant to understand in physical-organic chemistry. Early studies show that magnetic properties found from these systems can be used extensively in the electronics, computer technologies, and renewable energy fields. Unlike previously studied open-shell systems with kinetically trapped spin states, Biverdazyl biradicals are stable above room temperature to approximately 373.15 K which allows physical tuning to be conducted with ease. Two biverdazyl biradical's thermo-optical properties were examined, 1,1′,5,5′-tetramethyl-6,6′-dioxo-3,3′-biverdazyl (B1) and Methylene Bis(1,5-diisopropyl-6-oxoverdazyl) (B2), in high temperature, 300-400 K, UV-VIS experiments. As a change in temperature occurs, a photo-chemical color contrast can be observed driven by the singlet-triplet state equilibrium in the model. By following the model, their structure-property interactions can be studied by thermo-optical or magneto-optical response. The changes observed on the spectra can be analyzed using two techniques which can be combined to acquire the singlet-triplet spin gap of these biradicals, Curie-like population analysis and Beer's law analysis. By using this analytical framework, not only will the singlet-triplet spin gap be extracted, it can also differentiate between a singlet or triplet state excitation in the difference absorption spectrum (optical response) unlike electron paramagnetic resonance. Analysis of their photophysical properties suggests, stronger excitations are representative of $\pi \rightarrow \pi^*$ while the weaker excitations are representative of forbidden $\pi \rightarrow \pi^*$ transitions. Investigating the photophysical properties of B1 determined an average spin gap, Δ_0, for Curie population and Beer's Law analysis, found to be, 303.3 K and 369.0 K, respectively. Currently, only preliminary results are available for B2.

Poster 4 / Undergraduate Research

Presenter: Jesus Esquivel[1]

Co-authors: Dr. T. Thuy Minh Nguyen[1] and Dr. Mien Jao[2]

Mentor: Dr. Paul Bernazzani[1]

[1]Department of Chemistry and Biochemistry, Lamar University

[2]Department of Industrial and Environmental Engineering

Research in Forensic Chemistry

Remediation of Contaminants in Dredged Soil: A Gas Chromatography Analysis

The reuse of dredged materials (DM) is an important problem for waterways and port management systems. One of the key issues associated with dredged soils is the possible chemical contaminants they contain. The use of biochemical entrapments of contaminants to control this issue was investigated. The organic content of untreated and treated dredged soils was extracted using liquid-liquid extraction techniques and analyzed by gas chromatography. Results show that the biotreatment induced an 85% reduction of the most dominant contaminant. However, sample heterogeneity leads to challenges in the quantitation of the effects.

Poster 5 / Graduate Research

Presenter: Md Abrar Jamil[1]

Co-authors: Gregory D. Twing [1,2]

Mentors: Dr. Suying Wei[1] and Dr. Sylvestre Twagirayezu[1]

[1]Department of Chemistry & Biochemistry

[2]Department of Chemical Engineering, Lamar University

Research in Chemistry

Evaluation of Molecular Rotational Resonance Technique for Fast Monitoring Sulfur Dioxide in Ambient Air

As part of the efforts to determine the applications of molecular rotational resonance technique to SO_2 monitoring in ambient air, a K-band MRR Analyser has been employed to record MRR signatures of multiple synthetic air pollutants containing SO_2 and MRR signatures of SO_2. The observed MRR features reveal a rich rotational pattern due to MRR's sensitivity. The interferants matrices (i.e., air moisture), which typically challenge other conventional techniques, show no impact on MRR signatures of SO_2. The validity of MRR for SO_2 monitoring has been examined by measuring MRR signal response over a set of standard samples of SO_2 at different sampling pressures (5-15μTorr). The obtained linear correlations allowed the determination of recovery percentage (97-100%) and low detection of limit better than 1mg/m^3. Work to improve this analytical procedure is underway and will be reported in this talk.

Poster 6 / Undergraduate Research

Presenter: Mariela Marquez

Mentors: Dr. Paul Bernazzani and Dr. T. Thuy Minh Nguyen

Department of Chemistry and Biochemistry, Lamar University

Research in Forensic Chemistry

Gas Chromatographic Analysis of the Effect of Aniline on Plant Cell Lipids

Aniline is an important industrial chemical that has become a major environmental concern because of its toxicity. Natural remediation may be evaluated by exposing plant cells to this contaminant. We evaluated the ability of plant cells (Pinus Taeda leaves) to metabolize aniline in order to both survive and reproduce. Plant cells were exposed to aniline by growing in a media containing about 10 mM of contaminant. Membrane lipid content was extracted and analyzed using gas chromatography for both the absence and presence of the toxin used. Results show that the cells surviving the treatment had a significant number of new types of lipids.

Poster 7 / Undergraduate Research

Presenter: Poorna Menon[1]

Co-author: Dr. Ramkumar Menon[4]

Mentor: Dr. Lauren Richardson[2,3]

[1]University of Texas at Austin

[2]Department of Obstetrics & Gynecology, Division of Maternal-Fetal Medicine & Perinatal Research, The University of Texas Medical Branch at Galveston

[3]Department of Neuroscience, Cell Biology & Anatomy, The University of Texas Medical Branch at Galveston

[4]Department of Obstetrics & Gynecology, Division of Maternal-Fetal Medicine & Perinatal

Research, The University of Texas Medical Branch at Galveston

Research in Biology

The Effects of Extra Cellular Matrix Collagen Rigidity on 3-Dimensional Cultures of Fetal Membrane Cells

Objective: Human fetal membrane (amniochorion) lines the inner uterine cavity to hold amniotic fluid and the fetus during pregnancy. This study tested cell-collagen interactions and the impact of collagen rigidity in maintaining membrane integrity required to support pregnancy.

Methods: To determine the optimal substrate rigidity for 3-dimensional (3D) growth of amnion epithelial and mesenchymal cells (AECs and AMCs from fetal membranes) were cultured in a 6-well soft substrate plates coated with matrigel (1:50) and biocompatible elastomer with various rigidities (0.5, 2, 8, 16, 64kilopascal[kPa]). Cells were analyzed for morphology and viability (bright field microscopy and crystal violet staining), cellular transitions (vimentin/cytokeratin-18(CK-18) ratios) and inflammatory markers (ELISA). T-test was used for statistical analyses.

Results: Compared to control cells (standard culture conditions), AECs in each of the substrate rigidities formed spheroids and sheets (3D forms) and retained cell viability. AECs in the 8 kPa plates (determined as optimum rigidity) grew multiple mono-layer cell sheets, grew vertically into the media, remained viable, and maintained epithelial characteristics (CK-18/vimentin ratio; $p < 0.0001$) when transplanted into a normal culture environment. AMCs did not form 3D structures, yet cells remained viable, and had morphology and vimentin like AEC's suggesting that the environment (matrix and rigidity) favored mesenchymal to epithelial transition (MET).

Conclusion: An in vitro model recreated fetal membrane cell-collagen interactions occurring during pregnancy. Under an optimal environment, AECs proliferated, produced an amnion membrane sheet. MET of AMC may support sheet formation to aid fetal membrane remodeling. An interruption to this remodeling process can cause premature birth.

Poster 8 / Graduate Research

Presenter: Fatih Omeroglu

Mentor: Dr. Yueqing Li

Department of Industrial and Systems Engineering, Lamar University

Research in Industrial Engineering

Effect of Background Music on Task Performance

Music is a very big part of human lives. It affects mood, emotions, and even cognitive processes. The study aimed to identify how the human brain and short-term memory are affected when participants listen to the music, they prefer compared to the music they dislike. Electroencephalogram (EEG) brain signals were collected from individuals during the Corsi block tapping task (CBT) under 4 different background music conditions; preferred relaxing music, preferred energetic music, disliked music, and no background music. Results showed that participants achieved significantly better CBT scores while listening to their choice of relaxing music. Additionally, preferred energetic and relaxing music had a significant effect on theta power spectral density (PSD) on frontal lobe, alpha frontal asymmetry, and alpha parietal asymmetry. Results and analysis of this study can serve as a valuable guideline to understand the effects of sonic stimulations on cognitive performance and working memory.

Poster 9 / Graduate Research

Presenter: Anthony Osu

Mentor: Dr. Maryam Vasefi

Department of Biology, Lamar University

Research in Biology

Glutamate Receptor Interactions in Alzheimer's Disease

Brain cell deterioration indicated by memory loss, confusion, and changes in behavior are characteristics of cognitive decline that eventually progresses to Dementia. One of the most common forms of dementia is Alzheimer's disease (AD) and almost 6 million Americans have been currently diagnosed with this disease. One of the main hallmarks of AD is the accumulation of Beta- Amyloid (Aβ); a neurotoxic peptide that can initiate brain tissue damage. The progression of AD is correlated to Aβ oligomer aggregation and deposition in the brain. Aβ oligomer has the ability to bind with Metabotropic Glutamate receptor Subtype 5 (mGluR5) to alter receptor signaling in the cell. This alteration can induce excitotoxicity and cell death, but the underlying mechanism is not clear. In this research, we will be investigating if Aβ interaction with mGluR5 causes excitotoxic effects via changes in N-methyl-D-aspartate (NMDA) receptor activity and expression using western Blot and RT-PCR procedure. We are expecting to see mGluR5 signaling to change NMDA receptor blockade response in Alzheimer's disease. Suggesting that treatment with both mGluR5 antagonist and NMDA antagonist decreases the excitotoxicity of nerve cells in Alzheimer's disease condition.

Poster 10 / Undergraduate Research

Presenter: Joshua Smith[1]

Mentor: Dr. Sylvestre Twagirayezu[1]

Co-authors: Zhao Jianbao[2] and Brant Billinghurst[2]

[1]Department of Chemistry and Biochemistry, Lamar University

[2]Canadian Light Source Inc, Saskatoon, SK S7N 2V3

Research in Biochemistry

Synchrotron-based Attenuated Total Reflection (ATR) Infrared Spectroscopy of Artificial Gasoline Blend

Synchrotron-based ATR infrared spectra of artificially prepared gasoline blend have been recorded in the 600-4000 cm^{-1} region, at varied ethanol concentrations, using the Canadian Light Source Far-Infrared Beamline. The observed spectra reveal rich but distinct vibrational signatures of ethanol and gasoline. Whereas the vibrational spectrum of ethanol displays OH-stretch (3000-3600 cm^{-1}) and CO-stretch(1000-1150cm^{-1}), the spectrum of gasoline does not show any of those vibrational bands. The CO and C-C bands have been further analyzed to determine the shifts in forces constants. It is noted that the shift in force constant rises as the concentration of gasoline increases, and thus, confirming the impact of hydrocarbon on the ethanol in gasoline mixture. This work set the next stage for examining the exact nature of polar impurities in petroleum mixtures.

Poster 11 / Undergraduate Research

Presenter: Talon Weaver[1]

Mentors: Dr. Evgeny Romashets[2] and Dr. Cristian Bahrim[2]

[1]Department of Civil and Environmental Engineering, Lamar University

[2]Department of Physics, Lamar University

Research in Space Science

Toroidal magnetic clouds in solar wind

We adopt a dynamic model for the propagation of toroidal magnetic clouds from 2.5 solar radii to the Earth's orbit. In-situ magnetic and plasma measurements are fitted with Romashets and Vandas (Geophysical Research Letters, 2003) formulae for the determination of the size and orientation of the cloud near the Earth's orbit. We apply this information for finding the shape and speed of the toroid on its trajectory as it propagates through Heliosphere. Marubashi et al. (Solar Physics, 2015) applied this approach for finding the shape and speed of 53 toroidal clouds near the Earth's orbit. A detailed analysis is reported for the geomagnetic storm on September 25, 1998. The maximum speed of the cloud is close to 640 km/s when reaching the helio-distance r =3 solar radii. Conditions in the solar wind outside of the cloud are available from modeling. Thus, the quiet conditions in solar wind are determined in the period of one day prior to arrival of the cloud, given that the period provides almost constant values of density, velocity, and magnetic field. The average values inside the cloud are taken from measurements within the interval of Marubashi's list. The cloud's arrival time and speed near the Earth's orbit are in good agreement with observations from existing literature. The profiles of the particle density and the size of the cloud versus heliodistance are presented.

Breakout sessions

In alphabetical order

Talk / Doctoral Research - Advanced

Presenter: Nurul Azam

Mentor: Dr. Masoud Mahjouri-Samani

Department of Electrical and Computer Engineering, Auburn University, AL

Research in Material Sciences

Laser Based Synthesis of Two-Dimensional (2D) Quantum Materials

Two-dimensional (2D) layered materials, including transition metal dichalcogenides (TMDCs), exposed numerous bizarre properties that recently been at the center of the quantum materials and information sciences research. In the demand of the rapid progress of 2D materials filed, many efforts have concentrated on developing new approaches, including physical and chemical vapor deposition techniques. However, complex, uncontrolled gas-phase reactions, and flow dynamics have made the synthesis of these multi-component 2D crystals exceedingly challenging. In the response of these difficulties, here we demonstrate a novel laser-assisted synthesis technique (LAST), which significantly reduces the existing growth complexities and remarkably accelerates the growth of 2D materials. The uniqueness of this approach arises from the uses of laser for controlled vaporization of stoichiometric powder. We show that introducing laser permits pressure-independent decoupling of the growth and evaporation kinetics, enabling the use of stoichiometric powder as precursors for the growth of various high-quality mainstream 2D materials including MoS2, MoSe2, WSe2, and WS2.

Talk / Doctoral Research – In progress

Presenter: Rishi Bharadwaj[1]

Mentor: Dr. Cristian Bahrim[2]

[1]Philip Drayer Department of Electrical Engineering, Lamar University

[2]Department of Physics, Lamar University

Research in Photonics and Light-Matter Interaction

Energy suppression of a laser beam on a glass surface assisted by a stronger coupling laser

We are looking to store the energy of a continuous-wave (CW) TEMoo laser beam into the vibrations of atoms located on an insulating crown glass surface. Two CW laser beams from diode lasers of 650 nm (probe laser) and 532 nm (coupler laser) are irradiating simultaneously a 2mm wide glass area. A capacitor configuration with the crown glass used as dielectric medium between two aluminum plates, can increase the energy background of dipoles (including the vibration of nuclei) on the surface for better amplifying or reducing the coupling between the two lasers. Our experimental signal is the irradiance of the probe laser beam reflected by the glass surface and is measured within a region of 20 degrees wide centered at the Brewster angle, which is 56.6 degrees for crown glasses. At low voltage (0.3 volts), close to the Brewster region of width about 3 degrees we are measuring a regular interference pattern, with several minima located within. At high voltage (6 volts), the interference fringes form further out (about 1-2 degrees away) from the Brewster region. Our experimental signal clearly shows a typical pattern with evenly spaced fringes of interference located near the Brewster angle minimum of the parallel component of reflectance to the plane of incidence. The discussion about the suppression of probe laser's energy in interaction with a coupling laser assisted by the same electric dipoles on the surface is understood as being a destructive interference between the two lasers. The physical explanation associated to this new phenomenon of light-matter interaction at insulating surfaces can be inspired from Lorentz model. One interesting possible application of this new coupling mechanism aims toward the recording of optical information on insulating surfaces using optical bits, and another one is the suggestion of a new electro-optic switch.

Talk / Doctoral Research – Advanced

Presenter: Yi Liu

Co-author: Ruobing Zhao

Mentor: Dr. Yueqing Li

Department of Industrial Engineering, Lamar University

Research in Industrial and System Engineering

Effects of Directional Road Signs Combinations and Language Unfamiliarity on Driving Behavior

The study conducted a simulated driving experiment to explore the impact of language familiarity and the combination of directional road signs on driving performance and mental workload. Eight participants "drove" a simulated vehicle for one hour on a eight-lane rural highway. Data were aggregated from different scenarios (2 (Language: English, Spanish) × 2 (number of board: 1, 3). The results showed a significant main effect of language familiarity on driving performance. The higher standard deviations of speed and acceleration were found in Spanish condition. The research results showed that the impact of language familiarity on driving performance needs further research and attention.

Talk / Doctoral Research - Advanced

Presenter: Nader Madkour[1]

Co-authors: Dr. Seokyon Hwang[3], Dr. Jing Zhang[2], and Dr. Zhe Luo

Mentor: Dr. Berna Eren-Tokgoz[1]

[1]Department of Industrial Engineering, Lamar University

[2]Department of Computer Science, Lamar University

[3]Department of Construction Management, Lamar University

Research in Industrial and System Engineering

Drone and Artificial Intelligence-based evaluation of Debris for Waterways and Ports

There is a visible paradigm shift in debris management to developing framework for community resilience. Debris management has always been one of many competing priorities agencies must managed especially in waterways and shorelines. It is crucial that debris be properly managed to comply with regulations, conserve disposal capacity, protect human health and minimizing environmental impacts. A community should be prepared with a recovery plan for removing debris from waterways and sensitive habitats such as shorelines and wetlands before the presence of any event that might cause debris formation in order to recover fast and to have a better response towards the removal of the debris formed. In this research, the Port of Port Arthur was selected for the analysis of the debris formation along with the waterway streamline and assessing the debris formation by using remote sensing and spatial analysis. A Mavic 2 Pro drone which is a product of Dji enterprise was used to capture the videos from Port Arthur Independent School District, TX, with coordinates 29°55'41.0"N 93°52'18.1"W, and a height between 29 to 375 feet above the waterway. To assess the debris formed on the shores of the waterway of the port and inside the water streamline, the drone videos were analyzed by a deep learning neural network to segment water regions from video frames and the debris on the water surface were detected using an adaptive thresholding method.

Talk / Graduate Research

Presenter: Tyler Martin

Mentor: Dr. Daniel J. Preston

Co-authors: Aman Eujayl and Marquise D. Bell

Department of Mechanical Engineering at Rice University

Rice University, Houston, TX 77005 USA

Research in Material Science

Powering Soft Wearable Devices Using Body Heat

The emergence of pneumatically powered soft robots has enabled wearable assistive devices that aid users with limited mobility. However, these devices rely on bulky, noisy compressors or pumps that inhibit comfort and usability. Pneumatic power has been generated from heat by vaporizing a low-boiling-point fluid (LBPF) but has relied on electric heaters that have tethers or hard components. In this work, we developed a device that generates pneumatic power by vaporizing a LBPF using waste heat from the human body. We used a stacked lamination method to create a textile-based device with a warm chamber that absorbs body heat to pressurize the LBPF, a cool chamber that collects and condenses the LBPF after actuation, and an insulating layer between the chambers to prevent parasitic heat loss. Using a valve, the pressurized warm chamber inflates an actuator on demand, and the cool chamber depressurizes it. We used a thermal resistance network to model the pressures in each chamber, experimentally verified the pressures, and used the device to operate an actuator over a period of 45 minutes for 40 actuation cycles. In addition, the process was shown to be renewable, allowing the user to simply swap the chamber positions and continue powering wearable assistive devices. This work paves a path to self-powered wearable assistive devices for the upper body without hard components or tethers.

Talk / Undergraduate Research

Presenter: Vishal Mundodi

Mentor: Dr. Peter J. Christie

Department. Microbiology and Molecular Genetics

University of Texas Medical School at Houston, 6431 Fannin St. Houston, TX 77030

Research in Biology

Supported By: NIH Summer Undergraduate Research Supplement Award

Targeted Plasmid Delivery Using Surface Displayed Adhesions

The type IV secretion system (T4SS) is one of several types of secretion systems, which microorganisms use for the transport of macromolecules, such as proteins and DNA, across the cell envelope. It is the most versatile family of secretion systems and has been found in both Gram-positive and Gram-negative bacteria as well as in some archaea. The T4SS has been exploited to create engineered bacterial cells capable of delivering toxins and/or drugs to pathogens or eukaryotic cells. The objective of this project was to enhance DNA transfer frequency by engineering adhesions on a donor cell that encodes a T4SS and to develop a strong method of delivering a toxin or drug that could potentially be directed against specific cancer cells or pathogens. To achieve this, standard mating assays were used. The donor and recipient cultures were grown overnight and mixed in set proportions in a 96-well plate After conjugation the cells were plated on selection media and allowed to incubate overnight. After incubation the colonies were counted, and the transfer frequency was calculated. The results using the leucine zipper Fos and Jun binding system was expected to produce elevated transfer frequency. However, when tested minimal difference in the transfer frequency was observed. Targeting using nanobody-intimin (Nb-Int) and antigen-intimin (Ag-Int) to transfer the pKM101 plasmid showed that the Nb-Ag binding system showed elevated transfer frequency when compared to non-displayed binding. This targeting system worked well against a highly diluted recipient population, as a 4-log dilution of the targeted recipient in a mixed recipient showed high efficiency of targeted transfer frequency. The Nb-Ag adhesion system showed a 2-3 log higher efficiency than non-targeted binding. In the future we plan to use the surface displayed adhesion system to engage in targeted killing, possibly using CRISPR Cas9 to encode a killing plasmid.

Talk / Graduate Research

Presenter: Tyler Nelson

Co-authors: Gabriella Gagliano, Nahima Saliba, Sofía Vargas-Hernandez

Mentor: Dr. Anna-Karin Gustavsson

Gustavsson Lab – Rice University

Research in Applied Physics

Live-cell 3D Super-resolution Imaging

Super-resolution microscopy is a broad collection of techniques used to resolve cellular features and components that are smaller than the diffraction limit of light. One subgroup of super-resolution techniques, called single-molecule localization microscopy (SMLM), relies on the super-localization of individual stochastically blinking fluorescent molecules which are bound to a structure of interest. This super-localization is performed in post-processing by fitting the intensity distributions of single fluorescent molecules on the camera, called the point spread functions (PSFs), to mathematical functions to determine the precise position of each molecule. 3D information can also be obtained using phase masks to change the shape of the PSFs according to their distance from the focal plane.

Such techniques are powerful but have certain limitations for imaging in living cells. Specifically, the buffers needed to induce blinking in certain fluorescent dyes are often toxic and the dyes themselves are typically not cell permeable. Additionally, these dyes require high-power lasers, which can damage living cells. Super-localization also traditionally requires emitters to be sparsely distributed in each frame, meaning the blinking rate must be limited, which leads to long imaging times.

These limitations can be mitigated by, for example, far-red spontaneously blinking fluorescent molecules, light sheet illumination, advanced sCMOS cameras, and deep learning algorithms. Finding ways around these limitations will allow us to better study living cells in 3D at superb spatial and temporal resolutions, providing insight into the mechanisms behind cellular processes as well as the pathology of disease.

Talk / Graduate Research

Presenter: Roberto Obregon

Mentor: Dr. Paul Bernazzani

Research in Chemistry

Department of Chemistry and Biochemistry, Lamar University

Analysis of Oxidized Low-Density Polyethylene to Determine the Possibility of a Recycle Stream

Most synthetic polymers do not degrade easily at room temperature. Polyolefins in general are very durable due to chemical and biological inertness as a result of high molecular weight and lack of functional groups.[1] As a result, some plastics, such as low-density polyethylene (LDPE) must be recycled to extend their usability and decrease the overall carbon footprint. A not often used recycling option is the chemical conversion of a plastic into value-added compounds or basic starting material. This study investigates the chemical reactivity of LDPE at relatively low temperature to perform a partial oxidative degradation that could be used as the first step of a chemical recycling stream. Samples are held at 150°C for 3 days and analyzed for thermal and spectroscopy properties. FTIR demonstrates that partial oxidative degradation occurred. This study degrades LDPE thermally to force an oxidative addition of weak sites to the polymer chain. The results of this degradation are analyzed, and the products identified.

References

[1] Chamas, A.; et. al.; Degradation Rates of Plastics in the Environment; ACS Sustainable Chem. Eng. 2020, 8, 9, 3494–3511.

Talk / Graduate Research

Presenter: Dylan Palmer

Colorado School of Mines, Department of Mechanical Engineering, Golden, Colorado

Mentor: Dr. Brian Thomas, Professor Emeritus and Research Professor, University of Illinois

Research in Material Science and Mechanical Engineering

Finite Element Analysis of Defects in Continuously Cast Steel Slabs

To study the effect of defects in continuously cast steel products, a non-linear finite element model was constructed and compared against plant data. A complex constitutive model was implemented in ABAQUS to properly estimate the transient material properties of the material throughout the solidification process. Thermo-mechanical behavior of steel slabs has been simulated in the mold region for a variety of steel grades and casting conditions. Boundary conditions were implemented to capture the realistic loading caused by mold friction and mold taper issues. Heat flux disruptions, depressions, and longitudinal surface cracks are also modeled with this technique. The stress and strain profiles for different grades and casting conditions were studied with this technique, with insight gained for how each grade should be properly cast in the plant.

Talk / Graduate Research

Presenter: Saumi Patel

Co-author: Dr. Xinyu Liu

Mentor: Dr. Yueqing Li

Department of Industrial and Systems Engineering, Lamar University

Research in Industrial and System Engineering

Human Factor and Ergonomics Evaluation of in Vehicle Infotainment Touchscreen Display

There has been a rapid increase in 'In-vehicle touchscreens' usage over the last decade, particularly for information and entertainment functions. And because of the dynamic interface functionality, the touchscreen becomes a major attraction for the automobile industry. As a result, today most of the car manufacturer uses touchscreen instead of static push buttons. For display screen locations, there have been two legacy display locations in the car. One is a 'Head-up display' and 'Head-down display'. Head-up display is similar to jet plans mounted on top of the instrument panel board and head-down display - located on the car console. However, the HUD position won't work for touchscreen devices since the touchscreen required direct touch input from the driver for which HUD location either blocking the road view or out of the driver's reach. Besides, there are numbers of possibilities for HDD locations to enhance driver's interaction and driving experience.

In the research study, we are evaluating 8 different possible "in-vehicle touch-screen designs". (2 HDD locations for touch screen display- Top & Middle, 2 different main menu layouts- Horizontal & Vertical, 2 screen mount positions- Fixed screen vs Tilted screen according to user preference). The study focused on assessing possibilities for different HDD locations within proximity of the driver. This experiment aims to find the most effective and efficient touchscreen position with the least possible discomfort and distraction. Participants were instructed to perform a series of different Music, A/C, Seat control tasks on the developed In-vehicle infotainment prototype in the experiment. The experiment tasks were focused on controlled and real-life task-based scenarios.

Talk / Doctoral Research – In progress

Presenter: Prasad Pawar[1,2]

Co-authors: Pankti Joshi[1,2], Keal, Cleveland E[1,2], and Dinh, Tuoi T[1,2]

Mentor: Dr. Clayton S. Jeffryes[1,2,3]

[1]Nanobiomaterials and Bioprocessing Laboratory (NABLAB), Research in Chemical Engineering, Department of Chemical Engineering, Lamar University

[2]Center for Midstream Management and Science, Lamar University

[3]Center for Advances in Water & Air Quality, Lamar University

Research in Nanobiomaterials and Bioprocessing

Microwave-assisted demulsification of tight crude oil-water emulsions

The main objective of this study is to use microwaves to develop an energy efficient and economical method to demulsify stable crude oil-water emulsions. These emulsions are formed by high shear mixing of process water and crude oil during pumping, desalting and transportation through wellbores and pipelines and are stabilized by emulsifying agents that form interfacial films at the oil-water interface. These surface-active species, such as asphaltenes, resins, solids, waxes, or commercially available chemical emulsifiers are responsible for the formation of stable emulsions. Tight crude oil emulsions, characterized by suspended droplets on the order of submicron to tens of microns, often cause serious problems during extraction such as clogging, corrosion, and pump failures. To simulate field conditions, we mixed two crude oils to prepare samples with American Petroleum Institute (API) gravities between 28.9° and 46.0°. These crudes were mixed with water to create emulsions containing between 20% and 80% water. This array of Water-in-Oil (W/O) and Oil-in-Water (O/W) emulsions with different densities and viscosities were mixed at varying shear rates. Series of batch demulsification runs of these crude oil emulsions were done by exposure to microwaves under a well-defined set of parameters such as temperature, power, time, and salinity. To determine the efficiency of phase separation after treatment, final oil-phase water content was measured using Karl Fischer Titration. Under similar hold times and temperatures, microwave separation methods more effectively separated the phases than thermal separation methods. Energy input analysis was performed from the Power-Time data obtained from each demulsification run.

Talk / Doctoral Research - Advanced

Presenter: Premkumar Ravishankar[1]

Co-authors: Ibrahim X Khalilullah[2], Dr. Hwang[3], Dr. Zhang[2], Dr. Eren-Tokgoz[1] and Dr. Luo[3]

Mentor: Dr. Berna Eren-Tokgoz[1]

[1]Department of Industrial Engineering, Lamar University

[2]Department of Computer Science, Lamar University

[3]Department of Construction Management, Lamar University

Research in Industrial and System Engineering

Resilience framework of Pipeline Infrastructure Utilizing Drones and Image Processing Algorithm

Pipeline systems are a vulnerable section of the midstream industry, posing an immediate threat to human lives, other infrastructures, and the environment. The requirement for safe operation and effective preventive maintenance of pipelines grows as oil and gas demand rises. Timely identification of possible threats and defects can reduce the potential consequences. Drones are being used to improve the efficiency of pipeline inspection from humans. Data from drones are utilized to detect possible irregularities due to various defects occurring along the pipelines. This research introduces a resilience framework discussing misalignment, deformation, missing parts, cracks, soil movement, and broken components. The potential system disturbances and their short and long-term impacts on various components are investigated for regularly expected and severe events. The outcome of this research is to improve the midstream industry, enhance pipeline maintenance, increase system resiliency, and promote environmental and public safety.

Talk / Doctoral Research - Advanced

Presenter: Manthan A. Shah

Mentors: Dr. Cagatay Tokgoz and **Dr. Jing Zhang**

Phillip M. Drayer Department of Electrical Engineering

Research in Electrical Engineering

Efficient Radar Signature Prediction for Electrically Large Conducting Platforms Using Parallelization on the RED HPC Cluster at Lamar University

The radar signature of an object is a measure of how detectable it is by a radar system. Simulation of radar signature of an object becomes more challenging as its electrical largeness in terms of wavelength increases. Iterative physical optics (IPO) method is one of high frequency asymptotic techniques used to predict radar signatures of electrically large conducting objects. Although IPO accounts for multiple reflections, it does not properly include effects of diffractions from physical edges of an object. Therefore, a new hybrid approach is proposed to include edge diffractions using physical theory of diffraction (PTD) with IPO. In order to predict radar signature of an object, it is represented using surface mesh consisting of triangular facets that are a fraction of a wavelength in size. Hence, as frequency at which radar signature is predicted increases, the number of facets in surface mesh drastically increases, resulting in more computational cost in terms of time and memory. In this study, the IPO-PTD code that was developed based on C programming language for radar signature prediction has been parallelized on the RED HPC Cluster of Lamar University using message passing interface (MPI). Numerical results have been generated for radar signatures of well-known benchmark objects using the parallel version of the IPO-PTD code. The experimental results have been validated with the numerical results obtained using FEKO commercial electromagnetic simulation software. This study demonstrates that advanced numerical techniques can be accelerated using parallel computing to solve complex problems in computational electromagnetics with high computational efficiency.

Talks / Doctoral Research – In progress

Presenter: Ruobing Zhao

Co-author: Yi Liu

Mentor: Dr. Yueqing Li

Department of Industrial and Systems Engineering, Lamar University

Research in Industrial and System Engineering

A Preliminary Assessment of Driver's Workload in Partially Automated Vehicles and Conventional Vehicles

The study investigated driver's workload in partially automated vehicles and conventional vehicles under different traffic density conditions. Eight participants "drove" a simulated vehicle on a 10 mile straight, two-way rural interstate highway in 4 scenarios (2 (traffic density: Low, High) × 2 (vehicle type: Partially automated vehicle, Conventional vehicle) in random orders. In each scenario, participants were asked to perform lane change and overtaking when the vehicle ahead was moving at a speed much slower than the speed limit. Data was recorded using a STISIM DRIVE driving simulator, a Tobbi pro glasses 2 eye tracking device, and a NIRSport system. Workload was evaluated from subjective ratings (NASA-TLX questionnaire) and physiological methods (pupil dilation and oxygenated hemoglobin). A reduction in driver's workload was found when driving partially automated vehicles compared to driving conventional vehicles. Traffic density also has an impact on driver's workload, higher workload was found in high traffic density. Workload assessment helps to gain a deeper understanding of human-**automation** interaction, which will benefit the development of automated vehicles. The findings also indicate the importance of combining different approaches to evaluate workload in driving.

Presenter: Dr. Joseph C. Watso

University of Texas Southwestern Medical Center,

7232 Greenville Ave, Room 330, Dallas, TX 75231

Supervisor: Dr. Craig Crandall

Research in Applied Physiology

Adults with well-healed burn injuries have reduced pulmonary function decades after injury

Sub-acute (e.g., inhalation injury) and/or acute insults sustained during a severe burn injury impairs pulmonary function. However, previous work has not fully characterized pulmonary function in adults with well-healed burn injuries decades after an injury. Therefore, we tested the hypothesis that adults with well-healed burn injuries have reduced pulmonary function years after recovery. Our cohort of adult well-healed burn-injury survivors (n=41) had a lower forced expiratory volume in one second (Burn: 93±16 vs. Control: 103±10 %predicted, mean±SD; d=0.60, p=0.04), lower maximal voluntary ventilation (Burn: 84 [71-97] vs. Control: 105 [94-122] %predicted, median [IQR]; d=0.84, p<0.01), and a higher specific airway resistance (Burn: 235±80 vs. Control: 179±40 %predicted, mean±SD; d=0.66, p=0.02) than non-burned control participants (n=12). No variables were meaningfully influenced by having a previous inhalation injury (d≤0.44, p≥0.19; 13 of 41 had an inhalation injury), the size of the body surface area burned (R^2≤0.06, p≥0.15; range of 15-88% body surface area burned), or time since the burn injury (R^2≤0.04, p≥0.22; range of 2-50 years post-injury). These data suggest that adults with well-healed burn injuries have impaired pulmonary function decades after injury. Therefore, future research should examine rehabilitation strategies that could improve pulmonary function among adult burn-injury survivors.

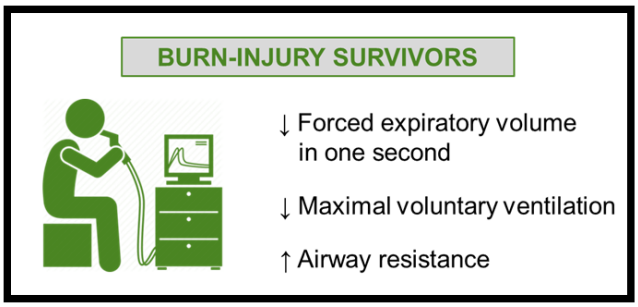

Summer Intern of the IEEM Summer Internship Program

Zaid Mohammed

Institute of Exercise and Environmental Medicine, 7232 Greenville Ave, Dallas, TX 75231

Supervisor: Dr. Craig Crandall, Director of the Thermal and Vascular Physiology Laboratory and Professor of Internal Medicine at UT Southwestern Medical Center

Collaborators: Dr. Joseph Watso, Dr. Luke Belval, and Dr. Josh Foster.

I interned at the Institute of Exercise and Environmental Science (IEEM) in Dallas, Texas. This is a research and clinical facility affiliated with Texas Health and UT Southwestern. I was in the Thermal and Vascular Physiology laboratory which focused on how the neural control of the cardiovascular system is influenced by thermal stress. My main focus was working on a data analysis project about whether pulmonary function improved after six months of community-based exercise training in burn survivors.

Due to their injuries, burn survivors experience several impairments to their body systems functions which places them at an increased risk of long-term complications. For pulmonary function specifically, it can be impaired for the rest of their lives if they had inhalation injuries and prolonged bed rest. Studies have shown that this negatively impacts their exercise tolerance and may be a causative factor for their low participation in physical activity. As a result, pulmonary function is lower in burn survivors than non-burn populations.

Looking at previous studies on this topic, only swimming exercise has been shown to improve pulmonary function in healthy adults. However, the evidence for exercise training improving pulmonary function is mixed. For burn survivor adults, a previous study has shown that there was no improvement in their pulmonary function from exercise training.

Our study has a larger sample size, lasts for six months, and is community based. Our hypothesis is that six months of exercise training will improve pulmonary function. The reasoning behind our hypothesis was that since burn survivors have such poor pulmonary function, an extended period of exercise training may be a stimulus that improves it.

When it comes to the criteria of selecting the participants, they were all at least 2 years post injury, and had not been part of a structured exercise regimen for the past 12 months.

The 36 participants were divided into 3 groups based on burn surface area (BSA): control (no BSA burned), less than 40% BSA, and greater than 40% BSA. During the six months of community-based exercise training, the first month focused on endurance.

The second and third months focused on endurance training and the beginning of resistance training albeit not too long or intense. Towards the end months, resistance and endurance training increased in time and intensity, and the regimen progressed to include some interval work.

The FITT model (frequency, intensity, time, type) was used to meet the exercise goals without overtraining the body.

Our results showed that there was a significant difference between the control groups for raw MVV values. MVV is a spirometry test that measures the largest volume that can be moved into and out of the lungs during a 10-15 second interval with voluntary effort. Our results did not show any significant difference between pre and post for any variables.

We can conclude that after six months of non-supervised community-based exercise training, pulmonary function did not improve in burn survivors.

Over the course of my internship, I assisted in three other projects.

- The first of the three projects I assisted with focused on the effects of battlefield analgesics on tolerance to hemorrhage. The goal of the study is to examine how a commonly used pain medication such as morphine affects heart and blood vessels.
- The second project I assisted with is testing cooling modalities to attenuate thermoregulatory and cardiovascular stress in burn survivors. We examined which cooling modality would be most effective in regulating their body temperature.
- Finally, I also worked on examining the cardiovascular consequences of heat waves on the elderly. Our goal was to record how their body reacts in a simulated, controlled setting, where a cardiologist was present.

I have learnt a lot from this internship and am deeply grateful to the Office of Undergraduate Research for providing me with this opportunity.


Texas Health
Presbyterian Hospital
DALLAS
IEEM WAITING ROOM

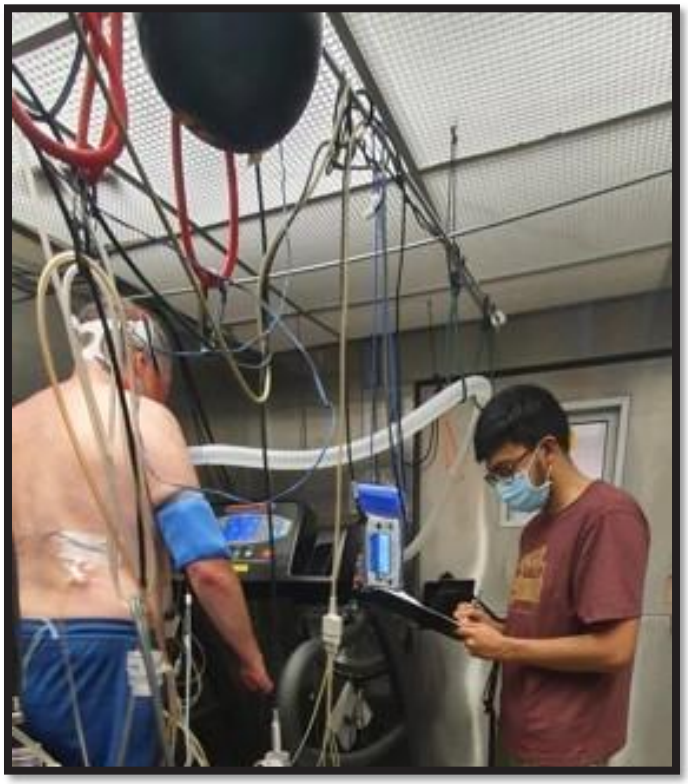

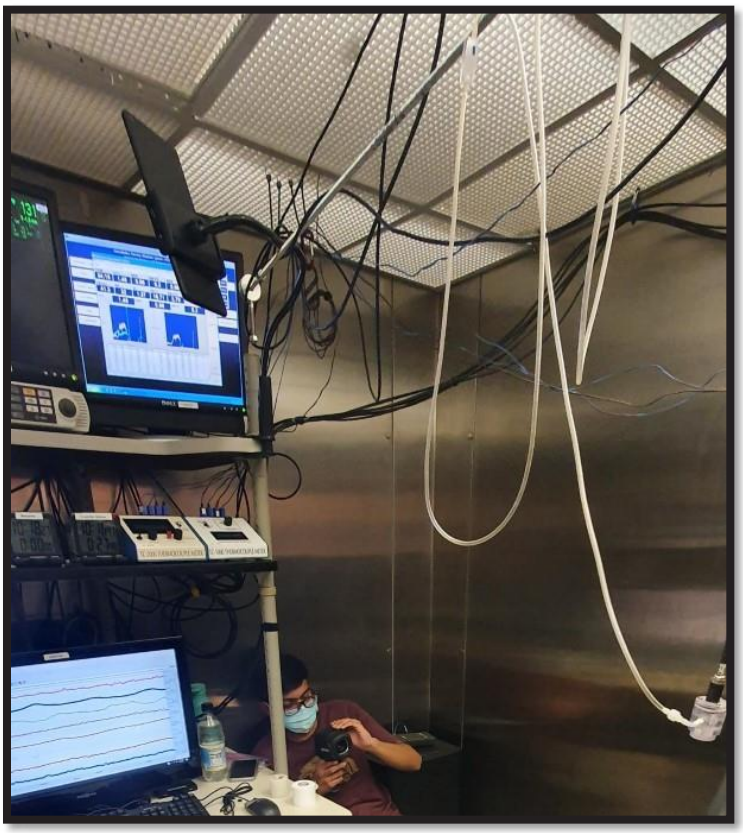

Join our student organization:

Lamar University Undergraduate Research Association (LURA)

"LURA was founded in fall 2019 to fulfill the need for a community *by* and *for* undergraduate students to discuss, collaborate, and learn how effectively one can conduct research. The consistent quality and volume of research conducted by undergraduate students at Lamar University has made it clear that there is a need for an organization to act as a vital resource for building young researchers. Thus, LURA provides an academic forum that connects all level students from freshmen to seniors with their professors and mentors, and facilitates communication between Lamar undergraduates and their peers around the nation.

LURA is a platform for offering panel discussions about

- Research opportunities inside and outside Lamar,
- Better ways to deliver undergraduate research results in poster and oral presentations,
- Ways to perform peer-mentoring,
- Organizing workshops and panel discussions on various topics, including how to successfully apply to graduate schools.

LURA is the premier student organization at Lamar University for any undergraduate student interested in doing research. The Office of Undergraduate Research provides strong support and offers logistics to this student organization. Contact URALamar@gmail.com or visit the Office of Undergraduate Research—Chemistry 115D

For More Information about O.U.R. programs

DR. CRISTIAN BAHRIM - ACTIVE DIRECTOR OF O.U.R.
OFFICE: CHEMISTRY 115B, PHONE: 409-880-8290,
E-MAIL: CRISTIAN.BAHRIM@LAMAR.EDU

MS. JENNA ERWIN - ADMINISTRATIVE ASSOCIATE
OFFICE - CHEMISTRY 115A, PHONE 409-880-8430,
E-MAIL: JERWIN6@LAMAR.EDU

HTTPS://WWW.LAMAR.EDU/UNDERGRADUATE-RESEARCH/INDEX.HTML

OFFICE OF UNDERGRADUATE RESEARCH
LAMAR UNIVERSITY

Please join us at our next conference

THE NINTH ANNUAL

Undergraduate Research & Creative activity Expo 2022

April 15, 2022

An event hosted by the Setzer Center


OFFICE OF UNDERGRADUATE RESEARCH
LAMAR UNIVERSITY


LAMAR
UNIVERSITY